이학박사 학위논문

Studies on growth and development of *Arabidopsis* in response to light and temperature signals.

빛과 온도 신호에 반응하는 애기장대의 성장 및 발달 연구

2018년 8월

서울대학교 대학원

화학부

하 준 호

ABSTRACT

Environmental stimuli, such as light, temperature, moisture, and nutrient limitation affect plant growth and development. Since the immovable nature of plants, they have to adapt to environmental changes to survive. Plants have developed adaptation strategies to cope with a variety of environmental changes. Previous studies have explored the molecular mechanisms that respond to various environmental changes. Studies on light responses generally have focused on photomorphogenesis that occurs in aboveground tissue. In addition, studies in response to temperature changes have been concentrated on thermomorphogenesis that proceeds at seedling stage. However, the adaptation strategies of plants to environmental changes vary depending on the plant tissue or specific growth stages. In this study, I investigated the light responses that occur in root tissues and the temperature responses that occur during early developmental stages.

In Chapter 1, Studies on the role of a root photoreceptor in response to light transmitted through the stem is described. Photoreceptors and associated signaling mechanisms have been extensively studied in plant photomorphogenesis with a major focus on the photoresponses of the shoot system. Accumulating evidence in recent years strongly support that light also influences root growth and development. However, how aboveground light influences the root system has not been systematically explored. Here,

I show that light is efficiently conducted through the stems to the roots, where photoactivated phytochrome B (phyB) triggers gene induction and protein accumulation of the positive photomorphogenic regulator ELONGATED HYPOCOTYL 5 (HY5). Accordingly, *Arabidopsis* plants that are defective specifically in root HY5 exhibited alterations in root growth and gravitropism. These findings demonstrate that the underground roots directly sense stem-piped light to monitor the aboveground light environment during plant environmental adaptation.

In Chapter 2, I discuss root development by shoot-to-root light response. The underground roots reside normally in darkness. However, they are often exposed to ambient light that penetrates through cracks of the soil layers, which would occur by wind, heavy rain, or temperature extremes. In response to light exposure, the roots produce reactive oxygen species (ROS), which promote root growth. It is known that the ROS-induced growth promotion facilitates rapid escape of the roots from non-natural light. Meanwhile, long-term exposure of the roots to light elicits ROS burst, which impose oxidative damages on cellular components, necessitating that cellular levels of ROS should be tightly regulated in the roots. Here, I demonstrated that the phyB stimulates the biosynthesis of abscisic acid (ABA) in the shoots and notably the shoot-derived ABA signals induce a peroxidase-mediated ROS detoxification reaction in the roots. Accordingly, while ROS accumulate in the roots of *phyb* mutant that exhibits a reduced

primary root growth in the light, such ROS accumulation did not occur in the dark-grown *phyb* roots that exhibited normal growth. These observations indicate that a mobile shoot-to-root ABA signaling links shoot phyB-mediated light perception with root ROS homeostasis to help the roots adapt to unfavorable light exposure. I propose that the ABA-mediated shoot-to-root phyB signaling contributes to the synchronization of shoot and root growth for optimal propagation and performance in plants.

In Chapter 3, thermal adaptation strategy during the autotrophic transition at high ambient temperature is described. Chlorophyll biosynthesis enables autotrophic development of developing seedlings. Upon light exposure, the chlorophyll precursor protochlorophyllide (pchlide) produces ROS. Developing seedlings acquire photosynthetic competence through the action of protochlorophyllide oxidoreductases (PORs) that convert protochlorophyllide to chlorophyllide (chlide), reducing ROS production that would otherwise induce cellular damages and chlorophyll bleaching. Here, I show that FCA mediates the thermostabilization of PORs to trigger the conversion of protochlorophyllide to chlorophyllide in developing seedlings. FCA also facilitates the thermal induction of *POR* genes through histone acetylation that promotes the accessibility of RNA polymerases to the gene promoters. The combined action of FCA maintains PORs at warm temperatures, shifting chlorophyll-ROS balance towards autotrophic development. I

propose that the FCA-mediated thermal adaptation of autotrophic development allows developing seedlings to cope with the heat-absorbing soil surface layer under natural conditions.

key words: Light signaling, phytochrome, root development, light transmission, abscisic acid, high ambient temperature, autotrophic development, chlorophyll biosynthesis, reactive oxygen species, FCA

Student number: 2014-21242

CONTENTS

ABSTRACT..... i

CONTENTS..... iv

LIST OF FIGURES..... viii

LIST OF TABLES..... xi

ABBREVIATIONS..... xii

CHAPTER 1: Stem-piped light activates phytochrome B to trigger light responses in *Arabidopsis thaliana* roots

INTRODUCTION..... 21

MATERIALS AND METHODS

1. Plant materials and growth conditions..... 24

2. Analysis of gene transcript levels..... 24

3. RNA sequencing..... 26

4. Micrografting..... 26

5. Fluorescence imaging..... 27

6. Immunoblot assays..... 27

7. Histochemical staining..... 28

8. Light transmission assay..... 29

RESULTS

Shoot light influences gene expression in the roots..... 31

Root phyB is required for shoot light–mediated gene regulation in roots..... 33

Root phyB mediates HY5 stabilization during root development.. 41

Stem-piped light activates root phyB..... 46

Aboveground light regulates root gravitropism through root phyB..... 69

DISCUSSION

ACKNOWLEDGEMENT

CHAPTER 2: Shoot phytochrome B modulates root ROS homeostasis via abscisic acid signaling in *Arabidopsis*

INTRODUCTION..... 81

MATERIALS AND METHODS

1. Plant materials and growth conditions..... 83

2. Analysis of gene transcript levels..... 83

3. Propidium iodide staining..... 84

4. Detection of ROS..... 85

5. Micrografting..... 86

6. Immunoblot assay..... 86

7. Hormone quantification..... 86

8. Growth hormone treatment..... 87

RESULTS

The primary root growth of *phyb* seedlings is sensitive to light..... 89

Shoot phyB suppresses ROS accumulation in the light-exposed roots 94

The phyB-mediated induction of ABA biosynthesis in the shoots is associated with root growth..... 96

Shoot phyB signals mediate root ROS homeostasis via ABA signaling..... 102

DISCUSSION

ACKNOWLEDGEMENT

CHAPTER 3: Thermo-induced maintenance of photo-oxidoreductases underlies plant autotrophic development

INTRODUCTION..... 123

MATERIALS AND METHODS

1. Plant materials..... 126

2. Plant growth conditions..... 127

3. Analysis of gene transcript levels..... 127

4. Transmission electron microscopy..... 129

5. Measurement of pigment contents..... 129

6. Immunoblot assays..... 130

7. Detection of ROS and treatment with ROS scavengers..... 131

8. Yeast two-hybrid assay..... 132

9. Chromatin immunoprecipitation assay..... 132

10. DNA methylation assay..... 133

RESULTS

FCA protects developing seedlings from albinism at 28°C..... 136

FCA is required for thermo-induced maintenance of POR proteins..... 139

FCA reduces ROS production at warm temperatures..... 156

FCA mediates RNA Pol II binding to *POR* Loci..... 159

DISCUSSION

ACKNOWLEDGEMENT

REFERENCES

PUBLICATION LIST

ABSTRACT IN KOREAN

LIST OF FIGURES

Figure 1. Shoot light influences gene expression in the roots..... 32

Figure 2. Gene expression of photoreceptors in the roots..... 34

Figure 3. Root phyB underlies the light-mediated induction of root genes..... 35

Figure 4. Root gene expression in grafted plants between Col-0 and *phyb* plants..... 37

Figure 5. Root gene expression in grafted plants between L*er* and *YVB* plants..... 38

Figure 6. Plant growth for fluorescence imaging of phyB and HY5 distribution in root tissues..... 39

Figure 7. Effects of shoot light on the nuclear localization of root phyB..... 40

Figure 8. Nuclear localization of root phyB by shoot light..... 42

Figure 9. Expression kinetics of *HY5* and its downstream genes in root cells..... 43

Figure 10. Shoot light stabilizes root HY5 via phyB during root development..... 44

Figure 11. Effects of shoot light on root HY5 stability in *phyb* mutant..... 45

Figure 12. Root phenotypes of grafted plants between Col-0 and *hy5* plants..... 47

Figure 13. Lateral root angle in grafted plants..... 48

Figure 14. Lateral root formation in grafted plants between Col-0 and *hy5* plants..... 49

Figure 15. Lateral root angle in *hy5* mutant..... 50

Figure 16. Primary root growth of soil-grown *hy5* mutant..... 51

Figure 17. Effects of growth hormones and sucrose on the nuclear import of phyB and the HY5 stability in root cells..... 53

Figure 18. Light transmission through stem-root segments..... 55

Figure 19. Normalized light transmission through stem and stem-root segments..... 56

Figure 20. Light transmission through stem or stem-root segments..... 57

Figure 21. Transmission of light with different spectral compositions through stem-root segments..... 58

Figure 22. Fluence rates and spectral composition of stem-piped light..... 59

Figure 23. Plant growth under soil light-block conditions..... 62

Figure 24. Effects of stem-piped light on the nuclear localization of root phyB..... 63

Figure 25. Effects of shoot illumination on root HY5 stability..... 64

Figure 26. Transcript accumulation of *HY5* and its targets in root cells..... 65

Figure 27. Experimental evaluation of the soil-cover treatments..... 66

Figure 28. GFP signals in the root cells of 35S:*PHYB-GFP* plants..... 67

Figure 29. GFP signals in the root cells of 35S:*HY5-GFP* plants..... 68

Figure 30. Spectral composition of FR-rich light..... 71

Figure 31. Effects of FR-rich light on the nuclear localization of root phyB..... 72

Figure 32. Effects of FR-rich light on root HY5 stability..... 73

Figure 33. Schematic diagram of stem-piped light signaling during root gravitropism..... 74

Figure 34. The primary root growth of *phyb* seedlings..... 90

Figure 35. Meristem cell numbers in *phyb* primary roots..... 91

Figure 36. Primary root growth of *phyb-5* seedlings in the light..... 92

Figure 37. Light sensitivity of *phyb* roots..... 93

Figure 38. Primary root growth of grafted seedlings between Col-0 plants and *phyb* mutant..... 95

Figure 39. ROS levels are elevated in the light-exposed primary roots of *phyb* seedlings..... 97

Figure 40. NBT staining of *phyb* primary roots..... 98

Figure 41. Endogenous ABA contents..... 99

Figure 42. Effects of ABA feeding on primary root growth..... 100

Figure 43. Effects of different concentrations of ABA on primary root growth..... 101

Figure 44. Quantification of endogenous growth hormones in *phyb*

seedlings..... 103

Figure 45. Effects of SA on primary root growth..... 104

Figure 46. Relative levels of *ABA1* and *ABA2* transcripts..... 105

Figure 47. Transcript levels of ABA biosynthesis genes in *phyb* seedlings..... 106

Figure 48. ABA is associated with root ROS over-accumulation in *phyb* seedlings..... 108

Figure 49. The primary root phenotype of *aba1-6* seedlings..... 109

Figure 50. Detection of ROS in *aba1-6* mutant..... 110

Figure 51. Relative levels of *ABI5* and *PER1* transcripts in *phyb* primary roots..... 112

Figure 52. Accumulation of ABI5 proteins in *phyb* roots..... 113

Figure 53. Evaluation of the anti-ABI5 antibody used..... 114

Figure 54. Primary root length of *abi5-3* mutants..... 115

Figure 55. Primary root length of *per1-2* mutant..... 116

Figure 56. DAB and H_2DCFDA stainings of light-grown primary roots..... 117

Figure 57. Schematic model for shoot phyB function in modulating root ROS homeostasis..... 118

Figure 58. *fca* seedlings exhibit albinism at high ambient temperatures 137

Figure 59. Effects of light intensities on albinism of *fca* seedlings at 28^{o}C..... 138

Figure 60. Effects of temperature on albinism..... 140

Figure 61. Seedling phenotypes of selected mutants..... 141

Figure 62. Chloroplast development at 28°C..... 143

Figure 63. Expression of *POR* genes..... 144

Figure 64. Effects of *fca* mutations on chlorophyll biosynthesis..... 145

Figure 65. Protein levels of PORs in *fca* mutants..... 146

Figure 66. Protein levels of PORA in *PORA*-overexpressing seedlings..... 148

Figure 67. Thermosensitive phenotypes during the dark-to-light transfer..... 149

Figure 68. Levels of PORs during the dark-to-light transfer..... 150

Figure 69. Chlorophyll contents and cotyledon lengths of the *fca* and *por* mutants..... 151

Figure 70. Protochlorophyllide contents in etiolated *fca-9* mutant at 28°C..... 153

Figure 71. Conversion of pchlide to chlide at 28°C..... 154

Figure 72. Reduction of chlide levels in *fca* seedlings at 28°C..... 155

Figure 73. Effects of *POR* overexpression on albinism of *fca-11* seedlings..... 157

Figure 74. ROS Accumulate in *fca* Seedlings at 28°C..... 158

Figure 75. Singlet oxygen accumulation in *fca* seedlings during the dark-to-light transfer..... 160

Figure 76. Hydrogen peroxide accumulation in *fca* mutants..... 163

Figure 77. Effects of protease and 26S proteasome inhibitors on POR accumulation..... 165

Figure 78. Yeast two-hybrid assays on interactions of FCA with PORs..... 166

Figure 79. Transcript level and protein stability of FCA at 28°C..... 167

Figure 80. Genomic structures of *POR* genes..... 168

Figure 81. ChIP assays on FCA binding to *POR* loci..... 169

Figure 82. Yeast two-hybrid assays on interactions of FCA with upstream regulators of *POR* expression..... 170

Figure 83. Histone modifications at *POR* chromatins..... 172

Figure 84. DNA methylation status at *PORA* and *PORB* loci..... 174

Figure 85. ChIP assays on RNA pol II binding to *POR* loci..... 175

Figure 86. phenotype of *fca* seedlings grown in soil at 28°C..... 176

Figure 87. *fca* seedlings exhibit albinism in warm soil..... 178

Figure 88. FCA is essential for thermal adaptation of autotrophic development..... 179

LIST OF TABLES

Table 1. Primers used in Chapter 1..... 30

Table 1. Primers used in Chapter 2..... 88

Table 1. Primers used in Chapter 3..... 135

ABBREVIATIONS

ABA	abscisic acid
ABA1	ABA DEFICIENT 1
ABA2	ABA DEFICIENT 2
ABA3	ABA DEFICIENT 3
ABI5	ABA INSENSITIVE 5
ANOVA	analysis of variance
B	blue
BiNGO	Biological Networks Gene Ontology tool
CaMV	cauliflower mosaic virus
CAO	CHLOROPHYLLIDE A OXYGENASE
ChIP	chromatin immunoprecipitation
CHLD	MAGNESIUM CHELATASE SUBUNIT D
CHLH	MAGNESIUM CHELATASE SUBUNIT H
chlide	chlorophyllide
CHLI-I	MAGNESIUM CHELATASE
CHS	CHALCONE SYNTHASE
Col-0	Colombia-0
CRD1	COPPER RESPONSE DEFECT 1
CRY2	CRYPTOCHROME 2

CT	threshold cycle
DAB	3,3'-diaminobenzidine
DAG	days after germination
DIC	differential interference contrast
FR	far-red
GFP	green flourescence
GO	gene ontology
G-R	green to red
GUS	b-glucuronidase
H2DCFDA	2',7'-dichlorodihydrofluorescein
H3K4me2	histone-3 lysine-4 dimethylation
HY5	ELONGATED HYPOCOTYL 5
IAA	indole-3-acetic acid
IR	infrared
JA	jasmonic acid
LDs	long days
Ler	Landsberg *erecta*
MeJA	methyla jasmonic acid
MeOH	methyl alcohol
MS	Murashige and Skoog
NBT	nitro blue tetrazolium
pchlide	protochlorophyllide
PER1	PEROXIDASE 1

Pfr	FR-absorbing form
PHR1	PHOTOLYASE 1
phyA	phytochrome A
phyB	phytochrome B
PI	protease inhibitor cocktail
PIF4	phytochrome-interacting factor 4
POR	protochlorophyllide oxidoreductase
Pr	R-absorbing form
R-nearIR	red to near-infrared
ROS	reactive oxygen species
RT-qPCR	quantitative real-time PCR
SA	salicylic acid
SB	soil light block
SEM	standard error of the mean
SOSG	singlet oxygen sensor green
TUB	α-tubulin
UV	ultraviolet
X-Gluc	5-bromo-4-chloro-3-indolyl-beta-D-glucuronic acid
YUC8	YUCCA8
YVB	constitutively active phyB
ZT	zeitgeber time

CHAPTER 1

Stem-piped light activates phytochrome B to trigger light responses in *Arabidopsis thaliana* roots

INTRODUCTION

Light regulates virtually all aspects of plant growth and developmental processes throughout the life cycle (Jiao et al., 2007). Various photoreceptors perceive a wide range of light wavelengths, such as ultraviolet (UV), blue (B), red (R), and far-red (FR), to monitor the plant's environment. The roles of photoreceptors and their associated signaling mechanisms have been extensively investigated mostly in the light-induced changes (photomorphogenesis) in the aerial (aboveground) structures (Xu et al., 2015; Lu et al., 2015), but light also influences growth and development of the underground root system (Dyachok et al., 2011; Warnasooriya et al., 2011; Correll and Kiss, 2005). For example, R and FR light-sensing phytochromes are present in the roots and mediate primary root elongation, gravitropism, and jasmonic acid responses (Correl et al., 2005; Costigan et al., 2011). Cryptochromes and phototropins, both of which sense B light, regulate primary root growth and root phototropism, respectively (Briggs et al., 2002; Canamero et al., 2002). In addition, UV-B light is known to trigger root photomorphogenesis (Tong et al., 2008; Leasure et al., 2009). These effects of light on root growth occur when roots are directly exposed to light in an experimental setting. Light signals perceived by the shoot also regulate root development through the transfer of signaling molecules from the shoot to the root. Activation of phytochromeA(phyA) and phyB

stimulates the shoot-to-root transport of the hormone auxin and promotes lateral root production (Salisbury et al., 2007). In phytochrome-deficient mutants, lateral root development is suppressed in both light- and dark-grown plants, showing that shoot phytochromes are required for this developmental process. It has been reported that phyB induces expression of *HY5* and promotes stabilization of the HY5 protein (Xu et al., 2015). The accumulated HY5 protein moves from the shoots to the roots, where it activates a gene encoding nitrate transporter to enhance nitrate uptake (Chen et al., 2016), consistent with the notion that shoot-sensed light signals are transmitted to the roots. It has been suggested that the roots directly sense light under natural soil conditions. Genes encoding photoreceptors are expressed in root cells (Salisbury et al., 2007; Sharrock and Clack, 2002) and can be activated by direct light stimulation (Briggs et al., 2002; Canamero et al., 2006; Tong et al., 2008; Leasure et al., 2009). Aboveground light might be conducted through the soil to the roots (Tester et al., 1987; Mandoli et al., 1990). However, light only penetrates a few millimeters into the soil, and the penetration rate is highly variable, depending on soil composition and layering. Alternatively, light could be conducted through plant tissues, such as the vascular system, to the roots (Sun et al., 2003; Sun et al., 2005). Here, I demonstrate that light was conducted from the shoots to the roots of the model plant Arabidopsis thaliana through the stem and that root phyB was directly activated by this stem-piped light. Stem-piped light promoted the nuclear import of activated phyB in the roots of soil-grown

plants, and this promoted accumulation of HY5 in the roots, triggering gravitropic responses. My findings are consistent with the hypothesis that the roots monitor the aboveground light environment by directly sensing stem-piped light under natural conditions.

MATERIALS AND METHODS

Plant materials and growth conditions

Arabidopsis thaliana lines used were of the Columbia (Col-0) background except for the *YVB* transgenic plants that express a constitutively active phyB in the Landsberg *erecta* (L*er*) background (Jeong et al., 2016). Sterilized *Arabidopsis* seeds were cold-imbibed at 4ºC for 4 days in complete darkness to synchronize germination. Plants were grown on Murashige and Skoog-agar (MS-agar) plates or in soil under long days (LDs, 16-h light and 8-h dark) at 22ºC with white light illumination (120 μmol/m^2s) provided by fluorescent FLR40D/A tubes (Osram, Seoul, Korea).

The *phya-211*, *phyb-9*, *chryptochrome2-1* (*cry2-1*), and *hy5-221* mutants have been described previously (Seo et al., 2009; Ma et al., 2002). To generate 35S:*PHYB-GFP* and 35S:*HY5-GFP* transgenic plants, a green fluorescence protein (GFP)-coding sequence was fused in-frame to the 3' ends of phyB- or HY5-coding sequences under the control of the cauliflower mosaic virus (CaMV) 35S promoter. The expression constructs were transformed into Col-0 plants by a modified floral dip method (Clough et al., 1998).

Analysis of gene transcript levels

Transcript levels were quantified by reverse transcription-mediated quantitative real-time PCR (RT-qPCR). For total RNA isolation, plant materials were ground in liquid nitrogen. One mL of Trizol reagent (Invitrogen, Carlsbad, CA) was added to each plant sample, and the mixture was centrifuged at 16,000 X g for 10 min at 4ºC. Two hundred μL of chloroform was added to the supernatants followed by centrifugation under the same conditions. The supernatant was transferred to a microcentrifuge tube containing 200 μL of isopropanol and 200 μL of high salt solution (0.8 M trisodium citrate and 1.2 M sodium chloride). The mixture was centrifuged under the same conditions for RNA precipitation. The RNA pellet was washed twice with 75 % ethanol and dried before it was suspended in 50 μL of RNase-free water.

RT-qPCR reactions were conducted according to the rules that have been proposed to guarantee reproducible and accurate measurements (Udvardi et al., 2008). RT-qPCR runs were performed in 96-well blocks of the Applied Biosystems 7500 Real-time PCR System with the SYBR Green I master mix in a volume of 20 μL. The two-step thermal cycling profile system employed was 15 s at 95ºC for denaturation and 1 min at 60-65ºC, depending on the calculated melting temperatures of PCR primers, for annealing and polymerization. The primers used are listed in Table 1. For internal control, an *eIF4A* gene (*At3g13920*) was used in each PCR reaction for normalization. All RT-qPCR reactions were performed in biological

triplicates using total RNA samples extracted separately from three independent plant materials that were grown under identical conditions. The comparative $\Delta\Delta C_T$ method was employed to evaluate relative quantities of each amplified product in the samples. The threshold cycle (C_T) was automatically determined for each reaction by the system set with default parameters.

RNA sequencing

Plants were grown on MS-phytagel media in plastic culture boxes at 22°C under LDs for 2 weeks. They were grown in the dark for 2 days to ensure complete phytochrome decay, and either the shoots or the roots were exposed to light or left in the dark for 1 additional day. The roots of the light-treated plants were harvested for total RNA extraction. Total RNA was extracted as described above. The RNA samples were then subjected to RNA-sequencing in Chunlab, Inc. (Seoul, Korea). Genes with P value < 0.15 and fold change ≥ 4 were regarded as differentially expressed genes. Gene ontology (GO) analysis was performed using the Biological Networks Gene Ontology tool (BiNGO) with Benjamini & Hochberg corrected P < 0.01. The network diagram shows significantly overrepresented GO terms.

Micrografting

Seedlings were grown on MS-agar plates for 4 days under short days (8-h light and 16-h dark) at 22°C before grafting. Grafting was performed as

described previously (Marsch-Martinez et al., 2013). Grafted plants were grown on MS-agar plates containing 0.5% sucrose for 1 week at 22ºC under LDs before appropriate assays.

Fluorescence imaging

The 35S:*PHYB-GFP* and 35S:*HY5-GFP* transgenic plants were grown in soil for 2-5 weeks at 22ºC under LDs. Root parts located approximately 4 cm below the soil surface were subjected to fluorescence imaging using a Carl Zeiss LSM710 confocal microscope (Carl Zeiss, Jena, Germany).

To examine the effects of growth hormones and sucrose on the subcellular localization and relative accumulation of phyB and HY5 in root cells, three-week-old plants were grown for 2 days in the dark and transferred to liquid MS culture containing either 100 mM sucrose, 100 μM methyl jasmonic acid, or 100 μM indol-3-acetic acid in the dark for 1 day before fluorescence imaging.

To investigate whether root phyB is activated under physiological light-dark periods, plants were grown in the dark for 16 h, and the shoots were exposed to light before fluorescence imaging of the root cells.

For FR-rich light illumination, the roots of 3-week-old plants grown in soil were grown in the dark for 48 h and exposed to FR-rich light with a R:FR ratio of 0.01 and a fluence rate of 15 μmol $m^{-2}s^{-1}$ provided by LED lamp (PARUS, Cheonan, Korea).

Immunoblot assay

Plants were grown in soil for 3-5 weeks. The root parts located approximately 4 cm below the soil surface were harvested for the extraction of total proteins. The root samples were ground in liquid nitrogen and mixed with protein extraction buffer (100 mM Tris-Cl, pH 6.8, 4% sodium dodecyl sulfate, 0.2% bromophenol blue, 20% glycerol, and 200 mM β-mercaptoethanol). The mixtures were incubated at 90ºC for 10 min and then centrifuged at 16,000 X g for 10 min. The supernatants were mixed with equal volumes of 2 X SDS-PAGE loading buffer and analyzed on 8% SDS-PAGE gel before transferring to polyvinylidene difluoride membrane. Anti-HY5 and anti-GFP antibodies (Santa Cruz Biotechnology, Dallas, Texas) were used for the immunological detection of HY5 and HY5-GFP proteins, respectively.

Histochemical staining

For β-glucuronidase (GUS) histochemical staining, a GUS-coding sequence was transcriptionally fused to the promoter sequences consisting of approximately 2 kbp upstream of the translational start sites of *PHYA*, *PHYB*, and *CRY2* genes. The constructs were transformed into Col-0 plants. Transgenic plants were grown on MS-agar plates at 22ºC for 2 weeks under LDs. They were then incubated in X-Gluc solution for 16 h at 37ºC in the dark (Jung et al., 2014).

Light transmission assay

Six-week-old Col-0 plants grown at 22ºC under LDs were used for light transmission assays. Light input was provided by fiber-coupled white light source (Thorlabs, Newton, NJ; Cat No. SLS201/M). Water-absorbed stem or stem-root segments were vertically oriented on coverslip. White light was applied into the upper part of the stem or stem-root segments using fiber optic cannula (Thorlabs; Cat No. CFM12L05). The stem-fiber junction was sealed with black paper tape to block light leakage. To obtain transmission spectra, transmitted light was measured with a confocal Raman spectrometer (Andor Technology, Belfast, UK; Shamrock 500i, monochromator, focal length = 50 cm) equipped with high NA objective lens (Olympus, Tokyo, Japan; M Plan Apochromat, 100x, 1.4 NA), which was connected to homemade EM-CCD-camera (Andor Technology, iXon3 897). As a negative control, the stem or stem-root segments were sealed with black paper tape to block light transmission. To enhance the signal-to-noise ratio, 1,000 spectra were sampled during light irradiation and averaged. Exposure time for each spectrum is 0.2 s.

Primers	Sequences	Usage
eIF4A-F	5'-TGACCACACAGTCTCTGCAA	RT-qPCR
eIF4A-R	5'-ACCAGGGAGACTTGTTGGAC	"
HY5-F	5'-TCGGAAAAGAAACTTCCGGT	"
HY5-R	5'-TCCCTCGCTTCCTTTGACTT	"
CHS-F	5'-ACATGCATCTGACGGAGGAA	"
CHS-R	5'-GCTTAGGGACTTCGACCAC	"
PHR1-F	5'-TTTGAAGGGAGCTTGGGAGT	"
PHR1-R	5'-CATGAAACCGTGCATTTTCC	"
PHYA-F	5'-ACAATGGCCAGTCATGCAGT	"
PHYA-R	5'-ACATCTCCAAATCCAAGGGC	"
PHYB-F	5'-TTGCATGCTAAAGGGTCCTG	"
PHYB-R	5'-TAACCCGCTTGTTTGCAGTC	"
CRY1-F	5'-AGCAGCGGAAGGAGAGAAAG	"
CRY1-R	5'-TTTGTGAAAGCCGTCTCCAG	"
CRY2-F	5'-GGTCTCCAGGATGGAGCAAT	"
CRY2-R	5'-GGCACACTGGAAAACGTGTC	"
PHOT1-F	5'-ACTGAAGGGGCCAAAGAAAA	"
PHOT1-R	5'-TTCATCGCTCTCCGATTTTG	"
PHOT2-F	5'-GCCAGACACCGACAAGAATG	"
PHOT2-R	5'-CCTGCATCCCAATGAACTTG	"

Table 1. Primers used in Chapter 1.

F, forward primer, R, reverse primer.

RESULTS

Shoot light influences gene expression in the roots

In an initial effort to understand the signaling link between light and root growth, I used genome-wide gene expression profiling using Arabidopsis plants under assay conditions that mimicked the natural root growth environment, in which roots remain in the dark. Either the shoots or the roots of dark-pretreated, wild-type Columbia (Col-0) *Arabidopsis* plants were exposed to light, and the roots of the light-treated plants were harvested for RNA sequencing analysis. Compared to transcripts in the roots of dark-treated plants, 988 transcripts differentially accumulated in the roots of root-illuminated plants (801 increased and 187 decreased) and 690 transcripts were differentially expressed in the roots of shoot-illuminated plants (606 increased and 84 decreased) (Fig. 1A).

Among the differentially expressed genes, 198 genes were regulated by both shoot-light and root-light conditions (Fig. 1B). Of these, 166 transcripts increased in abundance and 29 decreased under both conditions. The remaining three transcripts increased in abundance under shoot-light conditions but decreased under root-light conditions. These data suggest that aboveground light plays a role in regulating root gene expression, even when roots are not directly exposed to light. GO analysis revealed that the co-regulated root genes include those involved in various metabolic

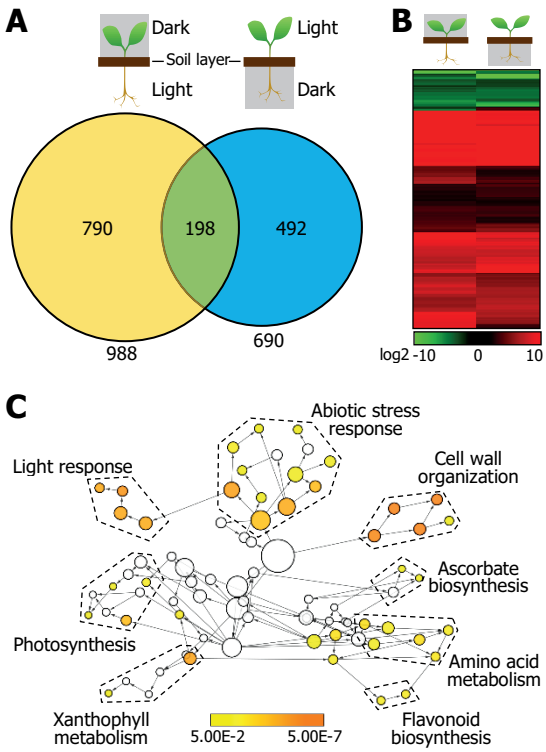

Fig. 1. Shoot light influences gene expression in the roots.

Two-week-old Col-0 plants grown on MS-phytagel media were grown in the dark for 2 d. Either the shoots or the roots were e exposed to light for 1 d, and total RNA was extracted from the roots for RNA sequencing. Biological triplicates were averaged.

(**A**) The Venn diagram of differentially expressed root genes.

(**B**) Heat map of co-regulated root genes by light treatments. Scale bar indicates fold changes ($\log_2$ values).

(**C**) GO analysis of differentially expressed root genes under both shoot-light and root-light conditions. Colored nodes in the network diagram represent significantly overrepresented GO terms (Benjamini & Hochberg corrected $P < 0.01$). Colored bar indicates P-values.

pathways, abiotic stress responses, and light responses (Fig. 1C). I was interested in the co-regulated root genes that are involved in light responses, in particular the gene encoding positive photomorphogenic regulator HY5, which plays a central role in plant photomorphogenesis (Cluis et al., 2004; Lee et al., 2007), and its direct target genes *CHALCONE SYNTHASE* (*CHS*) and *PHOTOLYASE* 1 (*PHR1*) (Lee et al., 2007; Castells et al., 2010).

Root phyB is required for shoot light–mediated gene regulation in roots

Photoreceptor genes are known to be expressed in the roots (Salisbury et al., 2007; Sharrock and Clack, 2002). Quantitative reverse transcription polymerase chain reaction (qRT-PCR) assays revealed that the abundance of *PHYA*, *PHYB*, and *CRY2* transcripts in root tissues was comparable to that found in shoot tissues (Fig. 2). The induction of HY5 and its target genes in the root under shoot-light conditions was largely suppressed in *phyb-9* plants (Fig. 3), indicating that phyB is primarily responsible for the induction of these genes in the root under these conditions.

Light-induced activation of phyB promotes HY5 activity at both the transcriptional and protein levels during shoot photomorphogenesis (Lee et al., 2007; Osterlund et al., 2000). Therefore, I asked whether the induction of HY5 in the root under shoot-light conditions was mediated by shoot phyB or root phyB. I performed micrografting experiments using Col-0 and

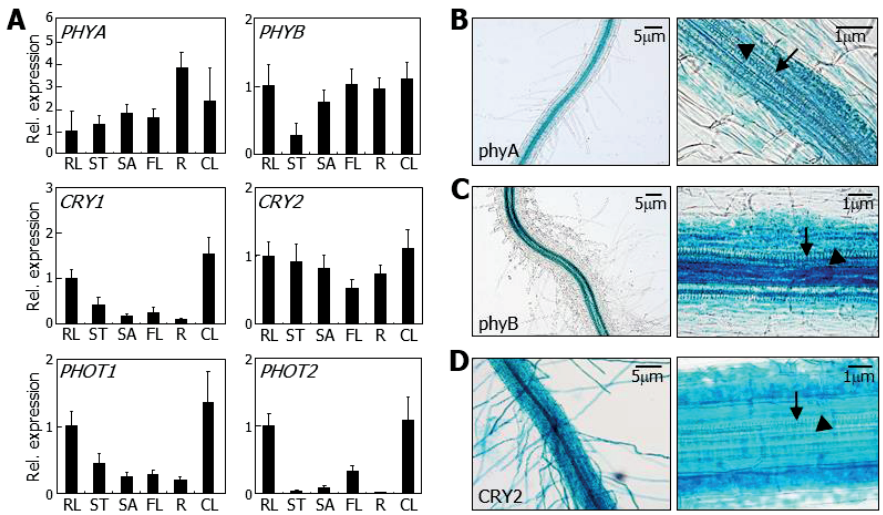

Fig. 2. Gene expression of photoreceptors in the roots.

(**A**) Transcript accumulation of photoreceptor genes. Col-0 plants were grown in soil at 23ºC under LDs until flowering. Plants were dissected into different organs for total RNA extraction. Transcript levels were examined by reverse transcription-mediated quantitative real-time PCR (RT-qPCR). Biological triplicates were averaged. Bars indicate standard error of the mean (SEM). RL, rosette leaf; ST, stem; SA, shoot apex; FL, flower; R, root; CL, cauline leaf.

(**B**, **C** and **D**) Histological detection of photoreceptor gene expression in root tissues. A b-glucuronidase (GUS)-coding sequence was fused in-frame to the 3' ends of the promoter sequences of approximately 2 kbp upstream of the translational start site of *PHYA* (B), *PHYB* (C), and *CRY2* (D), and the gene fusions were transformed into Col-0 plants. Transgenic plants were grown for 2 weeks on MS-agar plates before GUS staining. Arrows indicate protoxylem elements, and arrowheads indicate metaxylem elements.

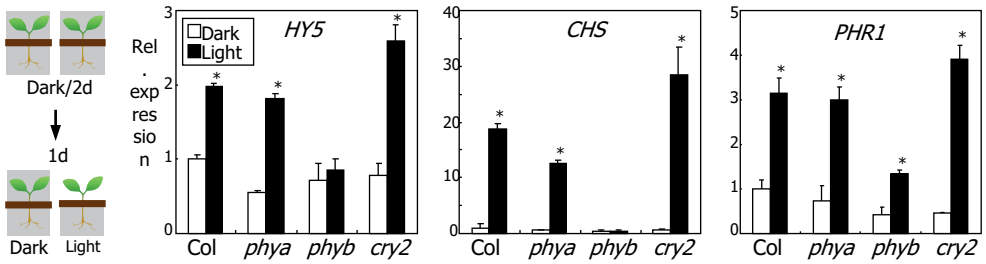

Fig. 3. Root phyB underlies the light-mediated induction of root genes.

Root gene expression in photoreceptor mutants. Two-week-old plants were exposed to light as illustrated. Transcript levels were examined by RT-qPCR. Biological triplicates were averaged. Statistical significance was determined by Student *t*-test (*$P < 0.01$)

phyb-9 plants and illuminated only the shoots of the grated plants. Grafting *phyb-9* mutant shoots onto Col-0 roots did not affect the expression of HY5 and HY5 target genes in the root, whereas grafting Col-0 shoots onto *phyb-9* roots significantly suppressed the expression of HY5 and HY5 target genes in the root (Fig. 4). These results indicate that root phyB is important for shoot light–induced root gene expression. It has been reported that shoot HY5 protein is moved to the roots, where it induces its own transcription and modulates nitrogen uptake (Chen et al., 2016). It is apparent that HY5 function in the roots is mediated by two distinct pathways: one by shoot HY5 and the other by root phyB.

A constitutively active form of phyB containing a Tyr-to-Val substitution at amino acid position 303 (hereafter phyB^{YVB}) has been reported to exhibit light-independent signaling activity in transgenic plants (Jeong et al., 2016). I performed grafting experiments with wild-type L*er* plants and phyB^{YVB} transgenic plants. Grafted plants were grown in the dark before harvesting root samples. As expected, expression of HY5 and HY5 target genes was greater in grafted plants with phyB^{YVB} roots than in those with phyB^{YVB} shoots (Fig. 5). In addition, shoot light triggered the nuclear import of phyB fused to green fluorescent protein (phyB-GFP) in root cells (Fig. 6 and Fig. 7). These observations indicate that root phyB mediates the induction of genes in the root in response to shoot light.

To examine whether the activation of root phyB occurs under physiological light-dark cycling, I grew plants in the dark for 16 hr and then

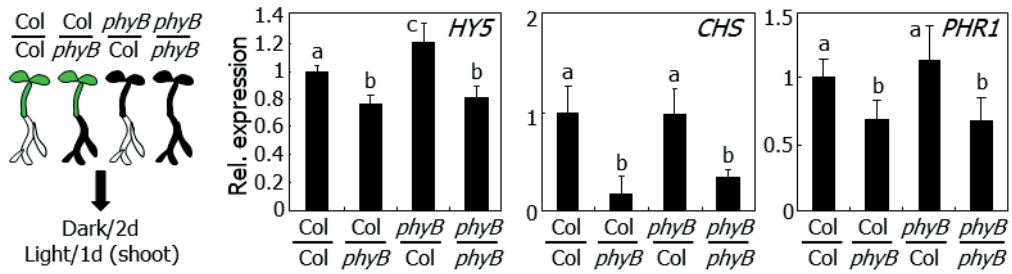

Fig. 4. Root gene expression in grafted plants between Col-0 and *phyb* plants.

Grafted plants were incubated under long days for 1 week and transferred to soil. Two-week-old plants were grown in the dark for 2 d to ensure complete phytochrome decay before exposing the shoots to light for 1 d. Different letters represent a significant difference ($P < 0.05$) determined by one-way analysis of variance (ANOVA) with *post hoc* Tukey test. Bars indicate SEM.

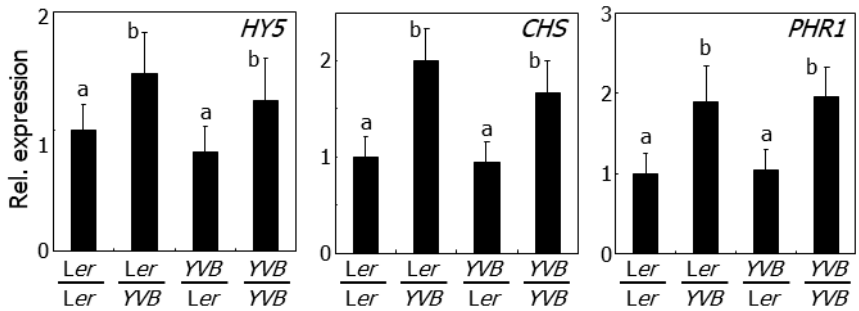

Fig. 5. Root gene expression in grafted plants between L*er* and *YVB* plants.

YVB plants have constitutively active phyB. Grafted plants were grown as described in Fig. 4. After dark treatments, plants were incubated in the dark for 1 d. Different letters represent a significant difference ($P < 0.05$) determined by one-way ANOVA with *post hoc* Tukey test. Bars indicate SEM.

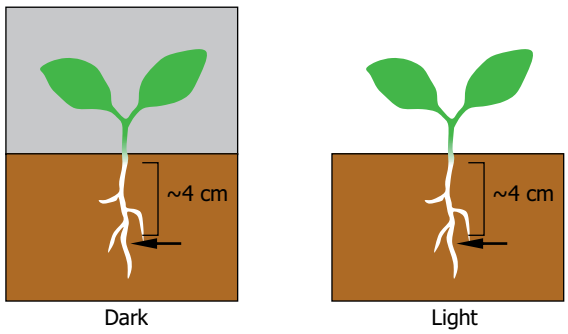

Fig. 6. Plant growth for fluorescence imaging of phyB and HY5 distribution in root tissues.

Two-week-old 35S:*PHYB-GFP* and 35S:*HY5-GFP* plants grown in soil were grown in the dark for 2 days. The shoots of the dark-grown plants were either left in the dark or exposed to light for 1 day. The root parts growing approximately 4 cm below the soil surface, as marked by arrows, were subjected to fluorescence imaging. I assume that the root parts used are not directly exposed to light through the soil layer under these growth conditions.

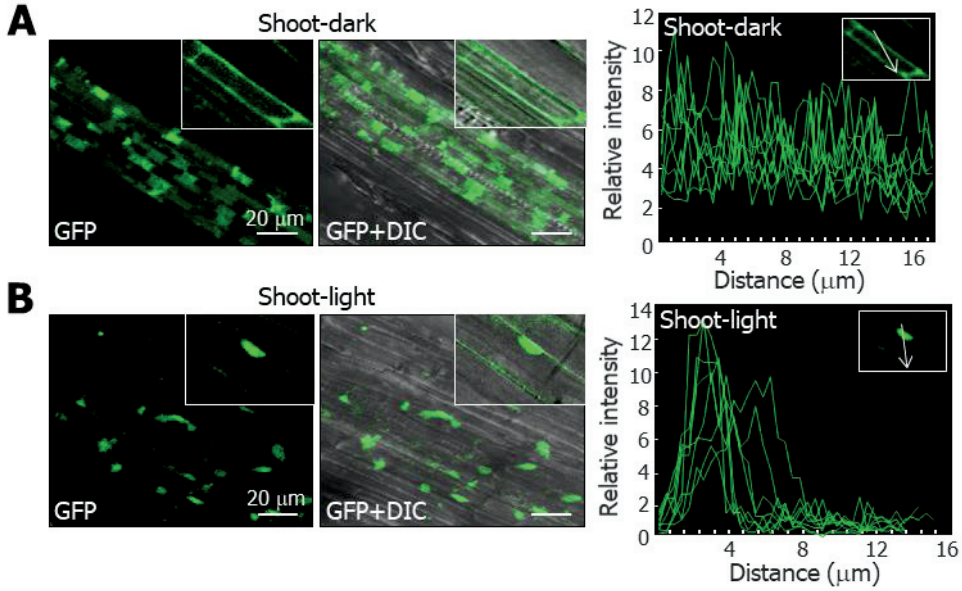

Fig. 7. Effects of shoot light on the nuclear localization of root phyB.

Two-week-old 35S:*PHYB-GFP* plants were grown in the dark for 2 d. Then, the shoots were either left in the dark (A) or exposed to light (B) for 1 d before fluorescence microscopy in root cells. DIC, differential interference contrast. Insets are enlarged views of representative single cells. Fluorescence intensities were measured across ten single cells during the distances of ~16 mm (Jung et al., 2014), as indicated by arrows in insets.

exposed only the shoots to light. I found that the nuclear import of phyB-GFP in the root initiated within 2 hr of exposure to light, reaching a peak nuclear accumulation within 4 hr after illumination (Fig. 8). Similarly, the expression of genes downstream of HY5 was rapidly induced within 4 hr under identical conditions (Fig. 9), consistent with the hypothesis that root phyB is activated by shoot light. Meanwhile, the expression of HY5 was not affected by shoot light under the assay conditions, suggesting that root HY5 protein is stabilized by root phyB-perceived light signals but not originated from the shoots during the early light response.

Root phyB mediates HY5 stabilization during root development

It is well known that phyB-mediated light signals stabilize the HY5 protein during plant photomorphogenesis (Osterlund et al., 2000). I therefore investigated whether root phyB contributes to the stabilization of HY5 in the roots of plants expressing *HY5* fused to GFP (HY5-GFP). In the roots under shoot-light conditions, shoot light enhanced the stability of root HY5-GFP (Fig. 10). Western blot analysis revealed that the abundance of root HY5 increased under shoot-light conditions (Fig. 11). However, the abundance of HY5 did not increase in the *phyb-9* mutant under identical assay conditions, consistent with a role for phyB in the accumulation of HY5 in the root.

Shoot light activated root phyB to stabilize HY5 in root cells. HY5 is known to be involved in primary and lateral root formation and root gravitropism (Oyama et al., 1997; Hardtke et al., 2000; Ang et al., 1998). A

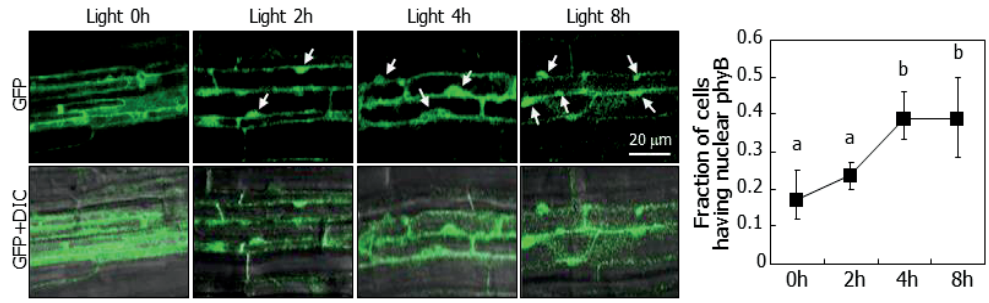

Fig. 8. Nuclear localization of root phyB by shoot light.

Two-week-old 35S:*PHYB-GFP* plants were grown in the dark for 16 h. The shoots were then exposed to light for up to 8 h before fluorescence microscopy in root cells. Arrows indicate nuclei. Fraction of root cells exhibiting nuclear phyB was measured (lower left panel). Four measurements, each with 15~25 root cells, were averaged and statistically treated. Different letters represent a significant difference ($P < 0.05$) determined by one-way ANOVA with *post hoc* Tukey test. Bars indicate SEM.

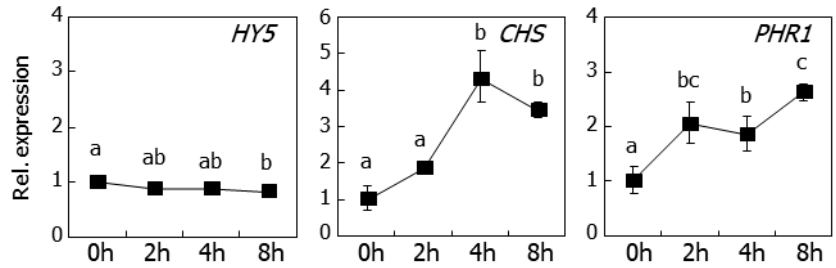

Fig. 9. Expression kinetics of *HY5* and its downstream genes in root cells.

Col-0 plants were treated as described in Fig. 8. Root samples were harvested for total RNA extraction. Transcript levels were examined by RT-qPCR. Biological triplicates were averaged. Different letters represent a significant difference ($P < 0.05$) determined by one-way ANOVA with *post hoc* Tukey test. Bars indicate SEM.

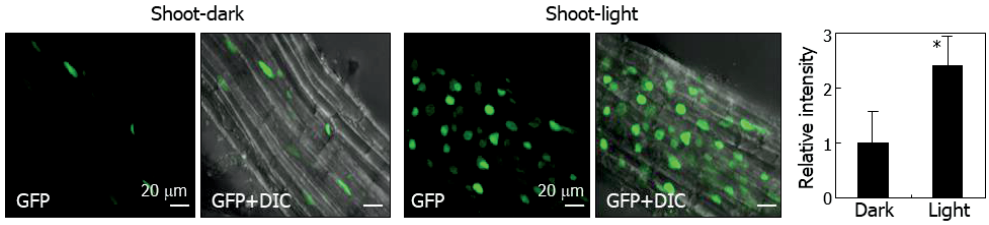

Fig. 10. Shoot light stabilizes root HY5 via phyB during root development.

Effects of shoot light on root HY5 stability. Two-week-old transgenic plants overexpressing a *HY5-GFP* fusion were grown in the dark for 2 d. The shoots were either left in the dark (left panel) or exposed to light (middle panel) for 1 d before fluorescence microscopy in root cells. Relative fluorescence intensities were averaged and statistically analyzed (*t*-test, $*P < 0.01$, $n = 10$) (right panel).

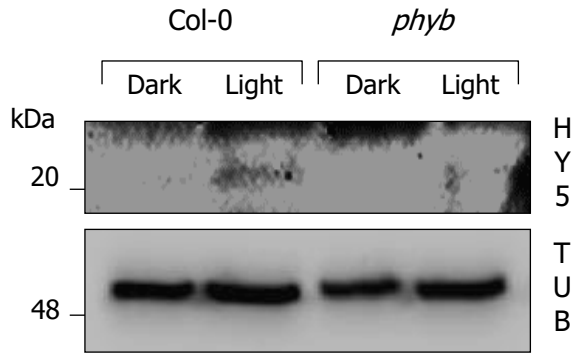

Fig. 11. Effects of shoot light on root HY5 stability in *phyb* mutant.

Three-week-old plants were treated with light as described above. The roots were harvested for western blot assays using an anti-HY5 antibody. Immunological detection of α-tubulin (TUB) was performed for protein quality control.

series of micrografting experiments between Col-0 plants and *hy5-221* plants revealed that primary root growth was impaired in grafted plants with *hy5-221* roots (Fig. 12). In addition, root gravitropism was also reduced in the grafted plants with *hy5-221* roots (Fig. 13), whereas lateral root formation was not affected by the *hy5* mutation in the root under my assay conditions (Fig. 14). These observations indicate that stabilization of HY5 by shoot light–activated phyB shapes root architecture.

I next analyzed the root morphology of *hy5-221* plants grown under shoot-light conditions, which mimicked the natural root growth environment. The mutant exhibited impaired root gravitropism (Fig. 15). However, primary root growth of the mutant was normal under identical assay conditions (Fig. 16). These observations indicate that the root phyB-HY5 module mediates shoot-sensed light signaling in root architecture with a primary role in root gravitropism among the root phenotypes examined.

Stem-piped light activates root phyB

A remaining question was how shoot light activated root phyB and stabilized HY5. I first investigated whether downstream mediators of light-induced signaling activate root phyB and HY5. Indole-3-acetic acid (IAA), methyl jasmonic acid (MeJA), and sucrose are among the molecules that are known to travel through plant tissues to mediate responses to light (Salisbury et al., 2007; Kircher and Schopfer, 2012; Suzuki et al., 2011). Treating dark-grown plants with any of these compounds did not influence

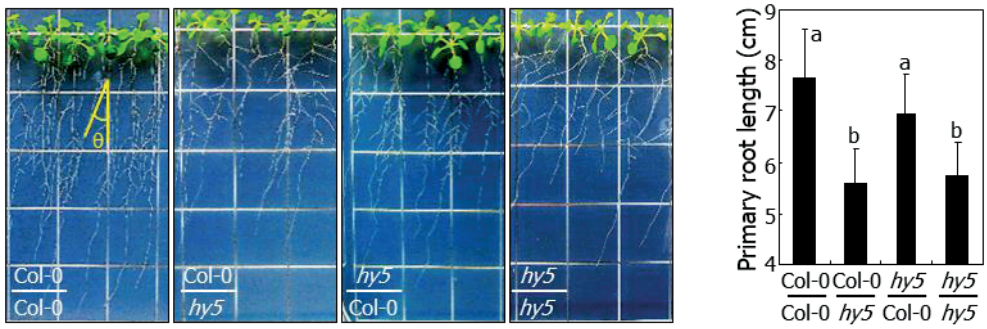

Fig. 12. Root phenotypes of grafted plants between Col-0 and *hy5* plants. Grafted plants were grown for 2 weeks on vertical plates containing 0.5 % sucrose. q, lateral root angle. Primary root lengths of ~20 grafted plants in were averaged. Different letters represent a significant difference ($P < 0.05$) determined by one-way ANOVA with *post hoc* Tukey test. Bars indicate SEM.

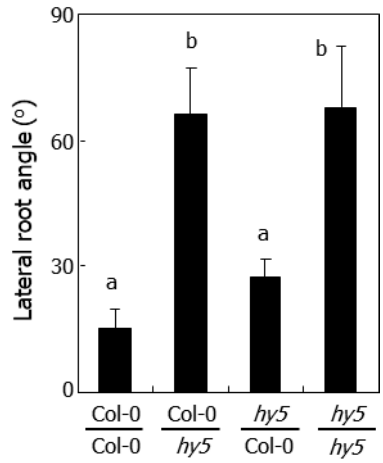

Fig. 13. Lateral root angle in grafted plants.

q values of ~20 grafted plants in Fig. 12 were averaged. Different letters represent a significant difference ($P < 0.01$) determined by one-way ANOVA with *post hoc* Tukey test. Longest lateral roots were used for q measurements. Bars indicate SEM.

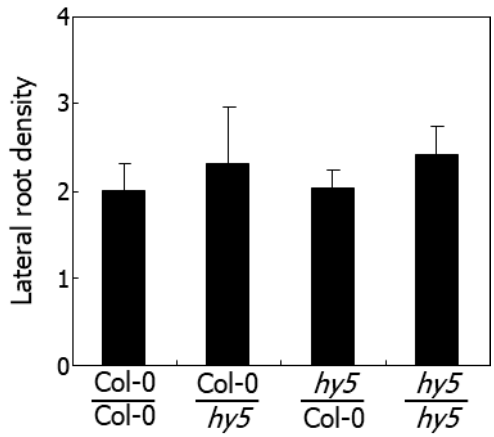

Fig. 14. Lateral root formation in grafted plants between Col-0 and *hy5* plants.

Four-day-old plants grown on MS-agar plates were used for micrografting experiments. Grafted plants were incubated under LDs for 2 weeks on vertical MS-agar plates containing 0.5% sucrose. Lateral root density (lateral root number/cm) was calculated by dividing total lateral root number by primary root length. Fifteen measurements were averaged. Bars indicate SEM. Note that lateral root density is not discernibly affected by the *hy5* mutation.

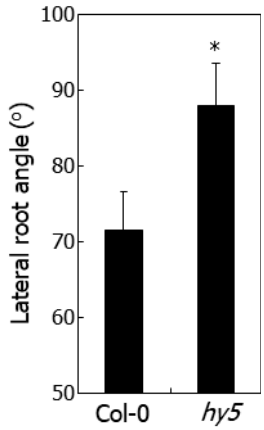

Fig. 15. Lateral root angle in *hy5* mutant.

Plants were grown for 2 weeks in plastic culture boxes containing MS-phytagel with the surface covered with a 3-mm soil layer. The lower part of the culture box was sealed with aluminum foil, ensuring that only the shoots are exposed to light. q was measured as described in Fig. 13. Roots of 4~7 plants were measured and statistically analyzed (*t*-test, $*P < 0.01$). Bars indicate SEM.

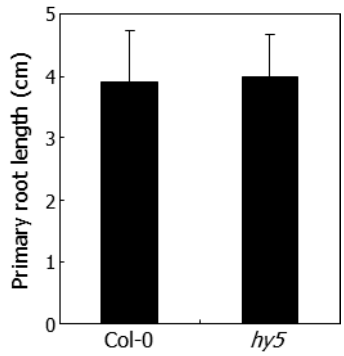

Fig. 16. Primary root growth of soil-grown *hy5* mutant.

Plants were grown in soil for 2 weeks under LDs before measuring primary root lengths. Fifteen measurements were averaged. Bars indicate SEM. Note that primary root growth is not affected by the *hy5* mutation when grown in soil.

the nuclear import of phyB and the stability of HY5 in root cells (Fig. 17), demonstrating that these mobile signals did not induce the photoactivation of phyB and HY5 in the root.

Another possibility was that shoot light was directly transduced through the stems to the roots (Sun et al., 2003; Sun et al., 2005). Using optical methods to investigate whether light is transduced through the plant body (Fig. 18), I used white light source in the B to near-infrared (B–nearIR) spectral range (400 to 1000 nm) with a peak at 700 nm (Fig. 19). I found that light in the R to near-infrared (R–nearIR) spectral range (670 to 1000 nm) was efficiently conducted through segments of tissue including both stem and root tissues with a peak conductance at 750 nm (Fig. 19 and Fig. 20, A and B). Light in the green-to-red (G–R) light spectral range (500 to 670 nm) was also conducted through the stem, although much less efficiently than light of longer wavelengths. Light transmission assays using a source emitting a different spectrum of light showed that light in a G–R spectral range was efficiently transmitted through stem-root segments (Fig. 21). Measurements of the fluence rates of light transmitted through stem-root segments with varying lengths revealed that the intensity of light wavelengths in a spectral range of 450 to 700 nm was more rapidly reduced compared to light of longer wavelengths (Fig. 22), which is likely due to the absorption of B and R light by chlorophyll.

To determine whether activation of phyB in the roots of shootilluminated plants could be the result of light penetrating the soil to

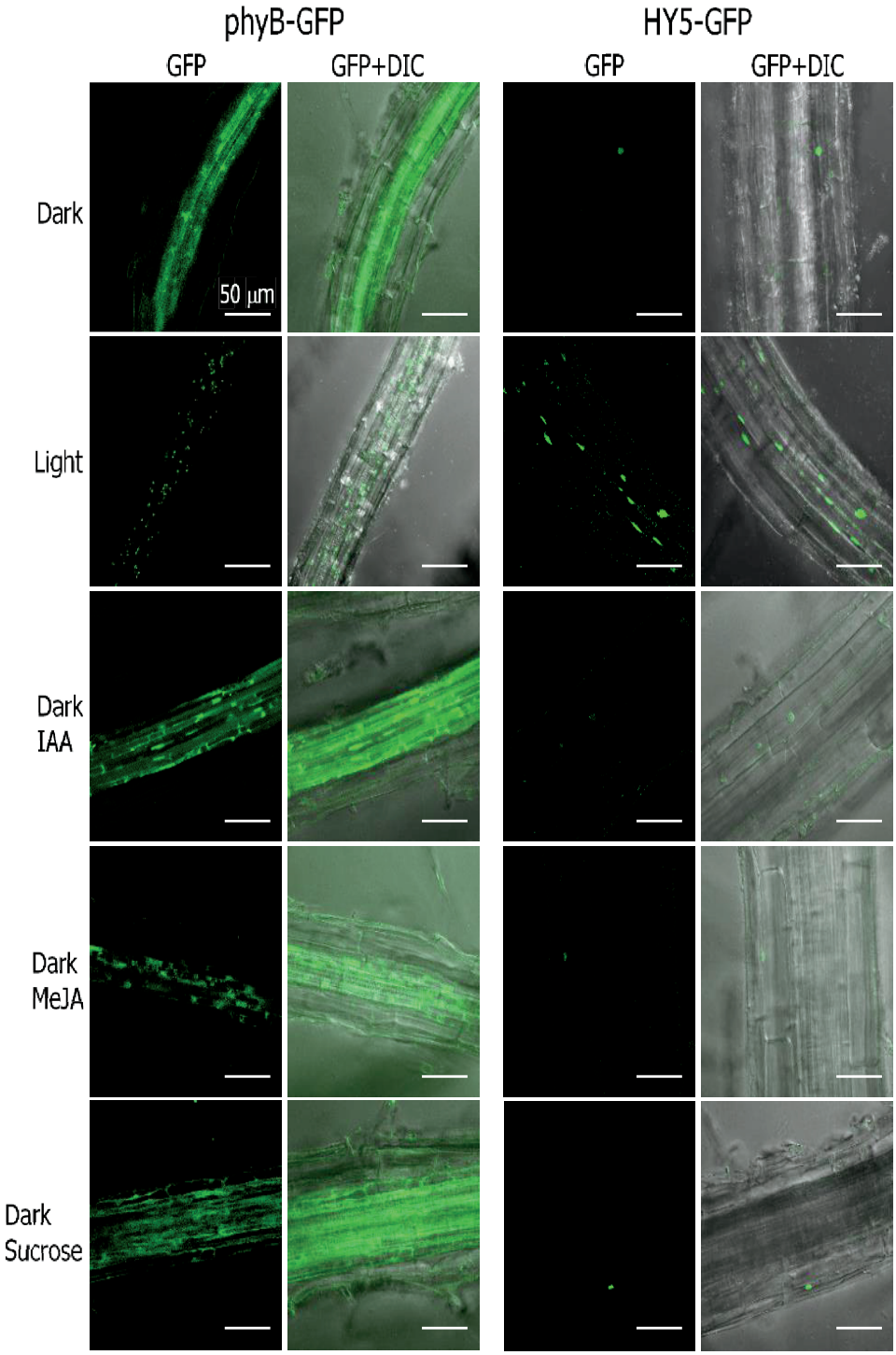
phyB-GFP
HY5-GFP
GFP
GFP+DIC
GFP
GFP+DIC
Dark
50 μm
Light
Dark
IAA
Dark
MeJA
Dark
Sucrose

Fig. 17. Effects of growth hormones and sucrose on the nuclear import of phyB and the HY5 stability in root cells.

Three-week-old 35S:*PHYB-GFP* and 35S:*HY5-GFP* transgenic plants grown in soil were grown in complete darkness for 2 days. The dark-treated plants were transferred to liquid MS cultures containing either 100 mM IAA, 100 mM MeJA, or 100 mM sucrose and incubated in the dark for 1 day. For light and dark treatments, the dark-treated plants were transferred to liquid MS cultures and grown either in the light or in the dark for 1 day. GFP signals in root cells were visualized by differential interference contrast (DIC) and fluorescence microscopy. Scale bars, 50 mm. Note that none of the tested chemicals influenced the subcellular distribution of phyB and the HY5 stability.

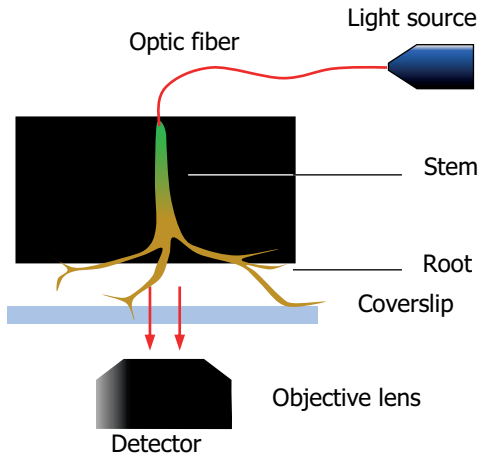

Fig. 18. Light transmission through stem-root segments.

Stem or stem-root segments of ~3.5 cm were prepared from six-week-old Col-0 plants. Schematic diagram of optical experiments is illustrated.

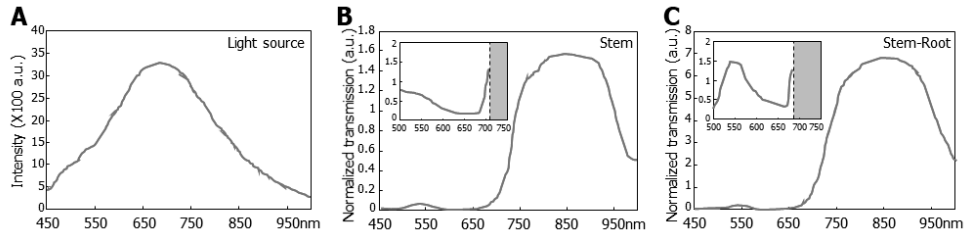

Fig. 19. Normalized light transmission through stem and stem-root segments.

Stem and stem-root segments of ~3.5 cm were prepared from six-week-old Col-0 plants grown in soil for light transmission assays.

(**A**) Spectrum of light source. Intensity of light source was measured in a range from 450 nm to 1000 nm for the normalization of transmitted light through stem and stem-root segments. a.u., arbitrary unit.

(**B** and **C**) Normalized light transmission. Intensity of transmitted light through stem (B) and stem-root (C) segments was divided by the intensity of light source in the wavelength range examined in (A). Insets are amplified light spectra from 500 nm to 750 nm. Gray boxes indicate measurement saturation.

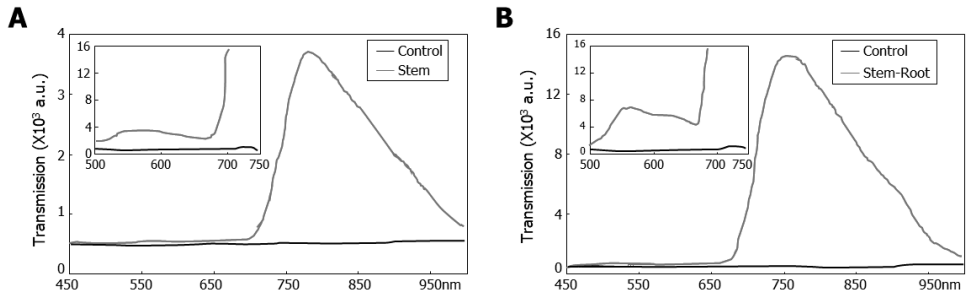

Fig. 20. Light transmission through stem or stem-root segments.

Stem or stem-root segments of ~3.5 cm were prepared from six-week-old Col-0 plants. Stem or stem-root segments were examined, respectively. Insets are amplified light spectra from 500 to 750 nm. a.u., arbitrary unit.

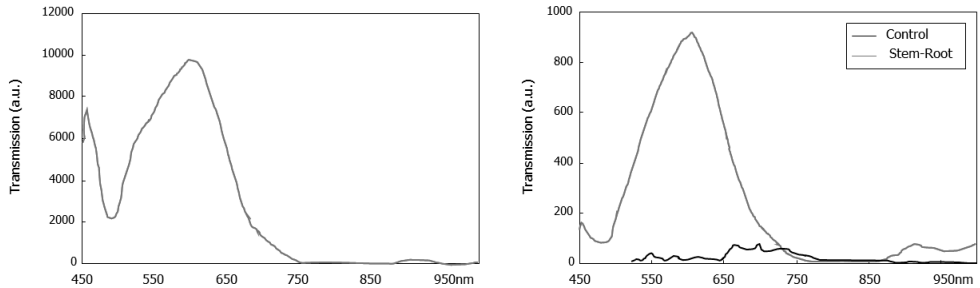

Fig. 21. Transmission of light with different spectral compositions through stem-root segments.

Light transmission assays were performed using stem-root segments of ~3.5 cm prepared from six-week-old Col-0 plants grown in soil. Fiber-coupled-warm white light source (Thorlabs, Cat No. MWWHF2), which emits light mostly in the green-to-red wavelength range (left panel), was applied into the upper end of stem-root segments. It is evident that the green-to-red light is efficiently transmitted through stem-root segments (right panel).

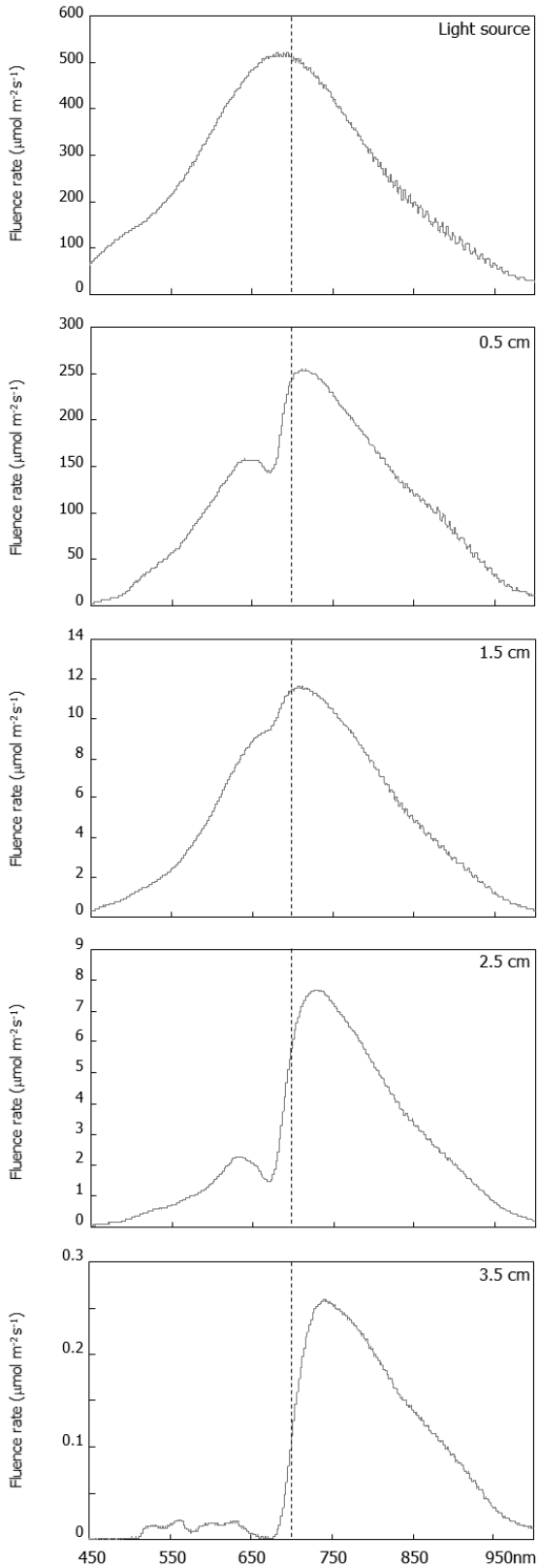
Light source
0.5 cm
1.5 cm
2.5 cm
3.5 cm
Fluence rate (μmol m-2s-1)
450
550
650
750
850
950nm

Fig. 22. Fluence rates and spectral composition of stem-piped light.

Stem-root segments with varying lengths (0.5 to 3.5 cm) were prepared from six-week-old Col-0 plants. Fluence rates were measured in a range from 450 nm to 1000 nm. Dotted lines denote 700 nm. Note that both fluence rates and spectral compositions of stem-piped light are affected by the different path lengths of light transmission. It is evident that the transmission of light with wavelengths of <700 nm is more rapidly reduced compared to that of light with longer wavelengths.

impinge on the roots, I completely blocked light transmission through the soil layer by covering the soil surface with aluminum foil and covering the foil with fine soil particles up to 3 mm in depth (Fig. 23). Root phyB-GFP was nuclearly localized in these plants, as observed in light-grown plants (Fig. 24). The abundance of HY5-GFP protein in the root also increased in the soil-blocked plants (Fig. 25) in response to shoot illumination, excluding the possibility that stabilization of HY5 is dependent upon light that penetrates the soil. Consistent with the activation of phyB and HY5 in the root by stem-piped light, the expression of *HY5* and HY5 target genes was increased in the soil-blocked plants, which is similar to what I observed in light-grown plants (Fig. 26).

To verify that the observed light responses of the roots are mediated by stem-piped light, I removed the shoots of soil-grown plants and then subjected the remaining roots to one of three different treatments: I took the remaining roots out of the soil and exposed them to light, left the remaining roots in the soil in the dark, or covered the soil surface with an additional layer of fine soil particles to a depth of 3mmand left the covered roots in the light (Fig. 27). Whereas the nuclear import of root phyB was stimulated when the amputated roots were exposed to light, it was not stimulated in roots maintained in the dark or in roots covered in soil after amputation of the shoot (Fig. 28). Similarly, HY5 stability in the soil-covered roots was not increased as observed in dark-treated roots (Fig. 29), indicating that there was no leak of light during my assays.

Fig. 23. Plant growth under soil light-block conditions.

Plants were grown in soil under LDs. After dark growth for 2 days, the plant pots harboring five-week-old plants were either exposed to light (left pot) or left in the dark (middle pot) for 1 day. For the soil-light block, the soil surface was covered with aluminum foil, and the foil was covered with fine soil particles (~3 cm in depth) to completely block light transmission through the soil layer and prevent direct contact between leaves and foil before exposing plants to light (right pot).

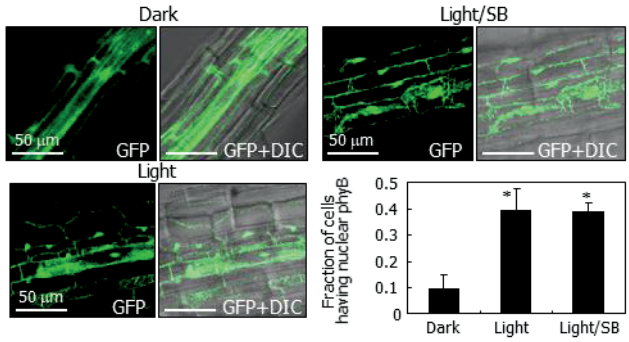

Fig. 24. Effects of stem-piped light on the nuclear localization of root phyB.

The 35S:*PHYB-GFP* plants were grown in soil for 5 weeks. The soil surface was covered with fine soil particles (~3 cm in thickness) and aluminum foil, termed soil light block (SB). After dark exposure for 2 d, the shoots were either left in the dark or exposed to light for 1 d before fluorescence microscopy. Fraction of root cells exhibiting nuclear phyB was measured as described in Fig. 3A. Four measurements were averaged and statistically analyzed (*t*-test, $*P < 0.01$). Bars indicate SEM.

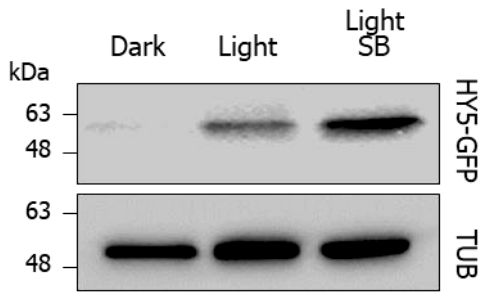

Fig. 25. Effects of shoot illumination on root HY5 stability

Five-week-old 35S:*HY5-GFP* plants were treated as described in Fig. 24. Total proteins were extracted from the roots for western blot analysis using an anti-GFP antibody.

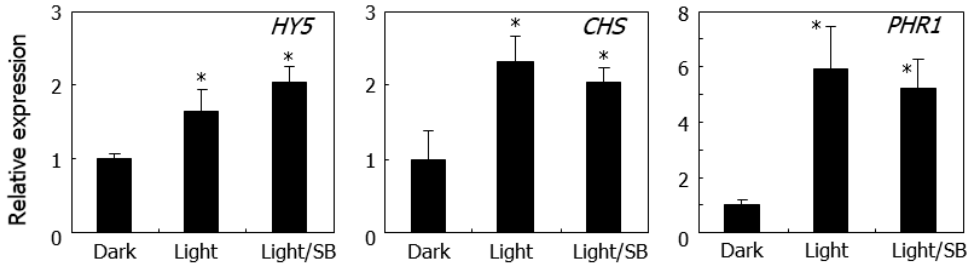

Fig. 26. Transcript accumulation of *HY5* and its targets in root cells.

Five-week-old Col-0 plants were treated as described in Fig. 24. Total RNA was extracted from the roots for RT-qPCR. Biological triplicates were averaged and statistically analyzed (*t*-test, $*P < 0.01$). Bars indicate SEM.

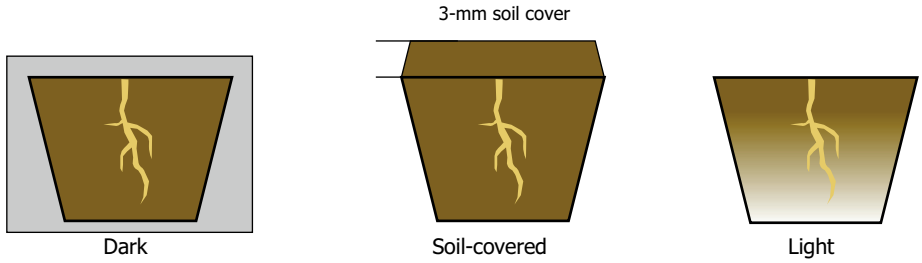

Fig. 27. Experimental evaluation of the soil-cover treatments.

Three-week-old 35S:*PHYB-GFP* and 35S:*HY5-GFP* plants grown in soil were grown in the dark for 2 days. The shoot scions were removed, and the root stocks were either exposed to light (Light) or covered with either a 3-mm depth of fine soil particles (Soil-covered) or aluminum foil (Dark).

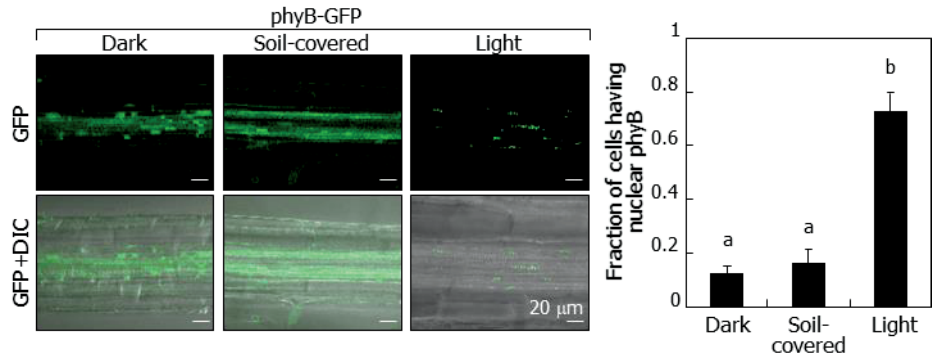

Fig. 28. GFP signals in the root cells of 35S:*PHYB-GFP* plants.

GFP signals in the root cells of transgenic plants were visualized by DIC and fluorescence microscopy. Fraction of cells exhibiting nuclear phyB was measured. For measurements, each with ~25 root cells, were averaged and statistically treated. Different letters represent a significant difference ($P < 0.05$) determined by one-way ANOVA with *post hoc* Tukey test. Bars indicate SEM.

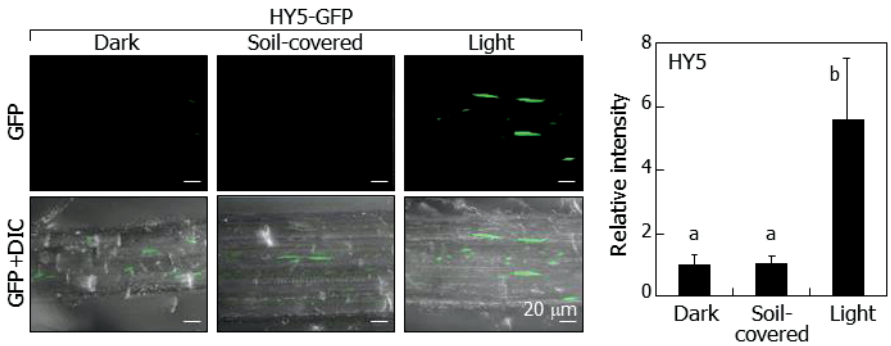

Fig. 29. GFP signals in the root cells of 35S:*HY5-GFP* plants.

GFP signals in the root cells of transgenic plants were visualized by DIC and fluorescence microscopy. Relative fluorescence intensities were averaged and statistically analyzed (n = 10). Different letters represent a significant difference ($P < 0.05$) determined by one-way ANOVA with *post hoc* Tukey test. Bars indicate SEM.

Aboveground light regulates root gravitropism through root phyB

Under low R-FR light conditions, the FR-absorbing form (P_{fr}) of phyB is converted to the physiologically inactive R-absorbing form (P_r) (Smith, 1982; Rensing et al., 2016). It has also been reported that phyB is translocated to the nucleus to trigger light responses during hypocotyl growth under FR-rich light conditions (Zheng et al., 2013). I found that the R/FR ratio of stem-piped light was relatively low (~0.01), raising the question as to whether or not the photon fluences and spectral compositions of the stem-piped light are sufficient to activate root phyB.

To directly test whether the spectrum of light that is piped through stems triggers light responses in the roots, I exposed roots to FR-rich light with an R/FR ratio of ~0.01, which is similar to the ratio observed in the stem-piped light (Fig. 30). Because total fluence of light is also important for phytochrome photoactivation (Casal et al., 1998), I calculated the total fluence of the stem-piped light in the assays. Under the light illumination conditions used (120 mmol m^{-2} s^{-1}), total fluences of the stem-piped light for 24 hr through stem-root segments of 3.5, 2.5, and 1.5 cm at 730 nm were about 5.5 × 103, 1.7 × 105, and 2.5 × 105 mmol m^{-2}, respectively. To irradiate generate total fluences similar to these light conditions, I exposed the roots to 15 mmol m^{-2} s^{-1} FR-rich light for 6 min, 3 hr, and 4 hr, which corresponds to 5.4 × 103, 1.62 × 105, and 2.16 × 105 mmol m^{-2}. PhyB-GFP rapidly translocated into nuclei after the FR-rich light treatment (Fig. 31). Whereas the nuclear import of phyB in roots of transgenic plants expressing

phyB-GFP was not evident 6 min after light treatments, most phyB was detected in the nuclei after 3-hour light treatments. Accumulation of HY5 protein was also initiated rapidly (<6min) after the FR-rich light exposure in Col-0 roots (Fig. 32). In contrast, HY5 accumulation occurred more slowly in *phyb-9* roots. These observations indicate that stem-piped light with a relatively low R/FR ratio efficiently activates phyB to induce HY5 accumulation in the roots (Fig. 33).

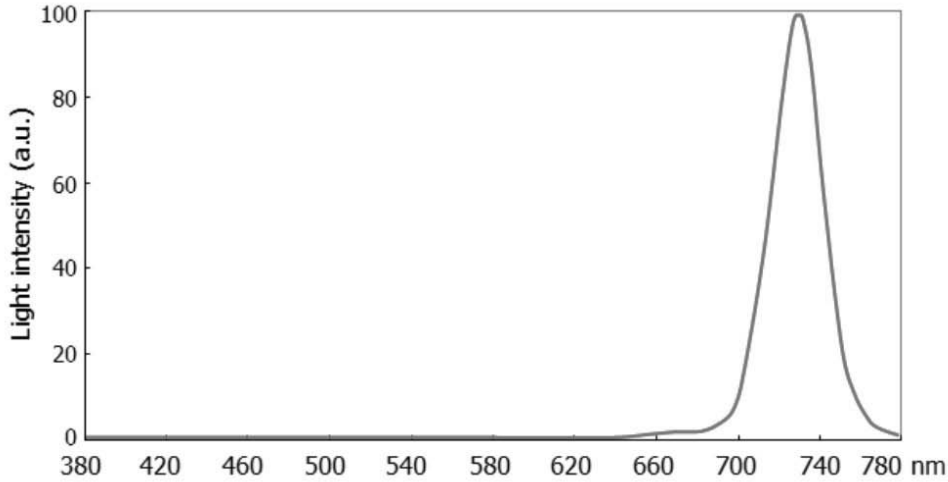

Fig. 30. Spectral composition of FR-rich light.

The spectral compositions of the FR-rich light source (Parus, Korea, Cat No. 111128-2) used in Fig. 31 were measured.

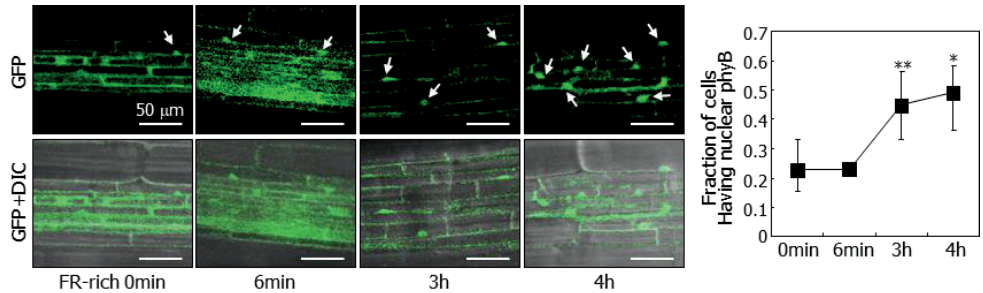

Fig. 31. Effects of FR-rich light on the nuclear localization of root phyB.

The roots of three-week-old 35S:*PHYB-GFP* plants were exposed to FR-rich light for up to 4 h before fluorescence microscopy. Fraction of root cells exhibiting nuclear phyB was measured. Four measurements were averaged and statistically analyzed (*t*-test, $*P < 0.01$, $**P < 0.05$). Bars indicate SEM.

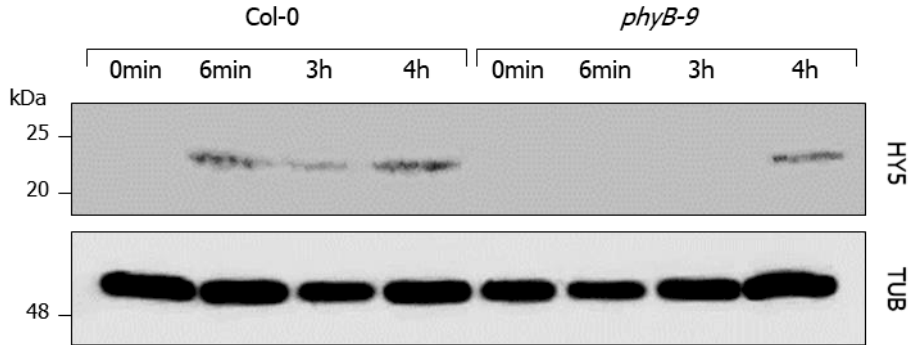

Fig. 32. Effects of FR-rich light on root HY5 stability.

The roots of three-week-old plants were exposed to FR-rich light for up to 4 h. Anti-HY5 and anti-tubulin antibodies were used for the immunodetection of endogenous HY5 and α-tubulin (TUB), respectively.

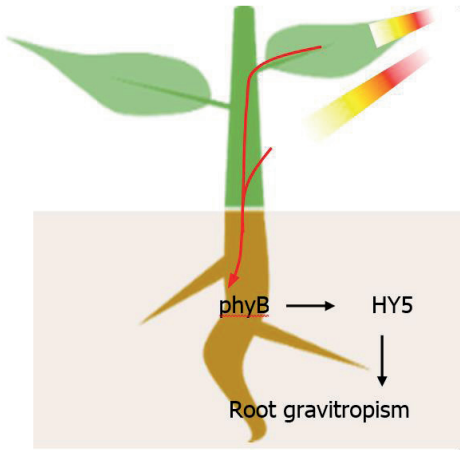

Fig. 33. Schematic diagram of stem-piped light signaling during root gravitropism.

DISCUSSION

It is widely documented that light influences a broad spectrum of root growth and developmental processes, including primary root growth and lateral root formation and patterning (Dyachok et al., 2011; Warnasooriya et al., 2011), and root responses to external stimuli, such as phototropic and gravitropic growth (Warnasooriya et al., 2011; Correll and Kiss, 2005). Photoreceptors and light-signaling molecules, such as auxin, jasmonic acid, and sucrose, have been proposed to play a role in the photoregulatory development of the root system (Salisbury et al., 2007; Kircher and Schopfer, 2014; Suzuki et al., 2011). However, most previous studies have been conducted using plants grown on agar medium, in which the roots are exposed to light during root growth assays. Therefore, how aboveground light influences the underground root system under natural conditions has not been explored.

Here, I used a plant culture system that mimics nature conditions, in which the roots of photomorphogenic mutants and grafted plants remain in the dark during root growth assays. My data show that in soil-grown Arabidopsis plants, aboveground light is efficiently transmitted through the stems to the roots and that this stem-piped light affects root architecture, and in root gravitropism in particular, through phyB-mediated stabilization of HY5 in the root. When grown on agar, the roots of a HY5-defective mutant

exhibited alterations in primary root growth and root gravitropism. In contrast, when grown in soil, root gravitropism was perturbed, but primary root growth was normal in the mutant. From these results, I infer that the activation of root phyB and HY5 by stem-piped light primarily plays a role in root gravitropism.

Together with previous reports on the roles of various signaling molecules and photoreceptors that influence root architecture (Dyachok et al., 2011; Warnasooriya et al., 2011; Correll and Kiss, 2005; Salisbury et al., 2007; Kircher and Schopfer, 2012; Suzuki et al., 2011), my data suggest that multiple light-signaling pathways downstream of different photoreceptors are involved in distinct aspects of root photomorphogenesis. It is also possible that the roots can directly sense aboveground light that is transmitted through the surface soil layer (Yakawa et al., 2015). The phyB-sensed light signals are most likely not mediated entirely by HY5, because several other signaling molecules are known to mediate light signaling downstream of multiple photomorphogenic processes (Salisbury et al., 2007; Kircher and Schopfer, 2012; Suzuki et al., 2011).

HY5 has been reported to be a mobile photomorphogenic regulator that is transported from the shoots to the roots, where it induces the expression of HY5 and NITRATE TRANSPORTER 2.1 to enhance nitrate uptake (Chen et al., 2016). It is thus likely that shoot light affects physiological and developmental processes in the roots through at least two distinct routes: one through the shoot-derived mobile HY5 and the other through the phyB-

mediated stabilization of HY5 in response to stem-piped light. It will be interesting to examine whether these two light-signaling pathways modulate distinct sets of physiological and developmental processes in the roots or regulate root processes in a coordinated manner.

I found that light in the FR–nearIR range was efficiently transmitted through the stems and roots, consistent with previous reports that examined light transmission through stem or root segments (Sun et al., 2003; Sun et al., 2005). Using sensitive light-detecting methods, I found that light in the G–R range is also transmitted through the stem and root segments, which is in contrast to the previous reports, in which it was reported that only FR light was transmitted through stems and root segments (Sun et al., 2003; Sun et al., 2005). Despite its lower transmission efficiency compared to that of FR light, light in this G–R wavelength range would be sufficient to activate phyB and possibly other photoreceptors in the roots, given the extremely high light sensitivity of these receptors (Schafer and Bowle, 2002; Taiz and Zeiger, 2010). In support of this, it has been observed that a small portion of phytochromes exists in the P_{fr} form even under low R-FR light conditions (Smith, 1982); this observation is consistent with the notion that at least a portion of root phyB is activated by stem-piped light of a relatively low R/FR ratio. The transmission of light in a broad wavelength range is also consistent with the notion that root architecture is modulated by multiple photoreceptors and light-signaling pathways.

Here, I demonstrated that stem-piped light activates root-localized phyB

and its target HY5 to modulate the development of the root system, particularly root gravitropism (Fig. 33). Sensing of stem-piped light by root phyB is part of the light adaptation mechanisms by which roots monitor fluctuations in the aboveground environment to optimize their growth and development under natural conditions. Although much more work is required to understand the molecular mechanisms underlying root photomorphogenesis, my findings provide a basis from which to continue the discovery of signaling molecules and pathways underlying root photomorphogenesis in plants.

ACKNOWLEDGEMENT

I thank H.J. Lee for helping this project. I also thank H. K. Choi and Z. H. Kim for performing light transmission assays. I appreciate Y. J. H and J. I. K for providing $phyB^{YVB}$ plants and discussing on biochemical activity of phyB.

CHAPTER 2

Shoot phytochrome B modulates root ROS homeostasis via abscisic acid signaling in *Arabidopsis*

INTRODUCTION

The root system is responsible for anchorage of plant body to the soil and mechanical support, absorption of water and nutrients, and storage of metabolites (Smith and De Smet, 2012). The roots also monitor changes in surrounding environments including water level, salinity, and light (Sun et al., 2008; Mo et al., 2015). Light influences virtually all aspect of root growth and developmental process. It has been reported that all photoreceptors are expressed in the roots and identified their specific function. For example, red/far-red photoreceptor phytochromes mediate primary root elongation, gravitropism, and hormone responses. In particular, phyB senses stem-piped light to modulate root growth and tropic responses (Lee et al., 2016a; Lee et al., 2016b). In addition, UV-B light also trigger root photomorphogenic development (Mo et al., 2015).

Moreover, shoot-to-root light signals through hormone and their signals also influence root growth and developmental processes. phyA and phyB regulates lateral root production by mediating shoot-to-root auxin transport (Salisbury et al., 2007). In *Lotus japonicas*, phyB regulates JA signaling that controls root nodulation (Suzuki et al., 2011). In addition, it has been identified that shoot-derived ABA promotes primary root growth in tomato and pea (McAdam et al., 2016).

On the other hand, direct light illumination is unfavorable to the roots in most cases. In nature, the roots normally reside darkness, however, they are often exposed to ambient light transmitted through small cracks of the soil layers, which occur under drought, heavy rain, wind, or high temperature conditions (Yokawa et al., 2014; Yokawa et al., 2016). The light-exposed roots produce ROS to promote root growth, allowing rapid escape of the roots from non-natural light illumination (Yokawa et al., 2014). Since prolonged exposure to light provoke ROS burst that cause photooxidative damages on cellular components in the roots, the levels of ROS should be tightly controlled. Yet, how plant roots control the levels of ROS under direct exposure to the light is largely unknown.

Here, I demonstrated that phyB facilitates induction of ABA biosynthesis genes in the shoot, and notably the shoot-derived ABA signals modulate ROS homeostasis through peroxidase-mediated ROS detoxification reaction in the roots. In *phyb* mutants, the contents of ABA hormone were declined, and ROS were highly accumulated, resulting in reduction of primary root growth. My finding indicated that ABA-mediated phyB signaling prevent ROS over-accumulation in the roots under unfavorable light conditions, contributing to the synchronization of shoot and root growth for optimal propagation and performance in plants.

MATERIALS AND METHODS

Plant materials and growth conditions

All *Arabidopsis thaliana* lines used were in this work were in Col-0 background except for L*er* background *phyb-5* mutant. The *phyb-9, phyb-5, aba1-6*, *per1-2* and *abi5-3* mutants have been described previously (Barrero et al., 2005; Lee et al., 2015; Jeong et al., 2016; Lee et al., 2016b).

Sterilized *Arabidopsis* seeds were cold-imbibed at 4°C for 3 days and germinate in a controlled growth chamber at 22°C with relative humidity of 60%. Plants were grown on 1/2 X Murashige and Skoog-agar (MS-agar) plates under long day conditions with white illumination (120 μmol $m^{-2}s^{-1}$) provided by FLR40D/A fluorescent tube (Orsram, Seoul, Korea). Seedlings grown for 3 days on horizontal MS-agar plates were transferred to vertical MS-agar (0.75%) plates and grew additional 10 days.

Analysis of gene transcript levels

Gene transcript levels were analyzed by RT-qPCR. The RT-qPCR reactions were performed according to the experimental guidelines that have been previously proposed (Udvardi et al., 2008). Total RNA samples were extracted from appropriate plant materials homogenized in liquid nitrogen with the TRIzol reagent (Invitrogen, Carsbad, CA). The suspension was centrifuged at 15,000 X g for 8 min at 4°C. The supernatant was mixed with

200 μl of chloroform, and the mixture was centrifuged under the same conditions. The aqueous part of the mixture was transferred to a fresh microcentrifuge tube and mixed with 200 μl of isopropanol and 200 μl of high salt solution containing 0.8 M trisodium citrate and 1.2 M sodium chloride. The RNA pellet was collected by centrifugation at 15,000 X g for 8 min at 4°C following incubation for 10 min at room temperature. The RNA pellet was rinsed with 80% ethanol and dissolved in triple-distilled water. The RNA sample was pretreated with RNase-free DNase to eliminate contaminating genomic DNA.

RT-qPCR reactions were conducted in 384-well plates with the Applied Biosystems QuantStudio 6 Flex Real-Time PCR System (Applied Biosystems, Foster City, CA) using 10 μl of SYBR Green I master mix. The entire PCR process has been described previously (Lee et al., 2016b). Primers used are listed in Table 1. An *eIF4A* gene (*At3g13920*) was included as internal control in the PCR reactions.

The PCR reactions were conducted in biological triplicates using total RNA samples prepared from three independent plant materials grown under the same conditions. The comparative $\Delta\Delta C_T$ method was employed to measure the levels of gene transcripts. The threshold cycle (C_T) value was calculated for each reaction by the process using default parameters.

Propidium iodide staining

Arabidopsis roots grown for two weeks were used for measurements. Roots were incubated in 10 mg / ml of propidium iodide solution (Sigma-Aldrich, St Louis, MO) for 5 min, and washed by water. Washed roots were mounted under a coverslip and detected by confocal microscope (LSM710, Carl Zeiss, Oberkochen, Germany).

Detection of ROS

The DAB staining solution (1 mg/ml) and H2DCFDA fluorescent staining solution (10 μM) were used for analyzing hydrogen peroxide and NBT staining solution (1 tablet / 50 ml) was used for superoxide detection. For DAB and NBT staining, the roots grown for two weeks on MS-agar plates in presence or absence of direct root illumination were incubated in each staining solution for 2 h at room temperature in complete darkness. The plant samples were de-stained by water and visualized by optical microscope (Olympus, Tokyo, Japan). The ImageJ system (http://rsb.info.nih.gov/ij/) was used for intensity quantification.

For H2DCFDA staining, roots grown for two weeks on MS-agar plates under LGs at 22ºC in presence or absence of direct root illumination were incubated in 10 μM of H2DCFDA staining solution for 20 min at room temperature. The roots were washed by water and used to measure fluorescent imaging by confocal microscope. The fluorescent intensity was quantified using ImageJ software.

Micrografting

Seedlings were grown vertically on MS-agar plates for 4 days under short days (8-h light and 16-h dark) at 22ºC prior to grafting experiments. Grafting was conducted as described previously (Marsch-Martinez et al., 2013; Lee et al., 2016b). Grafted plants were grown vertically on MS-agar plates with 0.5% sucrose for additional 2 weeks at 22ºC under LDs.

Immunoblot assay

The roots of two-week-old plants were harvested for the assays. Plant materials homogenized in liquid nitrogen were mixed with protein extraction buffer. The mixtures were boiled for 10 min before centrifugation at 15,000 X g for 15 min. The supernatants were loaded onto 10 % SDS-PAGE gel before transfer to polyvinylidene difluoride membrane. An anti-ABI5 antibody (ab98831; Abcam, Cambridge, UK) was used for the immunological detection of ABI5 proteins.

Hormone quantification

Seedlings were grown vertically on MS-agar plates for 10 days under LDs in presence of root-light. At least 50 mg of shoot and root samples were harvested for the extraction of hormones. Hormone quantification was performed as reported previously (Schäfer et al., 2016). Briefly, 50 mg of plant materials homogenized in liquid nitrogen was aliquoted into 96-well biotubes (Arctic White LLC, Bethlehem, PA) and closed with strips of 8-

plug caps (Arctic White LLC). For extraction, 800 µl of precooled (-20°C) acidified MeOH [MeOH:H_2O:HCOOH 15:4:1 (v:v:v)] was added to each sample containing the internal standards (for each sample 10 ng D4-ABA, 10 ng D6-JA, 10 ng D6-JAIle, 10 ng D6-SA and 1.5 ng D5-IAA). The tubes were sealed with a seal mate and incubated over night at -20°C. After incubation were homogenized, centrifuged and 600 ml of the supernatant was transferred to a new vial. Analysis was performed on a Bruker Elite EvoQ Triple quad-MS equipped with a heated electrospray ionization ion source. Samples were analyzed in multi-reaction-monitoring mode. Post-run analysis was done with the 'MS data Review' software of the 'Bruker MS Workstation' (Version: 8.1.2).

Growth hormone treatment

Seeds were germinated and grown on horizontal MS-agar plates for 3 days under LDs to synchronize germination. Three-day-old seedlings were transferred to vertical MS-agar plates containing various concentration of ABA and SA and further grown for 10 more days before measuring primary root lengths.

Primers	Sequences	Usage
ABA1-F	5'-GCGAACACGGAACCTATGTG	RT-qPCR
ABA1-R	5'-AAACTCGATGATGTCGGACG	"
ABA2-F	5'-CCAAGCATGCTGTTCTAGGC	"
ABA2-R	5'-TTAGTTGCAACCGCGTAAGG	"
ABA3-F	5'-CATAGCAGCCATCCGTCATG	"
ABA3-R	5'-TGACGTTGTGTGCATCCAAA	"
ABI5-F	5'-GGTGAGACTGCGGCTAGACA	"
ABI5-R	5'-GTTTTGGTTCGGGTTTGGAT	"
eif4a-F	5'-TGACCACACAGTCTCTGCAA	"
eif4a-R	5'-ACCAGGGAGACTTGTTGGAC	"
NCED2-F	5'-GCGGGCTATTTGGGTTAGTC	"
NCED2-R	5'-GCGGGCTATTTGGGTTAGTC	"
NCED5-F	5'-AACCGAGAGATTGGTTCAAGAG	"
NCED5-R	5'-CGATTCCAGAGTGACCATGTAG	"
NCED9-F	5'-GCGGGCTATTTGGGTTAGTC	"
NCED9-R	5'-CGGTAAATCGTCTTCGGACA	"
PER1-F	5'-CGTGCCCTTCATATTGTTGG	"
PER1-R	5'-GACGCCATCAACAACGAGTC	"

Table 2. Primers used in Chapter 2.

F, forward primer, R, reverse primer.

RESULTS

The primary root growth of *phyb* seedlings is sensitive to light

The red and far-red light-sensing phytochrome photoreceptors are known to modulate ROS production (Wei et al., 2008; Chai et al., 2015). They play a role in root development (Salisbury et al., 2007; Costigan et al., 2011). To investigate whether the phy photoreceptors are associated with the ROS-mediated promotion of root growth, I examined the root growth phenotypes of Arabidopsis mutants that are defective in either phyA or phyB. While the primary root growth of *phya* mutant seedlings was similar to that of wild-type Col-0 seedlings, it was significantly reduced in *phyb* mutant seedlings (Fig. 34). Anatomical analysis of the roots revealed that the reduced primary root growth of *phyb* seedlings is caused by a reduction of cell numbers in the meristematic zones (Fig. 35). A similar reduction of the primary root growth was also observed in L*er* plants lacking phyB (Fig. 36), supporting the functional linkage between phyB and primary root growth. Notably, the reduction of primary root growth did not occur when the roots were kept in darkness (Fig. 37). On the other hand, lateral root formation was suppressed in *phyb* seedlings both in the light and darkness, indicating that the phyB-mediated light response is associated specifically with the primary root growth.

The phyB photoreceptors exist in both the shoots and roots, where they

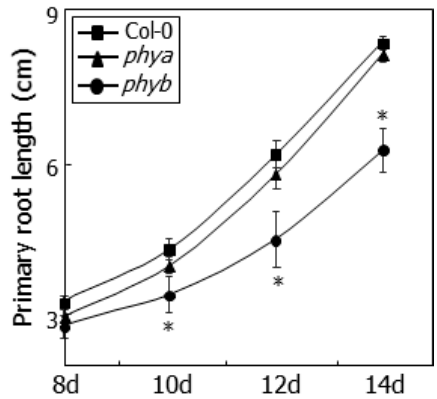

Fig. 34. The primary root growth of *phyb* seedlings.

Growth kinetics of *phya* and *phyb* primary roots. d, days after germination. fifteen measurements were statistically analyzed using Student *t*-test (*$P <$ 0.01). Bars indicate SEM.

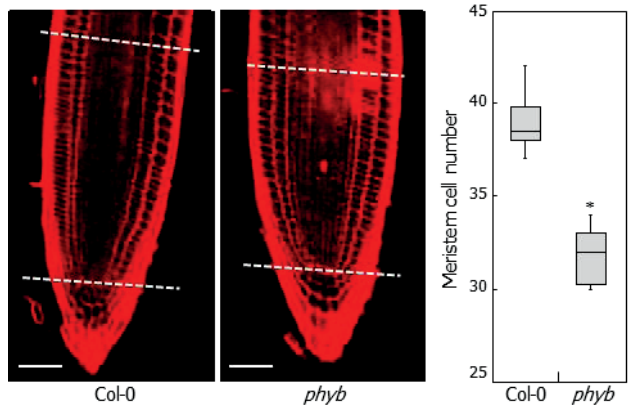

Fig. 35. Meristem cell numbers in *phyb* primary roots.

The roots of two-week-old seedlings were stained with propidium iodide. Dot lines mark the boundaries of elongation zones. Scale bars, 50 μm. Seven countings were statistically analyzed (*t*-test, $*P < 0.01$). Bars indicate SEM.

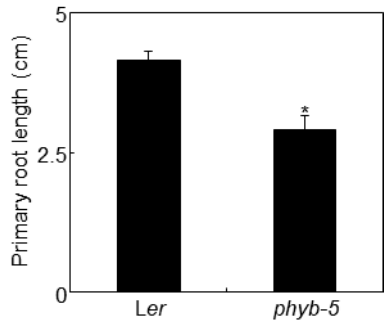

Figure 36. Primary root growth of *phyb-5* seedlings in the light.

Seedlings were grown on vertical MS-agar plates for two weeks with the roots exposed to light. Fifteen measurements were statistically analyzed using Student *t*-test (*$P < 0.01$). Bars indicate SEM. The *phyb-5* mutant in L*er* background has been described previously (Kim et al., 2008).

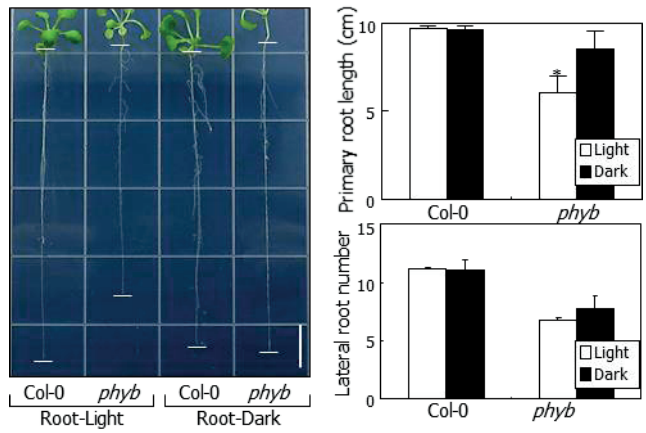

Fig. 37. Light sensitivity of *phyb* roots.

Primary root lengths and lateral root numbers of two-week-old seedlings were measured. Fifteen measurements were statistically analyzed using Student *t*-test (*$P < 0.01$). Scale bar, 1 cm.

play distinct roles (Lee et al., 2016b). To identify which phyB regulates primary root growth in the light, I performed grafting experiments using Col-0 and *phyb* seedlings. It was found that the reduction of primary root growth was observed in chimeric seedlings having the *phyb* scion but not in those having the Col-0 scion (Fig. 38). These observations indicate that shoot-localized phyB is important for the light-mediated regulation of primary root growth.

Shoot phyB suppresses ROS accumulation in the light-exposed roots

It is known that light-exposed roots produce low concentrations of ROS to promote primary root growth, which would help the roots rapidly escape from unfavorable light exposure (Yokawa et al., 2014; Yokawa et al., 2016). Meanwhile, high concentrations of ROS impose photooxidative stress on cellular components, causing physiological impairments and growth arrest (Tsukagoshi, 2016). I therefore anticipated that the growth reduction of the *phyb* primary roots under light conditions would be caused by ROS accumulation at high levels.

To confirm that ROS accumulation provokes the growth reduction of primary root growth in *phyb* mutants, I employed a chromogenic dye, 3,3′-diaminobenzidine (DAB), for hydrogen peroxide and a fluorogenic reagent, 2',7'-dichlorodihydrofluorescein diacetate (H2DCFDA), for the quantification of ROS intermediates in the primary roots (Mubarakshina et al., 2010; Tsukagoshi et al., 2010). The staining assays revealed that ROS

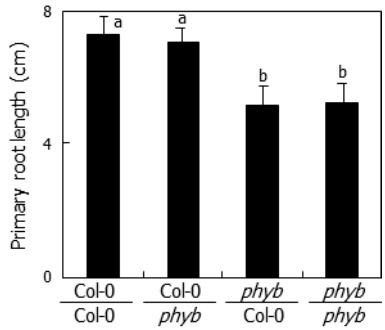

Fig. 38. Primary root growth of grafted seedlings between Col-0 plants and *phyb* mutant.

The grafted seedlings were grown for two weeks in the light before measurements. Different letters represent a significant difference ($P < 0.01$) determined by one-way ANOVA with *post hoc* Tukey test. Bars indicate SEM.

levels were similar in Col-0 and *phyb* roots when the roots were kept in darkness (Fig. 39, A and B). In contrast, when the roots were exposed to light, ROS levels were discernibly higher in the *phyb* roots than in Col-0 roots. Meanwhile, nitro blue tetrazolium (NBT) staining revealed that the levels of superoxide were similar in Col-0 and *phyb* roots regardless of light illumination (Fig. 40). Together with the reduced primary root growth in *phyb* seedlings (Fig. 37), these observations suggest that shoot phyB-mediated light signals suppress ROS accumulation in the roots under prolonged light exposure.

The phyB-mediated induction of ABA biosynthesis in the shoots is associated with root growth.

A critical question was how shoot phyB signals modulate primary root growth. It is known that phyB plays a role in the shoot-to-root transmission of diverse hormonal signals (Salisbury et al., 2007; Suzuki et al., 2011). Direct measurements of phytohormone contents showed that the levels of ABA were lower by more than 50% in the *phyb* shoots compared to those in Col-0 shoots (Fig. 41). In contrast, the ABA levels were similar in the roots of *phyb* and Col-0 seedlings. In addition, feeding with ABA in a physiological concentration range (0.1 μM - 1 μM) efficiently restored the reduced primary root growth (Fig. 42 and Fig. 43). These observations indicate that a shoot-derived ABA signaling mediator rather than ABA itself modulates the shoot phyB control

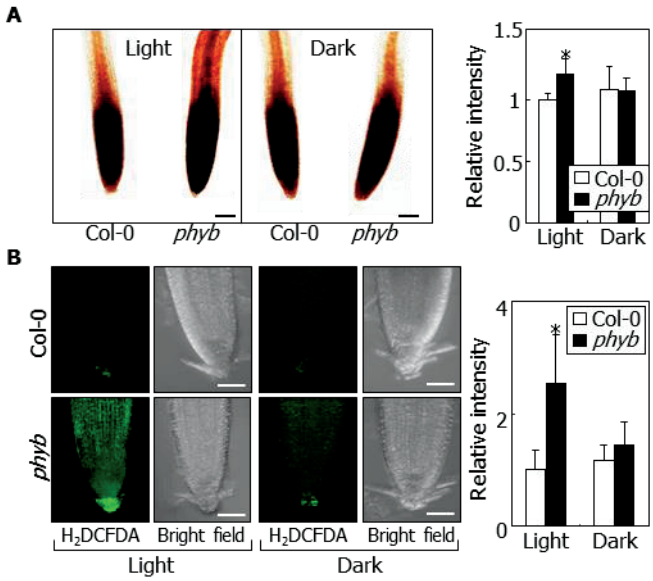

Fig. 39. **ROS levels are elevated in the light-exposed primary roots of *phyb* seedlings.**

In A, the roots of two-week-old seedlings grown on vertical MS-agar plates with the roots either exposed to light or kept in darkness were subjected to DAB staining for H_2O_2. Scale bars, 100 μm. Relative intensities were quantitated using the ImageJ software. Seven quantitation was statistically analyzed using Student *t*-test (*$P < 0.01$). Bars indicate SEM. In B, the root samples were subjected to confocal H_2DCFDA staining for ROS. Seven quantifications were statistically analyzed as described above. Scale bars, 50 μm.

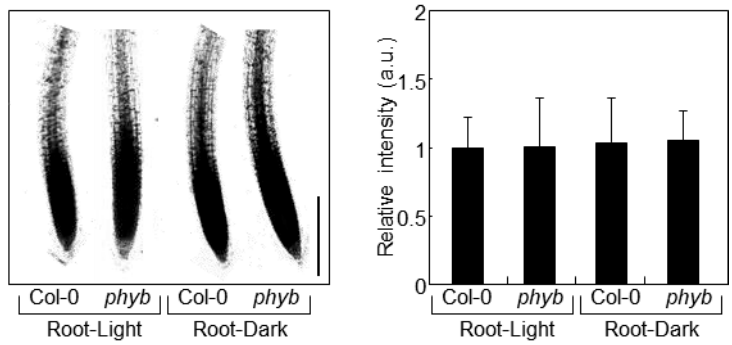

Fig. 40. NBT staining of *phyb* primary roots.

The roots of seedlings grown on vertical MS-agar plates for two weeks with the roots either exposed to light or kept in darkness were subjected to nitro blue tetrazolium NBT staining for superoxide radicles. Scale bar, 100μm. Relative intensities were quantified using the ImageJ software. Seven quantifications were statistically analyzed using Student *t*-test (*$P < 0.01$). Bars indicate SEM.

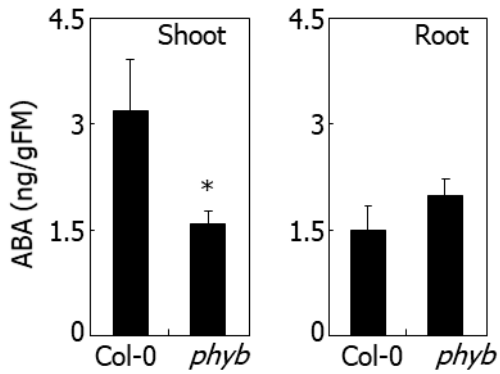

Fig. 41. Endogenous ABA contents.

Shoot and root samples were used for the measurements (n = 5). Seedlings were grown on vertical MS-agar plates for two weeks in the light. Measurements were statistically analyzed using Student t-test (*P < 0.01). Bars indicate SEM.

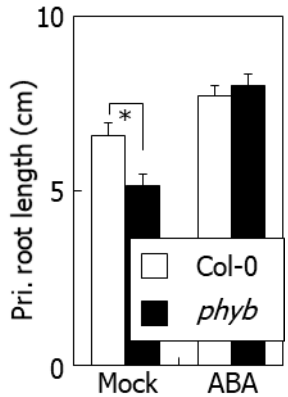

Fig. 42. Effects of ABA feeding on primary root growth.

Seedlings were grown in the presence of 1 μM ABA. Fifteen measurements were statistically analyzed. Measurements were statistically analyzed using Student *t*-test (*$P < 0.01$). Bars indicate SEM.

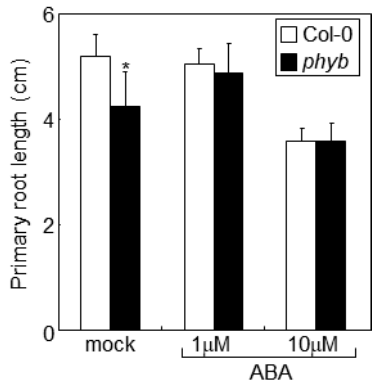

Fig. 43. Effects of different concentrations of ABA on primary root growth.

Seedlings were grown on vertical MS-agar plates in the presence of varying concentrations of ABA for two weeks in the light. Fifteen measurements were statistically analyzed using Student *t*-test (*$P < 0.01$). Bars indicate SEM.

of primary root growth. Notably, high concentrations of ABA (> 10 μM) inhibited primary root growth (Ghassemian et al., 2000) (Fig. 43), showing that ABA plays dose-dependent, contrasting roles in regulating primary root growth.

The levels of salicylic acid (SA) were also lower by ~50% in the *phyb* shoots (Fig. 44). However, SA feeding did not recover the reduced primary root growth of *phyb* seedlings (Fig. 45), indicating that SA is not related with the shoot phyB function in modulating primary root growth.

Consistent with the ABA feeding data, reverse transcription-mediated real-time PCR (RT-qPCR) assays revealed that the transcription of ABA biosynthetic genes, such as *ABA DEFICIENT* 1 (*ABA1*), *ABA2*, and *ABA3*, was reduced by ~60% in the *phyb* shoots (Fig. 46 and Fig. 47). In contrast, the transcript levels were not discernibly different in the roots, further supporting the notion that phyB signals promote ABA biosynthesis in the shoots. In conjunction with my data on ABA measurements and feeding assays, these observations strongly support that shoot phyB signals induce ABA biosynthesis and perhaps its signaling mediator in the shoots, which promote primary root growth when the roots are exposed to light.

Shoot phyB signals mediate root ROS homeostasis via ABA signaling

I next asked whether shoot ABA signals are associated with ROS accumulation in the roots. Histochemical staining assays with DAB and H2DCFDA revealed that treatments of the *phyb* roots with 1 μM ABA

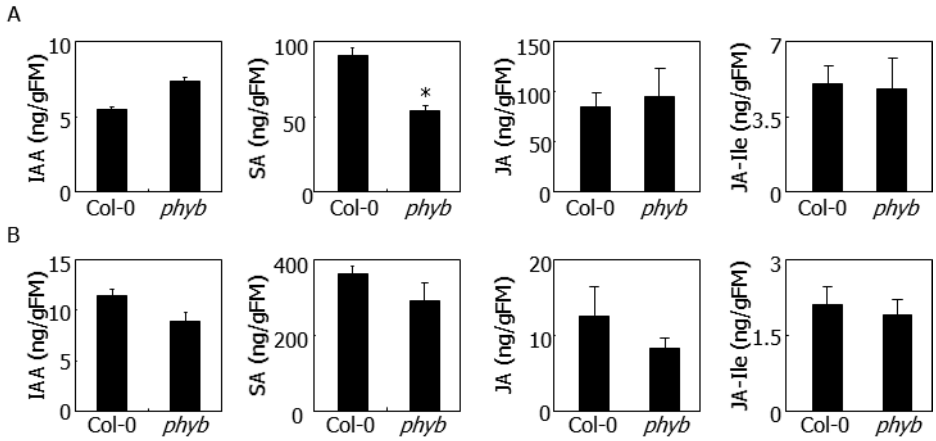

Fig. 44. Quantification of endogenous growth hormones in *phyb* seedlings.

The shoot and root samples (A, B, respectively) were prepared from two-week-old seedlings grown on MS-agar plates in the light. Five biologically independent samples were used for quantitation. Measurements were statistically analyzed using Student *t*-test (*$P < 0.01$). Bars indicate SEM.

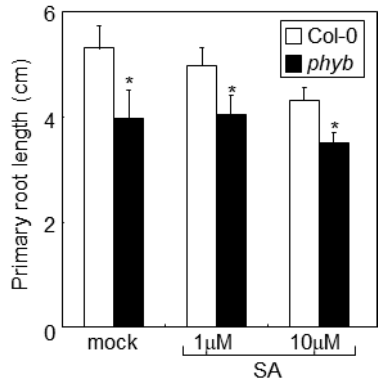

Fig. 45. Effects of SA on primary root growth.

Seedlings were grown on vertical MS-agar plates in the presence of varying concentrations of SA for two weeks in the light. Fifteen measurements were statistically analyzed using Student *t*-test (*$P < 0.01$). Bars indicate SEM.

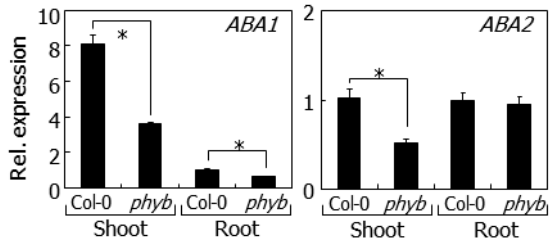

Fig. 46. Relative levels of *ABA1* and *ABA2* transcripts.

Total RNA was prepared from shoot and root samples. Transcript levels were analyzed by RT-qPCR. Biological triplicates were statistically analyzed. Bars indicate SEM.

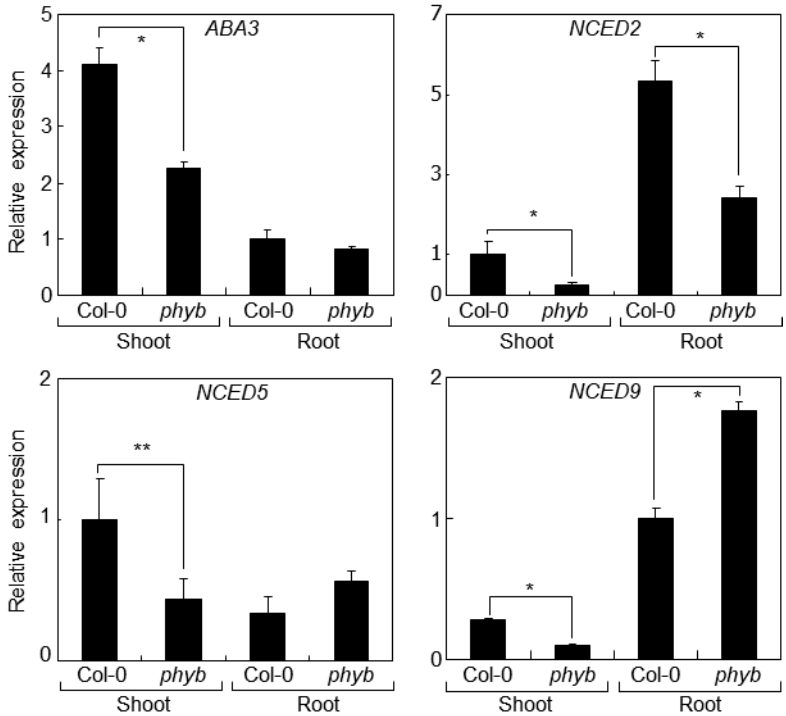

Fig. 47. Transcript levels of ABA biosynthesis genes in *phyb* seedlings.

Seedlings were grown for two weeks on vertical MS-agar plates in the light. Total RNA were prepared from the shoot and root samples. Transcript levels were examined by reverse transcription-mediated RT-qPCR. Biological triplicates were statistically analyzed (*t*-test, $*P < 0.01$, $**P < 0.05$). Bars indicate SEM.

attenuates the elevated contents of hydrogen peroxide to a level comparable to that in Col-0 roots (Fig. 48, A and B), showing that low concentration of ABA suppresses the accumulation of ROS in the roots. This is in contrast to the stimulation of ROS accumulation by high concentrations of ABA (Kwak et al., 2003; Böhmer and Schroeder, 2011).

Notably, a reduction of primary root growth was also observed in the ABA-defective *aba1-6* mutant in the light (Barrero et al., 2005), and the root phenotype was efficiently rescued by exogenous application of 1 μM ABA (Fig. 49), which were similar to what observed with the *phyb* mutant. Likewise, ROS levels were higher in the *aba1-6* roots than in Col-0 roots, but their levels were decreased to a level comparable to that in Col-0 roots in the presence of 1 μM ABA (Fig. 50, A and B). These observations further support the functional linkage between shoot phyB-mediated ABA accumulation and ROS metabolism in modulating primary root growth.

To investigate how shoot ABA signal detoxifies ROS accumulation in the roots, I examined the potential roles of ABA signaling mediators that modulate ROS detoxification in this signaling pathway. It has been reported that ABA induces the expression of *ABA INSENSITIVE 5* (*ABI5*) gene encoding a basic leucine zipper transcription factor that directly activates *PEROXIDASE1* (*PER1*) gene (Zhou et al., 2015; Lee et al., 2015), which encodes a hydrogen peroxidase that detoxifies ROS (Lee et al., 2015). RT-qPCR assays showed that the transcript levels of *ABI5* and *PER1* genes

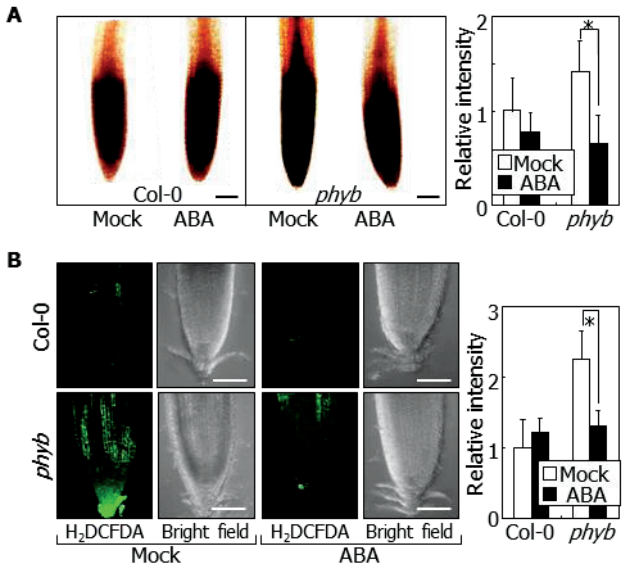

Fig. 48. ABA is associated with root ROS over-accumulation in *phyb* seedlings.

Seedlings were grown on vertical MS-agar plates for two weeks in the light. Measurements were statistically analyzed using Student *t*-test (*P < 0.01). Bars indicate SEM.

(**A** and **B**) Detection of ROS by DAB staining (A) and H2DCFDA staining (B) in *phyb* primary roots. Seedlings were fed with 1 μM ABA. Seven quantitation was statistically analyzed. Scale bars, 100 μm (A) and 50 μm (B).

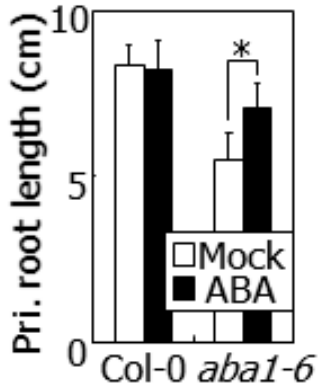

Fig. 49. The primary root phenotype of *aba1-6* seedlings.

Primary root length of *aba1-6* mutant. Primary root growth of *aba1-6* seedlings. Seedlings were grown in the presence of 1 μM ABA. Fifteen measurements were statistically analyzed. Measurements were statistically analyzed using Student *t*-test (*$P < 0.01$). Bars indicate SEM.

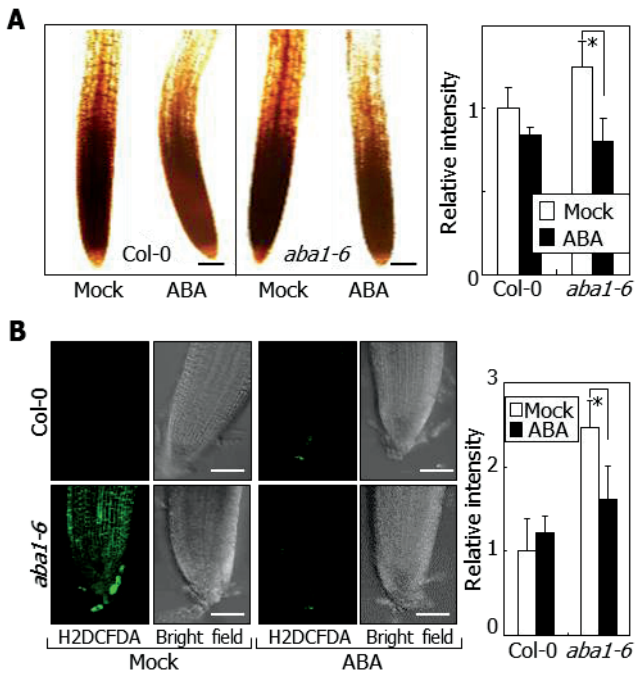

Fig. 50. Detection of ROS in *aba1-6* mutant.

ROS in the primary root tip were detected by DAB staining (A) and H_2DCFDA staining (B) in *aba1-6* mutants. At least five measurements were statistically averaged using Student *t*-test (*$P < 0.01$). Bars indicate SEM. Scale bars, 100 μm (B) and 50 μm (C).

were lower in the phyB roots with a more prominent reduction of the *PER1* transcripts compared to those in Col-0 roots (Fig. 51). However, the transcript levels of *ABI5* and *PER1* genes were similar in Col-0 and *phyb* roots when grown in the presence of 1μM ABA. It is known that ABA signals stabilize ABI5 proteins (Lopez-Molina et al., 2001; Seo et al., 2014). Immunoblot assays revealed that the levels of ABI5 proteins are significantly lower in the *phyb* roots but greatly elevated to a level comparable to those in Col-0 roots in the presence of 1μM ABA (Fig. 52 and Fig. 53). These observations indicate that ABA signals activate ABI5 both at the transcriptional and protein levels in the roots. Furthermore, the reduction of ABI5 and PER1 transcription and ABI5 abundance is consistent with the elevation of ROS in the *phyb* roots. Accordingly, ABI5-deficient *abi5-3* mutant and *PER1*-deficient *per1-2* mutant exhibited a reduced primary root growth in the light (Fig. 54 and Fig. 55). In addition, DAB staining and H2DCFDA fluorescent imaging revealed that ROS levels are higher in the mutant roots than in Col-0 roots (Fig. 56, A and B), further supporting the notion that ABA signals reduce ROS accumulation in the light-exposed roots.

Altogether, my findings describe a phyB-mediated light signal transduction pathway that involves a shoot-to-root ABA signaling. The shoot-derived ABA signals transcriptionally and post-transcriptionally elevate the abundance of ABI5 to activate *PER1* gene, leading to ROS detoxification in the roots (Fig. 57).

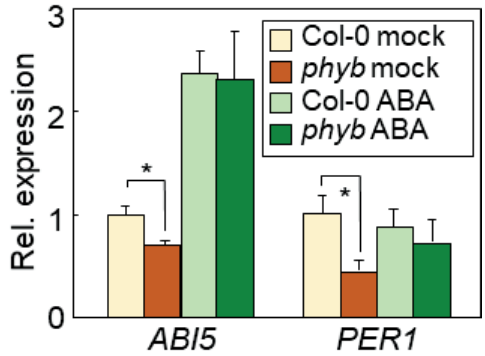

Fig. 51. Relative levels of *ABI5* and *PER1* transcripts in *phyb* primary roots.

Seedlings were grown in the light for two weeks in the presence of 1 μM ABA. Total RNA was prepared from root samples, and biological triplicates of RT-qPCR runs were statistically analyzed (*t*-test, $*P < 0.01$). Bars indicate SEM.

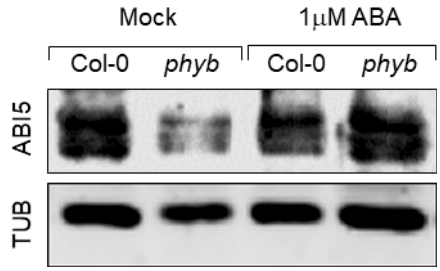

Fig. 52. Accumulation of ABI5 proteins in *phyb* roots.

Protein extracts were prepared from the roots of two-week-old seedlings. ABI5 proteins were immunologically detected using an anti-ABI5 antibody. α-Tubulin (TUB) proteins were also immuno-detected for loading control.

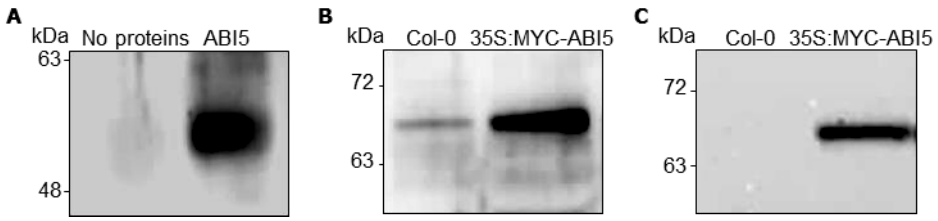

Fig. 53. Evaluation of the anti-ABI5 antibody used.

(A) Detection of ABI5 in cold imbibed seeds. Cold imbibed seeds for 3 days, in which a large quantity of ABI5 is present (Albertos *et al.,* 2015), were treated for 6 h with white light illumination were used for protein extraction. The polyclonal anti-ABI5 antibody was used for the immunological detection of ABI5 having a calculated molecular mass of 48 kDa. Note that ABI5 is detected as bands having higher molecular mass on SDS-PAGE (Albertos *et al.,* 2015).

(B and **C)** Detection of ABI5 in the roots. Proteins were extracted from the roots of two-week-old Col-0 and 35S:*MYC-ABI5* seedlings grown on vertical MS-agar plates in the light. MYC-ABI5 proteins were detected immunologically using either an anti-ABI5 antibody (B) or an anti-MYC antibody (C). Note that the efficiency and specificity of the anti-ABI5 antibody are high enough for the specific detection of ABI5 proteins.

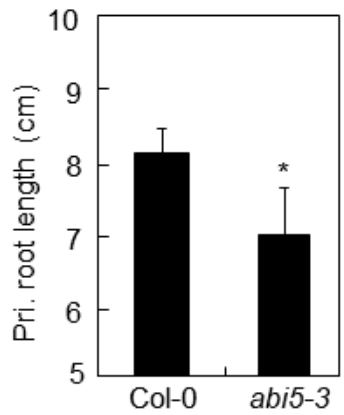

Fig. 54. Primary root length of *abi5-3* mutants.

The primary roots of two-week-old *abi5-3* mutants were used for measurement. Fifteen measurements were statistically analyzed (n = 15, t-test, *$P < 0.01$). Bars indicate SEM.

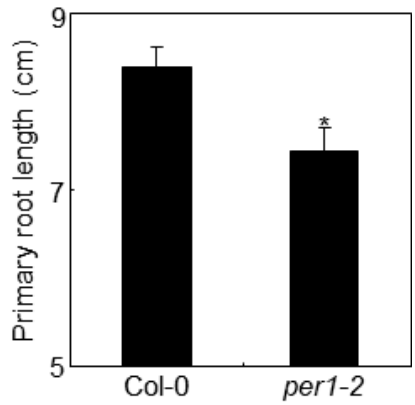

Fig. 55. Primary root length of *per1-2* mutant.

Plants were grown on MS- for two weeks under LD conditions in presence of root-light. Fifteen independent seedlings were analyzed using Student *t*-test (*P < 0.01). Bars indicate SEM.

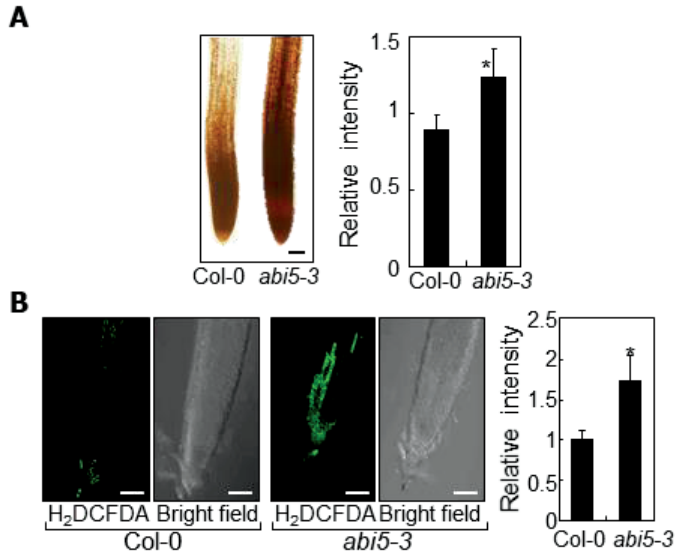

Fig. 56. DAB and H_2DCFDA stainings of light-grown primary roots.

ROS signals were detected by DAB (A) or H_2DCFDA (B) staining. Scale bars, 100 μm (A) and 50 μm (B). Seven quantitation was statistically analyzed (*t*-test, $*P < 0.01$). Bars indicate SEM.

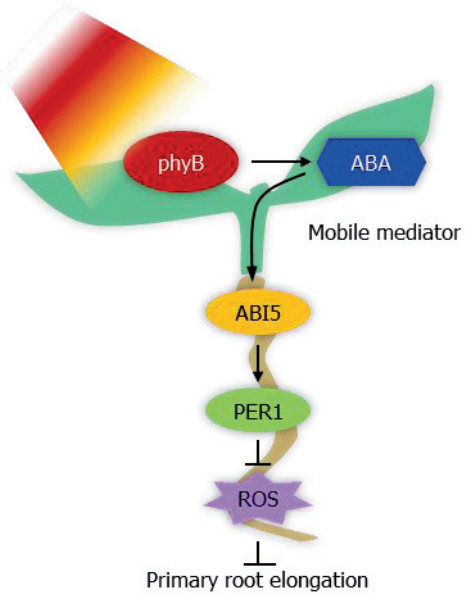

Fig. 57. Schematic model for shoot phyB function in modulating root ROS homeostasis.

Shoot phyB signals induce the biosynthesis of ABA, which triggers downstream signaling to the roots. The shoot-derived ABA signals activate ABI5, leading to the induction of *PER1* gene for ROS detoxification.

DISCUSSION

It has been reported that phyB-mediated light signals inhibit ABA biosynthesis (Kim et al., 2008). The phyB-mediated inhibition of ABA biosynthesis is modulated by SOMNUS, a CCCH-type zinc finger protein that is expressed specifically in the seeds (Kim et al., 2008). My data demonstrated that shoot phyB induces the expression of ABA biosynthetic genes in the shoots of growing seedlings. The previous and my own data support that phyB-mediated regulation of ABA biosynthesis occurs through multiple signaling pathways, depending on growth and developmental stages and varying environmental conditions.

Recently, it has been suggested that low concentrations of ABA stimulate primary root growth through interactions with auxin signaling (Li et al., 2017). It has been observed that auxin transport inhibitors block the effects of ABA on primary root growth and auxin transport mutants, which exhibit reduced primary root growth, are insensitive to ABA (Li et al., 2017). It is also known that phyB-mediated light signals affect auxin transport (Salisbury et al., 2007). However, I found that ABA feeding restored the reduced primary root growth phenotype of *phyb* mutant, indicating that ABA also affects primary root growth through an auxin-independent process. It is likely that ABA modulates primary root growth at least through two distinct routes: One through signaling crosstalks with auxin, and the other

through phyB-mediated ROS detoxification process.

I found that ABA synthesized in the shoots is not directly transported to the roots to trigger ROS detoxification. Instead, as-yet unidentified ABA signaling mediator produced in the shoots is transported to the roots. Meanwhile, it is known that ABA is transported from the shoots to the roots under stress conditions (Ikegami et al., 2009). It is notable that low concentrations of ABA (< 1 μM) are required for the activation of the ABI5-PER1 pathway for the induction ROS detoxification in the roots. Therefore, it is anticipated that under conditions when a low concentration of ABA is effective, ABA would be synthesized in the plants tissues that respond to environmental stimuli. However, when a large amount of ABA is required for its responses, such as drought stress conditions, it would be necessary that the plants tissues that respond to environmental stimuli would need more ABA that is to be transported from other tissues.

While my data strongly support that an ABA signaling mediator transmits light signals to the roots, it is still possible that ABA itself acts at least in part as the shoot-to-root mobile signal. I propose that the phyB-mediated light signaling modulates root ROS homeostasis to sustain root growth, thus providing an adaptive strategy that coordinates the growth of shoots and roots to achieve optimal growth and performance in nature.

ACKNOWLEDGEMENT

I thank Y.J. Park, H. J. Lee, S. G. Kim and H. J. sim for scientific discussions. I also thank G. Lee, R. Halitschke and I. T. Baldwin for measuring hormone contents. I appreciate J. I. Kim for providing *phyb-5* plants and scientific discussion on biochemical activity of phyB.

CHAPTER 3

Thermo-induced maintenance of photo-oxidoreductases underlies plant autotrophic development

INTRODUCTION

Upon exposure to light, the chlorophyll precursor pchlide produces ROS, which cause oxidative damage and chlorophyll bleaching in developing seedlings (Huq et al., 2004). Developing seedlings acquire photosynthetic competence as POR enzymes convert pchlide to chlide, producing chlorophylls to achieve autotrophic growth (Oosawa et al., 2000; Schoefs and Franck, 2003). Accordingly, autotrophic transition accompanies a reduction in ROS accumulation (Cheminant et al., 2011).

PORs are widely conserved in various plant species, ranging from angiosperm, such as barley (Oosawa et al., 2000), tobacco (Masuda et al., 2002), Amaranthus tricolor (Iwamoto et al., 2001), and Arabidopsis (Armstrong et al., 1995), to gymnosperm, including pine (Forreiter and Apel, 1993). In *Arabidopsis*, three POR isoforms, PORA, PORB, and PORC, are differentially regulated by light and developmental ages. PORA accumulates to a high level in etiolated seedlings. However, its gene expression decreases rapidly after light illumination (Armstrong et al., 1995). *PORB* gene is constitutively expressed in both etiolated seedlings and green seedlings (Armstrong et al., 1995). In contrast, the expression of *PORC* gene increases under identical conditions (Su et al., 2001). POR-bound, photoactive pchlide is converted to chlide by the action of PORs upon light exposure (Heyes and Hunter, 2005). On the other hand, photoinactive, free pchlide produces ROS

upon light illumination, which provoke oxidative damage leading to cell death (Paddock et al., 2010).

At high ambient temperature, developing seedlings exhibit a series of developmental changes, such as accelerated hypocotyl elongation, leaf hyponasty, and reduction of stomatal density (Box et al., 2015; Crawford et al., 2012; Gray et al., 1998; Koini et al., 2009), which are collectively termed thermomorphogenesis. Recent studies have shown that phytochrome-interacting factor 4 (PIF4) is a major regulator of these responses. Upon exposure to warm temperatures, the protein levels of PIF4 and its DNA-binding activity are elevated, triggering induction of auxin biosynthesis genes (Sun et al., 2012). These temperature responses help thermos-susceptible meristematic tissues in the shoot apex to rapidly move away from the heat-absorbing soil surface layer under natural conditions (Crawford et al., 2012; Gray et al., 1998). Notably, the effects of warm temperatures on hypocotyl growth are most prominent during 48–72 hr after germination, when heterotrophic-to-autotrophic transition occurs (Box et al., 2015). These observations predict that autotrophic transition is physiologically linked with thermal adaptation of developing seedlings.

FCA is a well-known floral activator functioning in the autonomous flowering pathway (Liu et al., 2010; Macknight et al., 1997). Notably, recent studies have shown that it also plays a role in temperature responses. Under heat stress conditions, FCA induces thermotolerance by triggering antioxidant accumulation (Lee et al., 2015). It directly interacts with

abscisic acid-insensitive 5 transcription factor during heat stress responses. Meanwhile, FCA attenuates thermomorphogenesis by inhibiting the DNA-binding activity of PIF4 (Lee et al., 2014). FCA directly interacts with PIF4, and the FCA-PIF4 complex binds to the promoter regions of PIF4 target genes, such as *YUCCA8* (*YUC8*). Under prolonged warm temperature conditions, FCA suppresses histone-3 lysine-4 dimethylation (H3K4me2) in the *YUC8* loci to inhibit its expression, compromising hypocotyl elongation.

In this work, I demonstrated that FCA plays a critical role in chlorophyll biosynthesis by enabling the thermo-induced maintenance of POR proteins. In FCA-defective mutants, POR proteins were destabilized at warm temperatures, and thermal induction of *POR* genes was also disturbed. As a result, the pchlide-to-chlide conversion was reduced, resulting in accumulation of pchlide, which acts as a photosensitizer and thus causes albinism. My findings indicate that FCA constitutes a thermoresponsive signaling pathway that directs chlorophyll biosynthesis in developing seedlings, which pass through the heat-absorbing soil surface layer under natural conditions.

MATERIALS AND METHODS

Plant materials

All *Arabidopsis thaliana* lines used in this work were in Columbia (Col-0) background. The FCA-defective *fca-9* and *fca-11* mutants have been described previously (Bäurle et al., 2007; Liu et al., 2007). The *flu* mutant (SAIL-136-E05), which has been described previously (Meskauskiene et al., 2001), was obtained from Drs. Chanhong Kim and Klaus Apel. The *pif4-101*, *abi5-3*, and *FRI*-Col plants have been described previously (Choi et al., 2011; Lorrain et al., 2008; Piskurewicz et al., 2008). To generate p*FCA*:*FCA-FLAG* transgenic plants, approximately a 11.4-kbp genomic fragment harboring *FCA* gene and its promoter were fused in-frame to the 5' end of FLAG-coding sequence, and the subcloned vector constructs were transformed into Col-0 plants. The *per1-1* (SALK-133714C), *fy-1* (CS57), *pora* (SALK-022639), *porb* (SALK-008867C), and *porc* (SAIL-1284-D05) mutants were isolated from a pool of T-DNA insertion lines deposited in the *Arabidopsis* Biological Resource Center (ABRC, Ohio State University, Columbus, OH). To generate 35S:*MYC-PORA*, 35S:*MYC-PORB*, and 35S:*MYC-PORC* transgenic plants, PORA-, PORB-, and PORC-coding sequences were fused in-frame to the 3' end of the MYC-coding sequence in the MYC-PBA vector (Seo et al., 2010). The expression constructs were

transformed into *fca-11* mutant by a modified floral dip method (Clugh and Bent, 1998).

Plant growth conditions

Sterilized *Arabidopsis* seeds were cold-imbibed at 4°C for 3 d in complete darkness and allowed to germinate in a controlled growth chamber at either 23°C or 28°C with relative humidity of 60%. Plants were grown either in soil or on sucrose-free, ½ X MS-agar plates under LDs with white light illumination (150 μmol $m^{-2}s^{-1}$) provided by fluorescent FLR40D/A tubes (Osram, Seoul, Korea).

Analysis of gene transcript levels

Transcript levels were analyzed by reverse transcription-mediated RT-qPCR. RT-qPCR reactions were performed according to the guidelines that have been proposed to guarantee reproducible and accurate measurements of transcript levels (Udvardi et al., 2008). For total RNA extraction, plant materials were ground in liquid nitrogen. The ground plant materials were suspended in 1 ml of TRIzol reagent (Invitrogen, Carlsbad, CA), and the suspension was centrifuged at 16,000 X g for 10 min at 4°C. The supernatant was mixed with 200 μl of chloroform and centrifuged under the same conditions. Five-hundred μl of the aqueous phase was transferred to a microcentrifuge tube containing 250 μl of high salt solution (0.8 M

trisodium citrate, 1.2 M sodium chloride) and 250 μl of isopropanol. The mixture was incubated for 15 min at room temperature and centrifuged at 16,000 X g for 10 min at 4°C to precipitate RNA molecules. The RNA pellet was washed with 75% ethanol and dissolved in deionized water. The RNA solution was pretreated extensively with RNase-free DNase to get rid of contaminating genomic DNA.

RT-qPCR reactions were conducted in 96-well blocks with an Applied Biosystems 7500 Real-Time PCR System (Foster City, CA) using the SYBR Green I master mix in a volume of 20 μl. The two-step thermal cycling profile employed was 15 s at 95°C for denaturation and 1 min at 60-65°C, depending on the calculated melting temperatures of PCR primers, for annealing and polymerization. PCR primers used are listed in Table 1. An *eIF4A* gene (*At3g13920*) was used as internal control in each PCR reaction to normalize the variations in the amounts of cDNAs used.

All RT-qPCR reactions were performed in biological triplicates using total RNA samples extracted separately from three independent plant materials that were grown under identical experimental conditions. The comparative $\Delta\Delta C_T$ method was employed to evaluate relative quantities of each amplified product in the samples. The threshold cycle (C_T) was automatically determined for each reaction by the system set with default parameters.

Transmission electron microscopy

Three-day-old seedlings were fixed in Karnovsky's fixative (2.5% glutaraldehyde and 2% paraformaldehyde in 0.1 M sodium cacodylate buffer, pH 7.2) for 4 h (Cho et al., 2011). The seedlings were then postfixed in 2% osmium tetroxide in 0.1 M cacodylate buffer for 2 h at 4°C and stained *en bloc* in 2% uranyl acetate for 1 h. The fixed samples were dehydrated through a series of ethanol and propylene oxide washes. After dehydration, the samples were embedded with Spurr resin (Sigma-Aldrich, St Louis, MO). Ultrathin sections were prepared using an EM UC7 ultramicrotome (Leica, Wetzlar, Germany). Chloroplasts in the seedling sections were visualized by a JEM 1010 transmission electron microscope (JEOL, Tokyo, Japan) operated at 80 kV.

Measurement of pigment contents

Chlorophyll contents were measured as described previously (Lee et al., 2015). Approximately 100 mg of seedlings grown for 7 d on MS-agar plates were used for each measurement. One ml of 90% acetone was added to the seedlings, and the mixture was incubated at 4°C for 24 h in complete darkness. The mixture was then centrifuged at 16,000 X g for 10 min at 4°C, and 1 ml of the supernatant was transferred to plastic cuvette. Absorbance was measured at 652, 665, and 750 nm using a nanodrop 2000 spectrophotometer (Thermo, Waltham, MA).

Seedlings grown for 2-7 d on MS-agar plates were used for the quantification of chlide contents. Approximately 30 mg of seedlings were incubated in 1 ml of 90% acetone at 4ºC for 24 h in complete darkness. The extract was then centrifuged at 16,000 X g for 10 min at 4ºC. The supernatant was measured using a Cary Eclipse fluorescence spectroscope (Agilent, Santa Clara, CA). Excitation wavelength was 416 nm, and emission wavelength was 672 nm. For the measurements of pchlide contents, excitation wavelength was 440 nm, and emission wavelength was recorded between 600 and 700 nm with a bandwidth of 5 nm (Reinbothe et al., 1999).

Immunoblot assays

Seedlings grown for 4-7 d on MS-agar plates or in soil were used for the extraction of total proteins. Plant materials were ground in liquid nitrogen and mixed with protein extraction buffer (100 mM Tris-Cl, pH 6.8, 4% SDS, 0.2% bromophenol blue, 20% glycerol, and 200 mM β-mercaptoethanol). The mixtures were boiled for 10 min and then centrifuged at 16,000 X g for 10 min. The supernatants were used for SDS-PAGE. The separated proteins were transferred to polyvinylidene difluoride membrane. Anti-POR (Agrisera, Vännäs, Sweden) and anti-FLAG antibodies (Sigma-Aldrich) were used for the immunological detection of POR and FCA-FLAG proteins, respectively. Anti-rabbit and anti-mouse IgG-peroxidase antibodies (Santa Cruz Biotechnology, Santa Cruz, CA) were used as

secondary antibodies for immunoblot assays using anti-POR and anti-FLAG antibodies, respectively.

For protease and 26S proteasome inhibitor treatments, 8% (w/v) protease inhibitor cocktail (Roche, Basel, Switzerland) and 5 μM MG132 (Merck Millipore, Darmstadt, Germany) were sprayed onto 3-day-old seedlings. Seedlings were harvested 24 h following the treatments.

Detection of ROS and Treatments with ROS Scavengers

The DAB staining solution (0.2 mg/ml) and the SOSG solution (100 μM) were used for analyzing hydrogen peroxide and superoxide, respectively (Lee et al., 2012). For DAB staining, seedlings grown for 3 d on MS-agar plates were exposed to 23ºC or 28ºC and incubated in the staining solutions for 24 h at room temperature in complete darkness. The plant samples were de-stained by soaking in 5 ml of 90% ethanol at room temperature for 24 h. The stain intensity was quantified using the ImageJ software (http://rsb.info.nih.gov/ij/).

For SOSG staining, seedlings were grown for 3 d on MS-agar plates under LDs at 23ºC or 28ºC and subsequently incubated in staining solution for 20 min at 23ºC followed by further incubation at either 23ºC or 28ºC for 20 min in the light before fluorescence detection. Confocal microscopy was employed to image SOSG fluorescence in cotyledons. Cary Eclipse fluorescence spectroscope (Agilent) was used to measure fluorescence intensity. Excitation wavelength was 480 nm and emission wavelength was

recorded between 500 nm to 600 nm with a bandwidth of 10 nm (Flors et al., 2006).

Yeast Two-Hybrid Assay

The FCA-coding sequence was fused in-frame to the C-terminus of GAL4 activation domain in the plasmid pGADT7. The PIF1-, EIN3-, and EIL1-coding sequences were fused in-frame to the C-terminus of GAL4-DNA binding domain in the plasmid pGBKT7. The expression constructs were transformed into yeast strain AH109, which harbors reporter genes *lacZ* encoding β-galactosidase and *HIS* mediating histidine biosynthesis under the control of the GAL1 promoter. Yeast transformants were grown on selective media lacking Leu, Trp, His, and Ade to screen for positive interactions.

ChIP Assay

ChIP assays were performed as described previously (Lee et al., 2014). Three-day-old seedlings grown on MS-agar plates were harvested at zeitgeber time (ZT) 24 and vacuum-infiltrated with 37 ml of 1% (v/v) formaldehyde for cross-linking. The plant materials were then ground in liquid nitrogen after quenching the cross-linking process. The grounded samples were resuspended in 30 ml of nuclear extraction buffer (1.7 M sucrose, 10 mM Tris-Cl, pH 7.5, 2 mM $MgCl_2$, 0.15% Triton-X-100, 5 mM β-mercaptoethanol, 0.1 mM PMSF) containing protease inhibitor (Sigma-

Aldrich) and filtered through miracloth (Millipore, Billerica, MA). The filtered mixture was then centrifuged at 4,300 X g for 20 min at 4ºC, and nuclear fractions were isolated by a sucrose cushion method (Abdalla et al., 2009). The nuclear fractions were lysed with lysis buffer (50mM Tris-Cl, pH 8.0, 0.5M EDTA, 1% SDS) containing protease inhibitor (Sigma-Aldrich) and sonicated to obtain chromatin fragments of 400-700 bp. Five μg of anti-FLAG (Sigma-Aldrich), anti-H3K4me2 (Millipore), anti-H3K9me3 (Millipore), anti-H3Ac (Millipore), or anti-RNA polymerase II (RNA pol II) (Abcam, Cambridge, UK) antibody was added to the chromatin solution and incubated for 16 h at 4ºC. The Protein-G or -A agarose beads (Millipore) were then added to the solution and incubated for 1 h to collect antibody. The mixture was centrifuged at 4,000 X g for 2 min at 4ºC. Following reverse-crosslinking of the precipitate, residual proteins were removed by proteinase K treatment. DNA fragments were purified using a silica membrane spin column (Promega, Madison, WI). To determine the amounts of DNA enriched in the chromatin preparation, quantitative PCR was performed, and the values were normalized to the amount of input in each sample. The primers used are listed in Table 1.

DNA Methylation Assay

DNA methylation assay was performed as described previously (Li and Tollefsbol, 2011). Genomic DNA was extracted using cetyltrimethylammonium bromide method from 3-day-old seedlings grown

on MS-agar plates and bisulfite-treated using the EpiTect Bisulfite Kit (Qiagen, Hilden, Germany) according to the manufacturer's instruction. Bisulfite-treated DNA samples were amplified by nested PCR using Taq polymerase. The PCR primers used are listed in Table 1. To amplify the promoter regions of *PORB* gene, the cycling program for the first-round PCR included 40 cycles, each consisting of 95°C for 5 sec, 40°C for 30 sec, and 72°C for 30 sec. For the second-round PCR, the cycling program was identical to that of the first-round PCR except for annealing at 50°C. The PCR products were cloned into the pTOP TA V2 plasmid using the TOP cloner™ TA core Kit (Enzynomics, Dae-Jeon, Korea) according to manufacturer's instruction. DNA methylation patterns were determined by direct DNA sequencing.

Primers	Sequences	Usage
eIF4A-F	5’-TGACCACACAGTCTCTGCAA	RT-qPCR
eIF4A-R	5’-ACCAGGGAGACTTGTTGGAC	“
FCA-F	5'-GCTCTTGTCGCAGCAAACTC	“
FCA-R	5'-GATCCAGCCCACTGTTGTTTAC	“
PORA-F	5’-GATGCCTCTCGATGTGTTGG	“
PORA-R	5’-GAAAGTGGCCCAAATGGTTT	“
PORB-F	5’-ATGCAAGAGTTTCACAGGCG	“
PORB-R	5’-TTTGCCTGACTCTGTTTCGG	“
PORC-F	5’-TCAGGATTGAATGGGCAAAA	“
PORC-R	5’-CGTCTGTGAAGCTCCTGCAT	“
CAO-F	5’-TTGCAAAAGGCTGGAGTGTC	“
CAO-R	5’-CGGGTTTTGATATCCCGATT	“
CHLI-1-F	5’-TGTAGTTGCAGGTGACCCGT	“
CHLI-1-R	5’-ACAAACCAGGCTCAAAGGCT	“
CHLH-F	5’-AGCTTACCTCGCTTCTTGGG	“
CHLH-R	5’-ACCTTTGGGTTTCTGATGGG	“
CHLD-F	5’-GTCGAATCCCCTAACGGTGT	“
CHLD-R	5’-ACCTGAAATGGCAATCCCTC	“
CRD1-F	5’-AGAATATTCCCTGCGGTGCT	“
CRD1-R	5’-GCGAAATCAACAGAGCCAGA	“
PORA1-F	5’-CACATTTTGTAATTGTCTTTAGGTTTATC	ChIP-PCR
PORA1-R	5’-AGCTAGAGCCCTAGAGGTATGAAAC	“
PORA2-F	5’-GTTTCATACCTCTAGGGCTCTAGCT	“
PORA2-R	5’-AAGATTATCTTTAGGGAAAGTTTTTGTC	“
PORA3-F	5’-GACAAAAACTTTCCCTAAAGATAATCTT	“
PORA3-R	5’-ACCAAAGAAGCAGCTTGAAGG	“
PORA4-F	5’-AGGCATTAGCCGAGACAGGT	“
PORA4-R	5’-GCCAAGTCCAAATGCATCAC	“
PORB1-F	5’-GCTCTTATTCATTGAATAAGGTTTGAG	“
PORB1-R	5’-GGAGATAGATAGAGCTAGTTGCTTGC	“
PORB2-F	5’-GACGACGTGGCAGATACTTAGTTC	“
PORB2-R	5’-GTGATTGCTGAAGAAAACTATCGTAG	“
PORB3-F	5’-CTACGATAGTTTTCTTCAGCAATCAC	“
PORB3-R	5’-GAAAGATGATGAAGAAGCATTCAAC	“
PORB4-F	5’-CGACAGCTAAAGAGCCTACTTACAG	“
PORB4-R	5’-CCAAACAAACATAACAATGATCAAA	“
PORC1-F	5'-GGTTGCGTACAGGTCAGAGC	“
PORC1-R	5'-CAGAACAACCCACAATTCTGTCT	“
PORC2-F	5'-CCGTTAAGTTGCCGCCTTCT	“
PORC2-R	5'-ATTGGGCCTTGAGATGGGCT	“
PORC3-F	5'-AAGCTGTAGCCTGGAAGACAC	“
PORC3-R	5'-AAGGTGCTAGAGTGTCACAGTG	“
PORAM-F	5’-TTTAATTTTYGAATTATTATTGGTTTTAAGAA	DNA methylation
PORAM-R	5’-ACTAAAACATTTAATTTTCCCTACAACC	“
PORAM-F2	5’-TTTTTTTATATATAAAGAGATGGAGTTT	“
PORAM-R2	5’-AAATAAAACACCRAACAAACTAAACTCTT	“
PORBM-F	5’-AATATTTAAGGAGAAGGAAATTTAATTTT	“
PORBM-R	5’-AACTTAAAAAACCATTATTAATACTCRAAC	“
PORBM-F2	5’-ATGTTAAAGGGTATGGAATTTTATTAA	“
PORBM-R2	5’-AAACATTCAACTTCRCATCTTTACRAAC	“

Table 3. Primers used in Chapter 3.

F, forward primer, R, reverse primer.

RESULTS

FCA protects developing seedlings from albinism at 28ºC

I have recently reported that the RNA-binding protein FCA attenuates high ambient temperature-induced hypocotyl elongation by inhibiting the DNA binding of PIF4 that modulates auxin biosynthesis (Franklin et al., 2011; Lee et al., 2014). While working on the effects of warm temperatures on hypocotyl growth, I found that FCA-defective *fca* mutants exhibit early seedling albinism with retarded growth at 28ºC (Fig. 58A). The phenotypic alterations were more severe in *fca-11* seedlings than in *fca-9* seedlings, which might be due to different effects of the mutations.

While the splice acceptor site AG at the 30 end of eighth intron is mutated to AA in *fca-9* mutant (Liu et al., 2007), glutamine 537 is mutated to the stop codon in *fca-11* mutant (B€aurle et al., 2007). The chlorophyll contents were reduced by more than 80% in the mutant seedlings (Fig. 58B). Interestingly, the albino phenotype disappeared when the mutant seedlings were germinated and grown for longer than 3 days at 23ºC before transfer to 28ºC (Fig. 58A). In addition, the albino phenotype of *fca* seedlings was not observed at low light intensities (<10 mmol m^{-2} s^{-1}) (Fig. 59), indicating that the albinism occurs only in the presence of moderate or higher light intensities.

To systematically examine the effects of warm temperatures on the

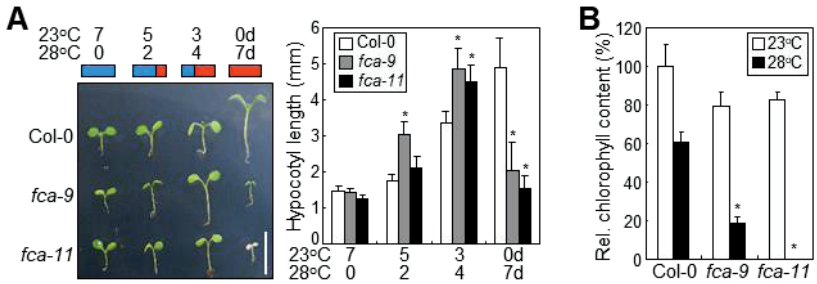

Fig. 58. *fca* seedlings exhibit albinism at high ambient temperatures

Length of hypocotyls was measured using ~20 seedlings and statistically treated using Student *t*-test (*$P < 0.01$). Bars indicate SEM. Scale bars, 5 mm. Blue and red boxes indicate time durations at 23°C and 28°C, respectively.

(**A** and **B**) Induction of albinism at 28°C. Seedlings were grown for 7 d under different combinations of temperature regimes (A). In (B), three measurements were statistically treated (*t*-test, *$P < 0.01$, difference from 28°C-treated Col-0).

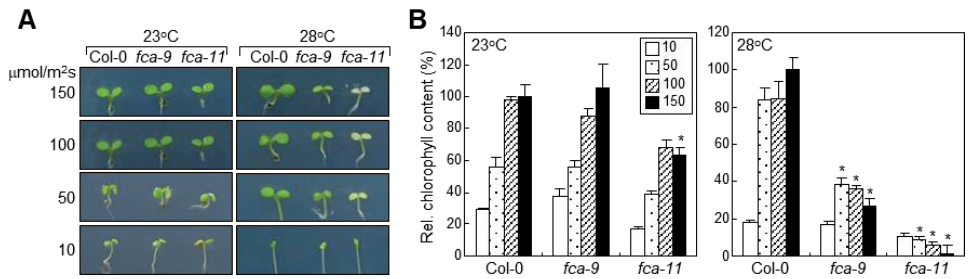

Fig. 59. Effects of light intensities on albinism of *fca* seedlings at 28°C.

Seedlings were grown on MS-agar plates for 3 d at either 23°C or 28°C under different light intensities (A). Three measurements of chlorophyll contents were averaged and statistically treated (*t*-test, $*P < 0.01$, difference from Col-0) (B). Bars indicate SEM.

albino phenotype of *fca* seedlings, I germinated mutant seeds and grew them at 28ºC for up to 72 hr before transfer to 23ºC. The *fca* seedlings exhibited albinism when they were grown at 28ºC for longer than 24 hr before transfer to 23ºC (Fig. 60A). In contrast, the mutant seedlings exhibited normal growth when they were incubated at 23ºC for longer than 24 hr before transfer to 28ºC (Fig. 60B). It is known that the heterotrophic-to-autotrophic transition occurs during 24–72 hr after germination in Arabidopsis (Mansfield et al., 1996; Vidal et al., 2014). It was therefore suspected that the *fca* seedlings are hypersensitive to warm temperatures during the autotrophic transition. FCA directs diverse developmental and environmental responses, such as flowering induction, thermal control of hypocotyl elongation, and induction of heat resistance, by regulating various genes (B€aurle et al., 2007; Lee et al., 2014, 2015). To examine whether genes belonging to the FCA-mediated signaling are involved in the thermal responses of developing seedlings, I examined the early seedling growth of the mutants at 28ºC. None of them exhibited albinism unlike *fca* mutants (Fig. 61), indicating that FLC and other known FCA-related signaling mediators are not related with the FCA-mediated regulation of the thermosensitive seedling development.

FCA is required for thermo-induced maintenance of POR proteins

Significant reduction of chlorophyll contents and lethal growth defects in *fca* mutants at 28ºC indicate that the mutant phenotypes are not associated

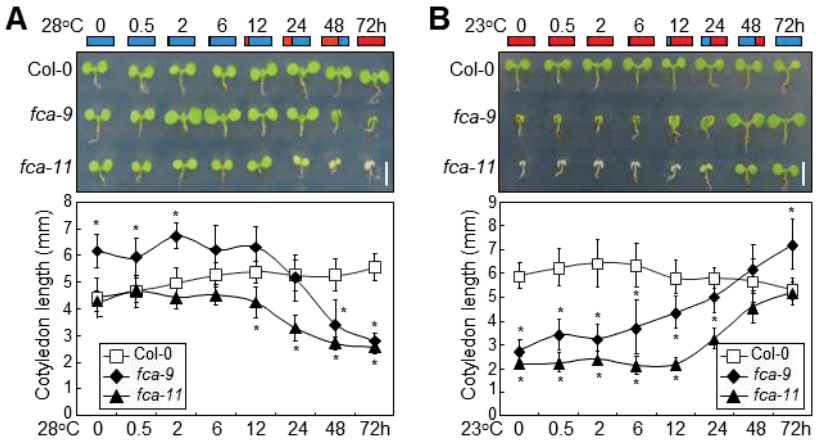

Fig. 60. Effects of temperature on albinism.

Length of cotyledons was measured using ~20 seedlings and statistically treated using Student *t*-test (**P* < 0.01). Bars indicate SEM. Scale bars, 5 mm. Blue and red boxes indicate time durations at 23°C and 28°C, respectively.

(**A**) Effects of thermal duration on albinism. Seedlings grown at 28°C for various time durations were transferred to 23°C for up to 7 d.

(**B**) Effects of seedling ages on albinism. Seedlings grown at 23°C for different time durations were exposed to 28°C for up to 7 d.

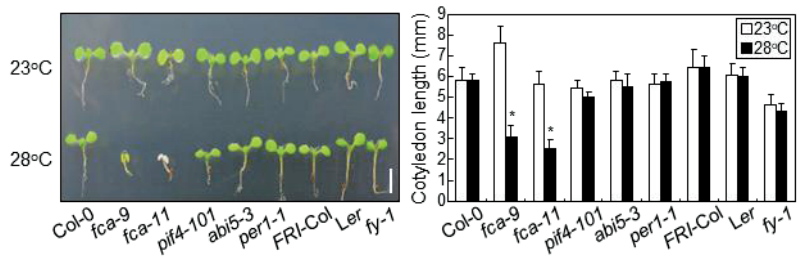

Fig. 61. Seedling phenotypes of selected mutants.

Seedlings were grown for 7 d at either 23ºC or 28ºC. Fifteen measurements were quantified and statistically treated using Student *t*-test (*$P < 0.01$). Bars indicate SEM. Scale bars, 5 mm.

with thermomorphogenic responses but instead are caused by loss of photosynthesis. Damaged chlorophyll biosynthesis often correlates with malformation of chloroplasts (Tomas, 1997). Since albino phenotypes were observed in light-grown *fca* seedlings, I decided to analyze biochemical properties under light conditions.

Transmission electron microscopic examination of *fca* cotyledons revealed that thylakoid membranes are severely disrupted at 28ºC (Fig. 62). Expression assays of genes mediating chlorophyll biosynthesis and chloroplast development showed that whereas *PORA*, *PORB*, and *PORC* genes are significantly induced 3 days after germination (DAG) at 28ºC in Col-0 seedlings, they were not induced in *fca-9* seedlings and even suppressed in *fca-11* seedlings under identical conditions (Fig. 63). Expression of other genes was not discernibly altered in Col-0 seedlings at 28ºC (Fig. 64), suggesting that *POR* genes would be functionally related to high temperature responses. To verify whether the reduced expression of *POR* genes in *fca* mutants affects protein accumulation, I performed immunoblot assays using an anti-POR antibody (Hu et al., 2015; Lin et al., 2014). While the levels of POR proteins were similar or slightly elevated at 28ºC in Col-0 seedlings, they were completely diminished in *fca* seedlings (Fig. 65). Together with the expression data that POR transcripts were highly induced at 28ºC in Col-0 but not in *fca* seedlings, these results indicate that induction of POR genes by FCA contributes to maintaining POR protein levels under warm temperature conditions.

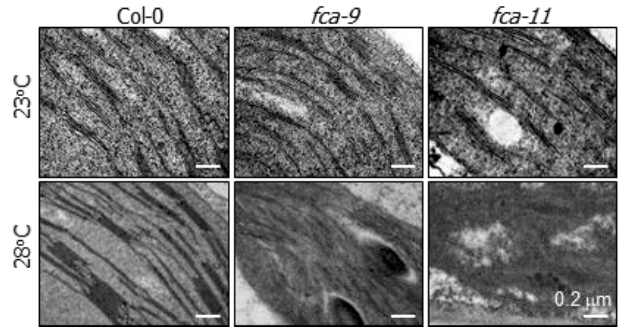

Fig. 62. Chloroplast development at 28°C.

Cotyledons of 3-day-old seedlings were subjected to transmission electron microscopy. At least five biological replicates were analyzed.

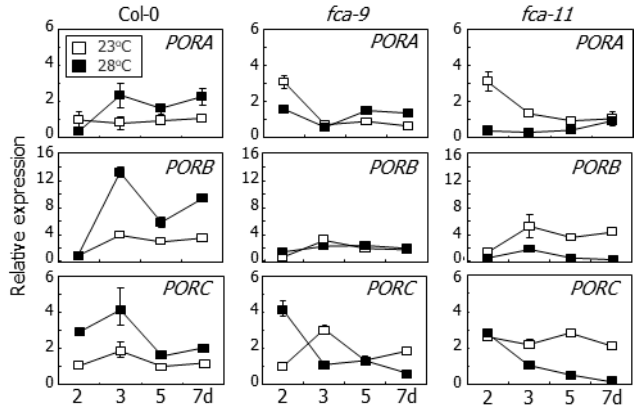

Fig. 63. Expression of *POR* genes.

Transcript levels were examined by RT-qPCR using total RNA samples extracted from seedlings grown for up to 7 d. Biological triplicates were averaged and statistically treated (*t*-test, $*P < 0.01$). Bars indicate SEM.

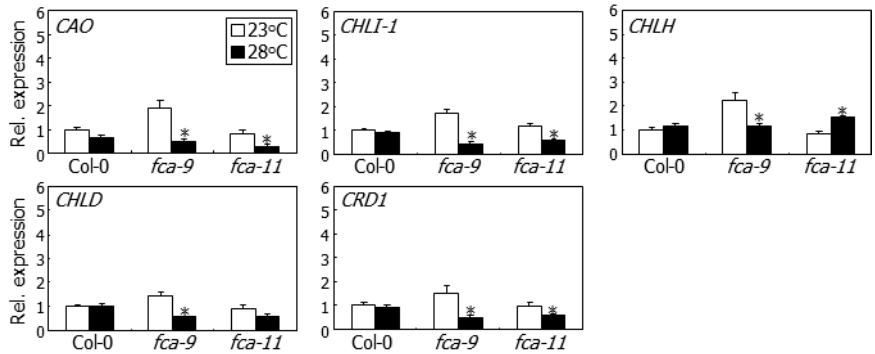

Fig. 64. Effects of *fca* mutations on chlorophyll biosynthesis.

Expression of chlorophyll biosynthesis genes. Three-day-old seedlings grown at either 23°C or 28°C were harvested at ZT 24 for total RNA extraction. Transcript levels were examined by reverse transcription-mediated RT-qPCR. Biological triplicates were averaged and statistically treated (*t*-test, $*P < 0.01$). Bars indicate SEM. Genes examined included those encoding chlorophyllide a oxygenase (*CAO*, *AT1G44446*), magnesium chelatase (*CHLI-1*, *AT4G18480*), magnesium chelatase subunit h (*CHLH*, *AT5G13630*), magnesium chelatase subunit d (*CHLD*, *AT1G08520*), and copper response defect 1 (*CRD1*, *AT3G56940*).

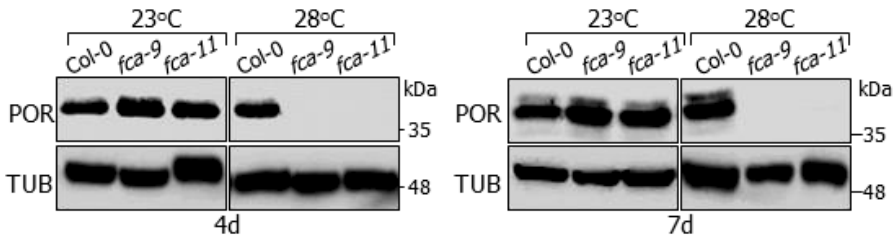

Fig. 65. Protein levels of PORs in *fca* mutants.

Total proteins were extracted from seedlings grown at either 23°C or 28°C for 4 and 7 d. An anti-POR antibody was used for the immunodetection of POR proteins. α-Tublin proteins were used for protein quality control.

It is notable that POR proteins were not detected in *fca* mutants at 28ºC. I therefore hypothesized that FCA is also required for stabilizing POR proteins at warm temperatures. I overexpressed a *MYC-PORA* fusion driven by the *CaMV 35S* promoter in Col-0 plants and *fca-11* mutant. It was found that the levels of PORA proteins were similar at 23ºC and 28ºC in Col-0 seedlings (Fig. 66). In contrast, PORA proteins were not detected in *fca-11* seedlings at 28ºC, showing that FCA is required for the thermostability of POR proteins.

To confirm the role of FCA in sustaining POR function, I transferred dark-incubated seedlings to the light, thus mimicking developing seedlings passing through the autotrophic transition under natural conditions. Under the assay conditions, *fca* seedlings exhibited albino phenotypes at 28ºC (Fig. 67). In addition, the level of POR proteins was reduced to a basal level in the mutant seedlings (Fig. 68), further supporting the notion that FCA mediates POR production.

Arabidopsis mutants lacking multiple PORs are defective in chlorophyll biosynthesis and chloroplast development (Frick et al., 2003; Paddock et al., 2010), similar to what is observed in *fca* seedlings at 28ºC. To examine the role of *POR* genes in high-temperature responses, I observed growth phenotypes of *pora*, *porb*, and *porc* seedlings at 28 ºC. At 23 ºC the *pora* mutant exhibited reduced growth, while the *porb* and *porc* seedlings showed normal growth as described previously (Fig. 69) (Frick et al., 2003; Paddock et al., 2012). However, the *porb* mutant exhibited retarded growth

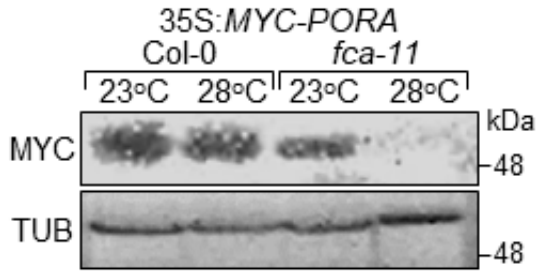

Fig. 66. Protein levels of PORA in *PORA*-overexpressing seedlings.

Transgenic seedlings overexpressing a *MYC-PORA* fusion driven by the CaMV 35S promoter in Col-0 and *fca-11* were grown at either 23ºC or 28ºC for 4 d before harvesting whole seedlings. An anti-MYC antibody was used for the immunodetection of MYC-PORA protein.

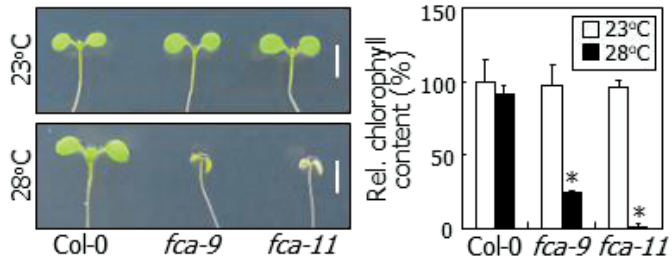

Fig. 67. Thermosensitive phenotypes during the dark-to-light transfer.

Seedlings were grown at either 23°C or 28°C. They were grown for 3 d in darkness and then transferred to the light for 3 d before taking photographs (left panel). Three measurements of chlorophyll contents were averaged and statistically treated (*t*-test, $*P < 0.01$) (right panel). Bars indicate SEM. Scale bars, 0.2 cm.

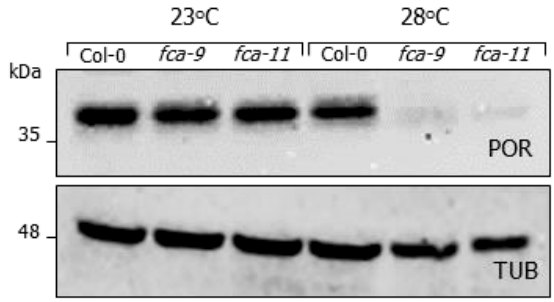

Fig. 68. Levels of PORs during the dark-to-light transfer.

Total protein extracts were prepared from the plants described in Fig. 67. An anti-POR antibody was used for the immunological detection of PORs (upper panel). Immunological detection of α-tubulin (TUB) was performed in parallel as protein quality control (lower panel).

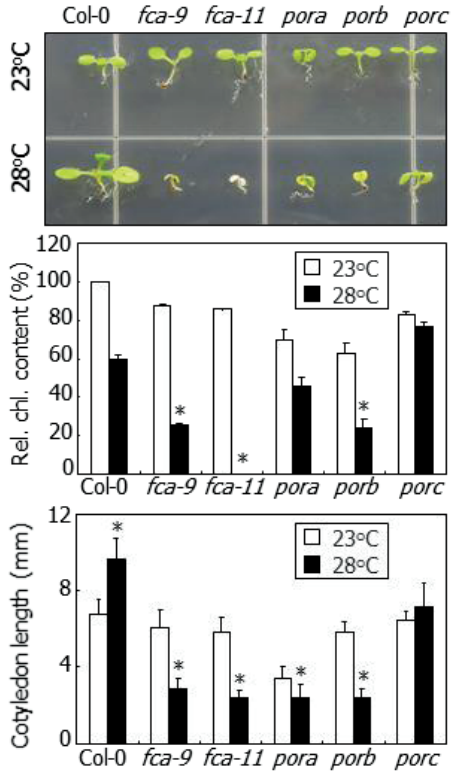

Fig. 69. Chlorophyll contents and cotyledon lengths of the *fca* and *por* mutants.

Early seedling growth of *por* mutants at 28°C. Seedlings grown for 7 d at either 23°C or 28°C were photographed (upper panel). Chlorophyll contents were measured (*P < 0.01, difference from 28°C-treated Col-0) (middle panel). Cotyledon lengths were measured (*P < 0.01, difference from 23°C) (bottom panel). Eighteen seedlings were used for the measurements. Biological triplicates were averaged and statistically treated (t-test, *P < 0.01). Bars indicate SEM.

with reduced chlorophyll contents similar to *fca* seedlings at 28 ºC (Fig. 69). The *pora* mutant exhibited only slight reduction of chlorophyll contents, and the *porc* mutant did not exhibit any changes in chlorophyll levels in comparison with Col-0, suggesting that PORB is a major regulator of chlorophyll biosynthesis at high ambient temperatures.

Since POR proteins convert pchlide to chlide (Oosawa et al., 2000; Schoefs and Franck, 2003), I investigated the levels of pchlide and chlide in *fca* seedlings. The *fca-11* mutant exhibited very severe growth defects at 28ºC. I therefore used the *fca-9* mutant in most biochemical assays. Measurements of pchlide contents in dark-grown seedlings revealed that its contents were similar in *fca-9* and Col-0 seedlings at both 23 ºC and 28 ºC (Fig. 70), suggesting that FCA is not involved in pchlide biosynthesis. Upon light exposure, pchlide was rapidly converted to chlide within 5 min in Col-0 plants at both 23ºC and 28ºC (Fig. 71), as previously reported (Huq et al., 2004). However, while the level of pchlide was not significantly reduced, the level of chlide was decreased in *fca-9* seedlings at 28ºC, indicating that the pchlide-to-chlide conversion is impaired in *fca-9* seedlings at high ambient temperatures. In light-grown seedlings, chlide contents were lower in *fca-11* seedlings than in Col-0 and *fca-9* seedlings at 23ºC, and the lower level was more prominent in *fca-9* and *fca-11* seedlings at 28ºC (Fig. 72), further supporting that FCA is associated with POR function during the pchlide-to-chlide conversion.

To further examine the functional linkage between FCA with POR, I

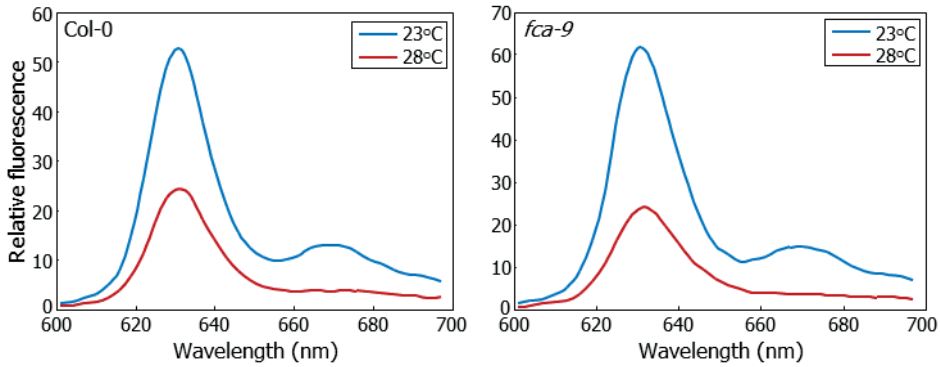

Fig. 70. Protochlorophyllide contents in etiolated *fca-9* mutant at 28°C.

Seedlings were grown on MS-agar plates for 4 d at either 23°C or 28°C in darkness. Protochlorophyllides were extracted with 90% acetone, and the extracts were incubated at 4°C for 24 h in darkness. Protochlorophyllide contents were measured by a fluorospectrometer (Cary Eclipse fluorescence spectroscope). Excitation wavelength was 440 nm, and emission spectra were recorded between 600 and 700 nm with a bandwidth of 5 nm (Huq et al., 2004).

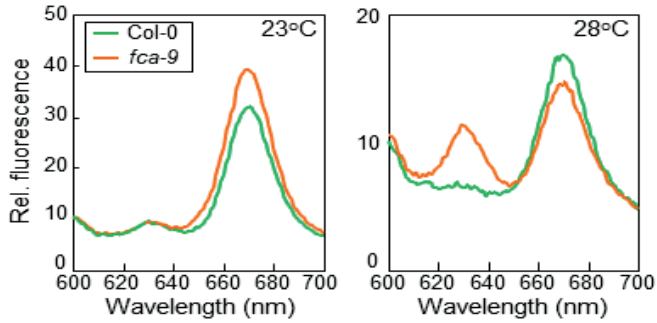

Fig. 71. Conversion of pchlide to chlide at 28°C.

Seedlings were grown for 3 d in the dark and then exposed to the light for 5 min at either 23°C or 28°C. Three biological replicates were averaged. Note that the peak at 633 nm indicates pchlide, and the peak at 667 nm indicates chlide.

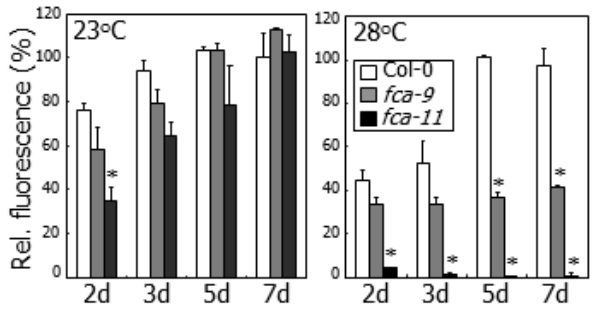

Fig. 72. Reduction of chlide levels in *fca* seedlings at 28°C.

Seedlings were harvested at the indicated time points after germination. Biological triplicates were averaged and statistically treated (*t*-test, $*P < 0.01$). Bars indicate SEM.

overexpressed POR-coding sequences driven by the *CaMV 35S* promoter in *fca-11* mutant. I found that seedling growth defects and reduced chlide accumulation were partially recovered by overexpression of individual POR genes at 28ºC (Fig. 73, A, B and C), further supporting the notion that FCA mediates the maintenance of POR proteins at 28 ºC. The *PORB* and *PORC* overexpressions were more effective than *PORA* overexpression in rescuing the *fca-11* seedling phenotypes, consistent with the previous report (Reinbothe et al., 1995, 1996) in which PORA protein was rapidly degraded upon light illumination. Together, these observations indicate that FCA is functionally linked with POR in developing seedlings at 28ºC.

FCA Reduces ROS Production at Warm Temperatures

PORs play a photoprotective role by metabolizing pchlide, which otherwise acts as a photosensitizer that produces ROS in response to light (Buhr et al., 2008; Huq et al., 2004; Paddock et al., 2010). I therefore measured ROS levels in *fca* seedlings. To measure the levels of singlet oxygen, I used the singlet oxygen-specific fluorescence probe Singlet Oxygen Sensor Green (SOSG). It has been shown that the fluorescence intensity of SOSG is proportional to the level of singlet oxygen (Flors et al., 2006). At 23 ºC, SOSG fluorescence was similarly low in Col-0 and *fca* seedlings (Fig. 74, A, B and C). However, its fluorescence intensity was largely elevated in *fca* seedlings grown at 28 ºC. It is likely that the conversion of pchlide to chlide is suppressed due to the lack of POR induction and, thus, pchlide triggers

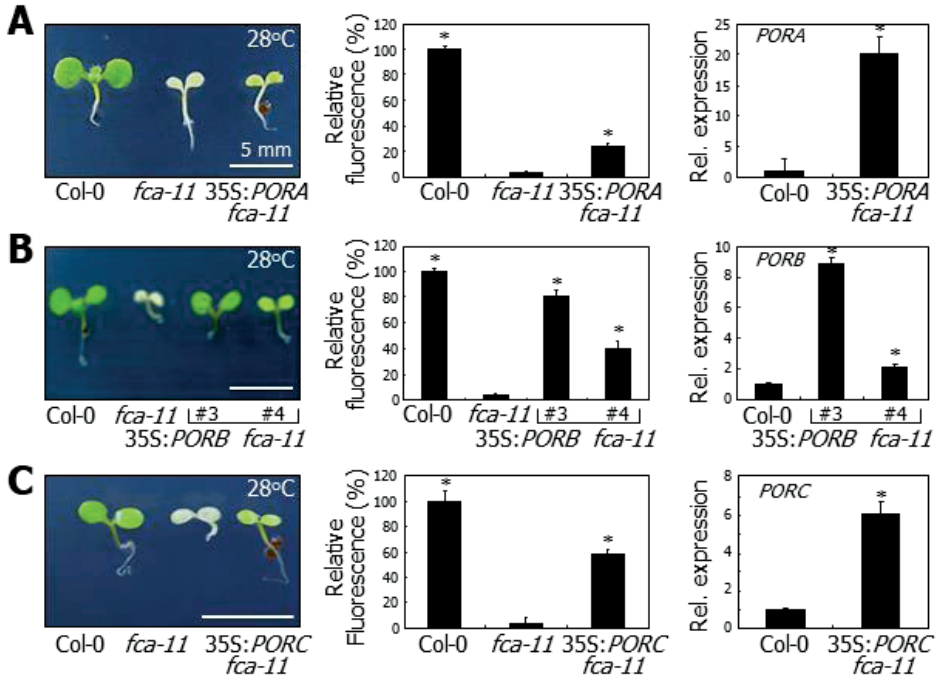

Fig. 73. Effects of *POR* overexpression on albinism of *fca-11* seedlings.

(**A**, **B** and **C**) *POR*-coding sequences were overexpressed driven by the CaMV 35S promoter in *fca-11* mutant. Three-day-old seedlings grown at 28°C were transferred to 23°C and further grown for 3 additional days. Six-day-old seedlings grown at 23°C were harvested for analyzing *POR* expression. Biological triplicates were averaged and statistically treated (*t*-test, $*P < 0.01$). Bars indicate SEM.

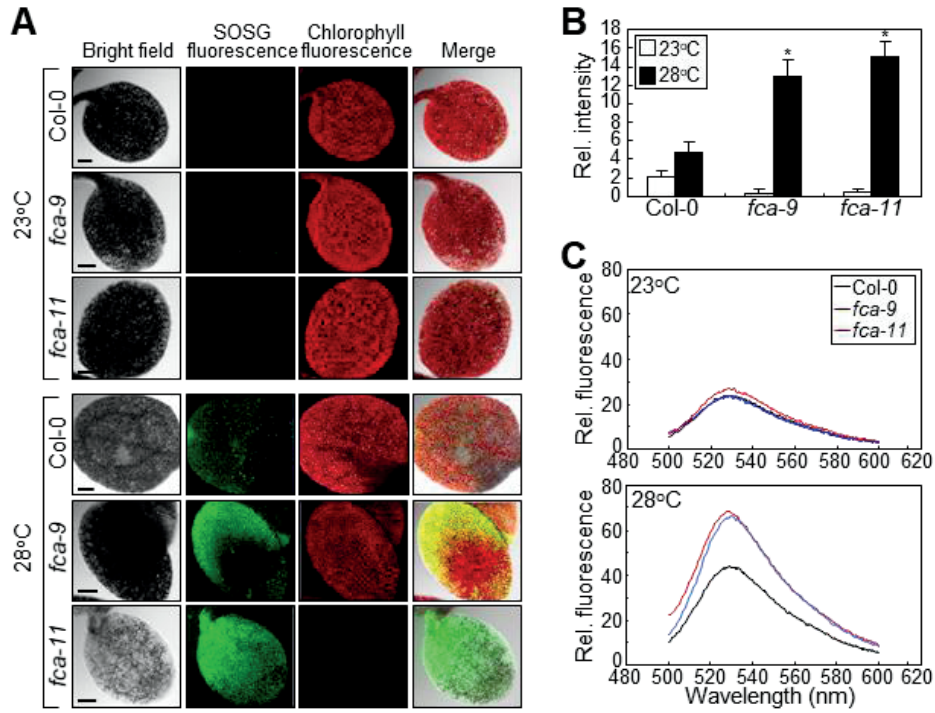

Fig. 74. ROS accumulate in *fca* seedlings at 28°C.

(**A**, **B** and **C**) Singlet oxygen accumulation. Seedlings grown for 3 d either at 23°C or 28°C were subjected to SOSG staining for the visualization of singlet oxygen. Confocal microscope was employed for fluorescence imaging (A). Scale bars, 200 μm. In (B), fluorescence intensities were quantified using ImageJ software. Three measurements were averaged and statistically treated using Student *t*-test (*$P < 0.01$). In (C), SOSG fluorescence was measured using fluorescence spectrophotometer.

the production of singlet oxygen in *fca* seedlings. In addition, the reduced chlorophyll fluorescence in *fca-11* mutant is also consistent with my observation that the chlide level was significantly reduced in *fca-11* mutant grown at 28 ºC for 3 days (Fig. 72).

I next investigated whether the production of singlet oxygen occurs under natural conditions. To mimic natural conditions, I first grew seedlings in darkness for a few days and transferred them to the light before analyzing SOSG fluorescence at either 23 ºC or 28 ºC. It was found that SOSG fluorescence was much higher in the *fca* seedlings than in Col-0 seedlings at 28 ºC (Fig. 75), further supporting that production of singlet oxygen is elevated in the higher temperature-treated mutant.

I also measured hydrogen peroxide levels by DAB staining. While the hydrogen peroxide levels were similar in Col-0 and *fca* seedlings at 23 ºC, they were significantly elevated in *fca* seedlings at 28 ºC (Fig. 76). These results indicate that FCA is associated with the reduction of ROS accumulation by converting pchlide to chlide under high ambient temperature conditions.

FCA Mediates RNA Pol II Binding to *POR* Loci

My data indicate that FCA modulates POR function at both the transcriptional and protein levels at warm temperatures. I investigated the biochemical nature of the FCA-mediated thermostabilization of POR proteins by employing inhibitors of proteases and 26S proteasome. None of

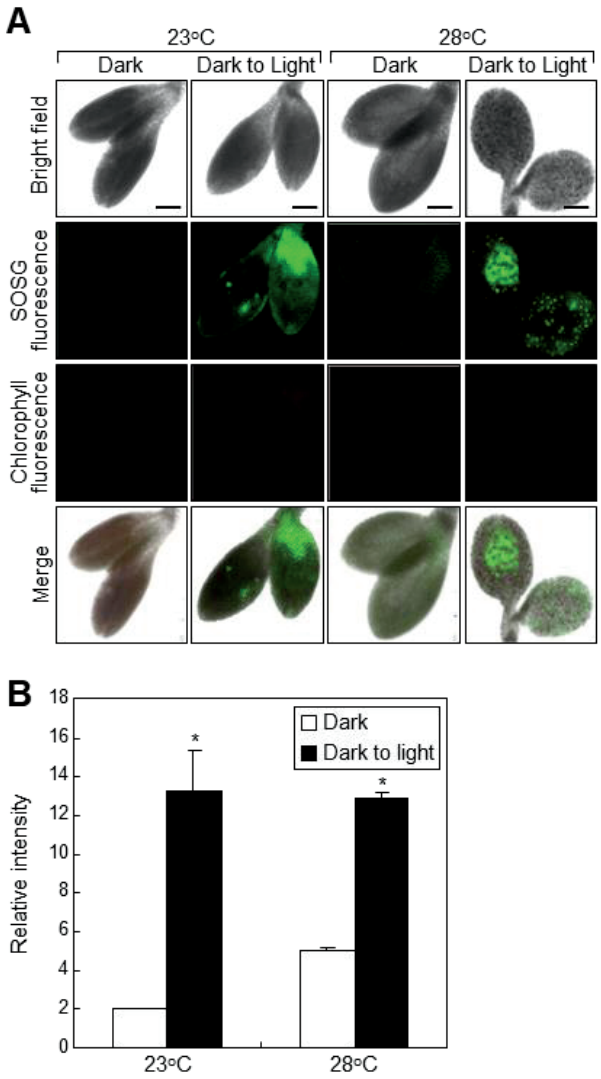
A
23°C
28°C
Dark
Dark to Light
Dark
Dark to Light
Bright field
SOSG fluorescence
Chlorophyll fluorescence
Merge
B
Relative intensity
Dark
Dark to light
*
*
0
2
4
6
8
10
12
14
16
18
23°C
28°C

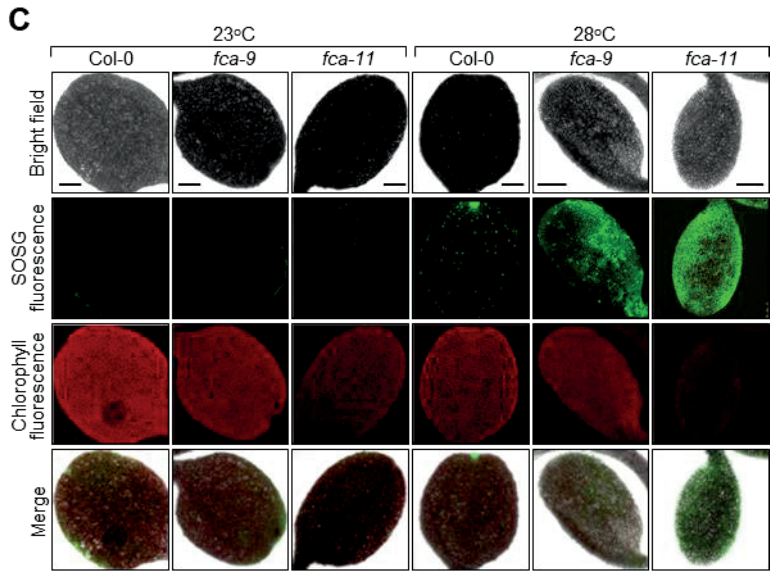
C
23°C
28°C
Col-0
fca-9
fca-11
Col-0
fca-9
fca-11
Bright field
SOSG fluorescence
Chlorophyll fluorescence
Merge

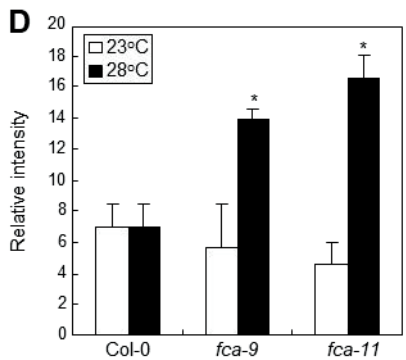
D
Relative intensity
23°C
28°C
0
2
4
6
8
10
12
14
16
18
20
*
*
Col-0
fca-9
fca-11

Fig. 75. Singlet oxygen accumulation in *fca* seedlings during the dark-to-light transfer.

(**A** and **B**) Singlet oxygen accumulation in *flu* mutant. The *flu* seedlings grown for 3 d on MS-agar plates in darkness were transferred to the light for additional 3 d at either 23ºC or 28ºC. Seedlings were subjected to SOSG staining for the visualization of singlet oxygen. Confocal microscopy was employed for fluorescence imaging (A). Scale bars, 200 mm. In (B), SOSG fluorescence intensities were quantified using the ImageJ software (http://rsbweb.nih.gov/ij/). Measurements of three different seedlings were averaged and statistically treated using Student *t*-test (*$P < 0.05$). Note that SOSG fluorescence was observed only in light-treated *flu* mutant, as described previously (Schoefs and Franck, 2003), indicating that the intensities of SOSG fluorescence reflect the levels of singlet oxygen and support the relevance of the assay system employed.

(**C** and **D**) Singlet oxygen accumulation in *fca* seedlings. Three-day-old seedlings grown on MS-agar plates in darkness were treated with light as described in (A). SOSG fluorescence images were obtained as described in (A) and (C). Scale bars, 200 mm.

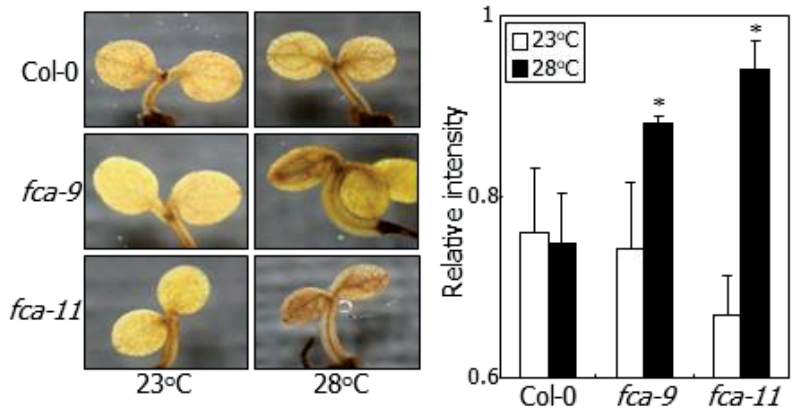

Fig. 76. Hydrogen peroxide accumulation in *fca* mutants.

Seedlings were grown as described in Fig. 74. Hydrogen peroxide levels were examined by DAB staining. Relative intensities were quantitated by the ImageJ software. Five measurements were averaged and statistically treated using Student *t*-test (*$P < 0.01$). Bars indicate SEM.

the chemical inhibitors recovered the reduced levels of POR proteins in *fca* mutants at 28 ºC (Fig. 77). In addition, yeast two-hybrid assays revealed that FCA does not interact with PORA and PORB (Fig. 78). It seems that FCA modulates POR stability through as yet unidentified protein-stabilizing pathways.

I next investigated how FCA modulates POR transcription at 28 ºC. I observed that both FCA transcription and its protein stability were not discernibly affected by warm temperatures, although FCA transcription was slightly changed throughout the time course (Fig. 79, A and B). Recent studies have shown that FCA regulates gene expression by binding to gene promoters (Lee et al., 2014; Liu et al., 2007). I therefore investigated whether FCA binds to conserved sequence elements in the *POR* loci (Fig. 80). The results showed that FCA bound to the *PORA* and *PORB* promoters only when seedlings were grown at 28 ºC (Fig. 81), suggesting that high ambient temperature induces DNA binding of FCA.

It has been reported that ETHYLENE-INSENSITIVE 3 (EIN3) and EIN3-LIKE 1 (EIL1) proteins bind directly to *PORA* and *PORB* promoters, while PIF1 binds to *PORC* promoters (Moon et al., 2008; Zhong et al., 2009). Since FCA lacks a DNA-binding domain, I hypothesized that FCA might interact with the transcription factors to bind to the *POR* promoters. Yeast two-hybrid assays showed that FCA does not interact with any of the transcription factors (Fig. 82).

I next examined whether FCA affects *POR* chromatin modifications,

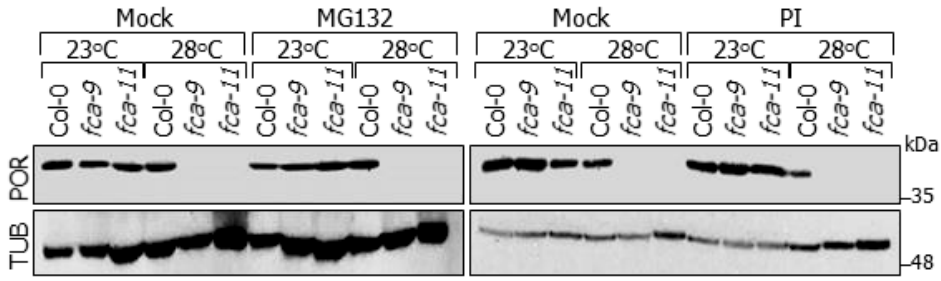

Fig. 77. Effects of protease and 26S proteasome inhibitors on POR accumulation.

Two-day-old seedlings grown on MS-agar plates at either 23°C or 28°C were treated with 5 μM MG132 or 8% protease inhibitor cocktail (PI) for 24 h.

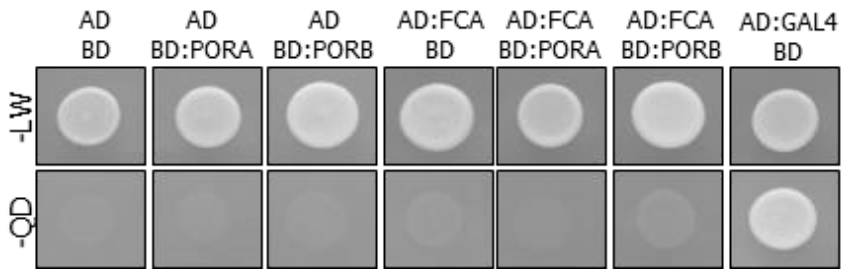

Fig. 78. Yeast two-hybrid assays on interactions of FCA with PORs.

Yeast cell growth on selective media lacking Leu, Trp, His, and Ade (-QD) represents positive interaction. AD, activation domain; BD, binding domain.

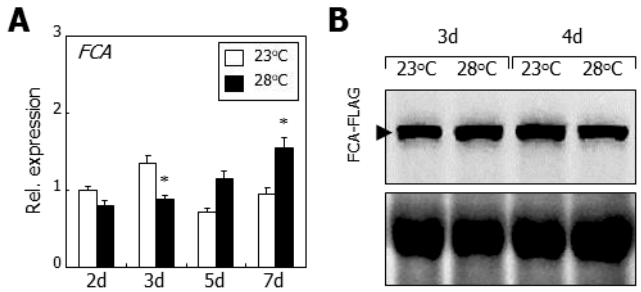

Fig. 79. Transcript level and protein stability of FCA at 28°C.

(**A**) Seedlings grown for the indicated time durations at either 23°C or 28°C were harvested at ZT 24 for total RNA extraction. Levels of *FCA* transcripts encoding a functional FCA protein were analyzed by RT-qPCR. Biological triplicates were averaged and statistically treated (*t*-test, $*P < 0.01$). Bars indicate SEM.

(**B**) Transgenic seedlings expressing a *FCA-FLAG* fusion driven by an endogenous *FCA* promoter consisting of approximately 3.0 kbps from the translation start site were grown for 3 or 4 d at either 23°C or 28°C. Whole seedlings were used for total protein extraction. An anti-FLAG antibody was used for the immunological detection of *FCA-FLAG* protein. Part of Coomassie blue-stained gel containing rubisco was shown at the bottom for loading control.

Fig. 80. Genomic structures of *POR* genes.

Black boxes, exons. White boxes, untranslated regions. Sequence elements used for ChIP assays are marked.

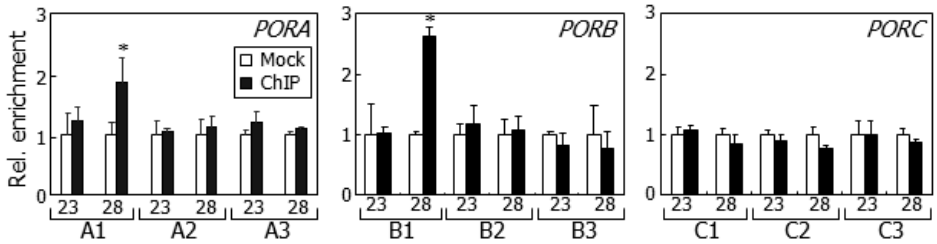

Fig. 81. ChIP assays on FCA binding to *POR* loci.

Three-day-old p*FCA:FCA-FLAG* seedlings were used. Three measurements were averaged and statistically treated (*t*-test, $*P < 0.01$). Bars indicate SEM. Mock indicates no antibody control. The analytical sequence regions were annotated in Fig. 80.

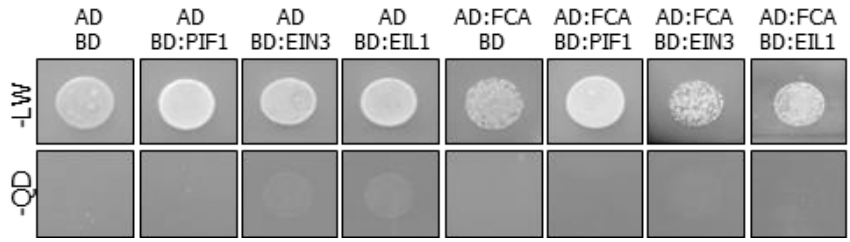

Fig. 82. Yeast two-hybrid assays on interactions of FCA with upstream regulators of *POR* expression.

The assays were performed as described in Fig. 78. The -QD media were supplemented with 50 mM 3-amino-1,2,4-triazole.

since it is known that FCA-directed regulation of gene expression is mediated by histone modification and DNA methylation (B€aurle et al., 2007; Lee et al., 2014; Liu et al., 2007). Chromatin immunoprecipitation (ChIP) assays showed that histone-3 acetylation, which is related to transcription activation (Lee et al., 1993), was significantly increased in 28 ºC grown Col-0 seedlings but did not exhibit any changes in *fca* seedlings (Fig. 83, A and B).

Other histone modification patterns, such as H3K4me2 and H3K9me3, did not match with the patterns of *POR* expressions in Col-0 and fca-9 seedlings at 28 ºC (Fig. 83, A and B). In *fca-9* mutant, the levels of *PORA* transcripts were similar at 23 ºC and 28 ºC (Fig. 63). ChIP data showed that the level of H3K4me2, indicative of inductive transcription, was much higher at 28 ºC than at 23 ºC (Fig. 83A). In contrast, the level of H3K9me3, indicative of repressive transcription, was significantly lower at 28 ºC than at 23 ºC. Similarly, the patterns of PORB transcription are not correlated with the levels of H3K4me2 and H3K9me3. In *fca-9* mutant, the levels of PORB transcripts were similar at 23 ºC and 28 ºC (Fig. 63). However, the levels of H3K4me2 were higher at 28 ºC compared with those at 23 ºC in the mutant (Fig. 83B). In Col-0 seedlings, while *PORB* transcription was upregulated at 28 ºC, the levels of H3K9me3 were similar at 23 ºC and 28 ºC. These observations indicate that H3K4me2 and H3K9me3 modifications are not directly involved in the thermal induction of *POR* genes.

FCA is also related with DNA methylation, which is known to affect

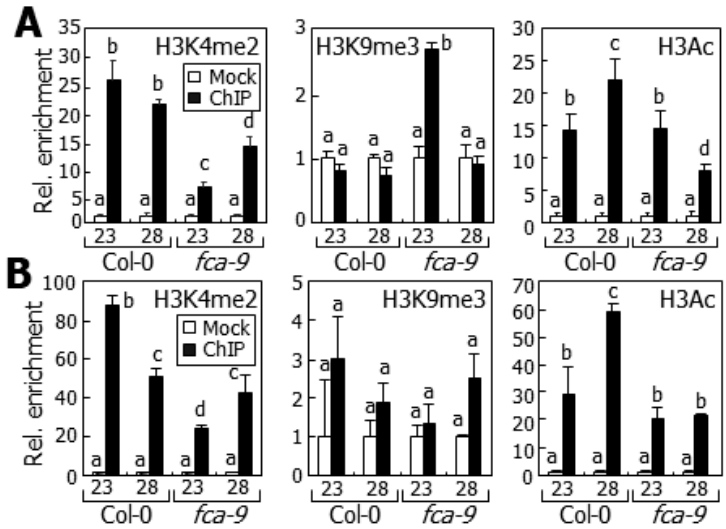

Fig. 83. Histone modifications at *POR* chromatins.

ChIP assays were performed as described in Fig. 81. Anti-H3K4me2, H3K9me3, and H3Ac antibodies were used for immunoprecipitation. Histone modifications at A1 (A) and B1 (B) sequence regions were analyzed by ChIP-qPCR. Three measurements were statistically treated. Different letters represent a significant difference ($P < 0.05$) determined by one-way ANOVA with post hoc Tukey test. Bars indicate SEM.

transcriptional activation in plants (B€aurle et al., 2007; Shibuya et al., 2009). I therefore examined DNA methylation patterns in the *POR* loci. The levels of DNA methylation in *PORB* promoter were elevated in Col-0 seedlings at 28 ºC, while they were slightly reduced in heat-treated *fca* seedlings (Fig. 84). However, DNA methylation in *PORA* promoter exhibited opposite patterns, implying that DNA methylation would not be directly involved in *POR* expression at high ambient temperatures.

I next investigated whether FCA mediates RNA polymerase II (pol II) binding to *POR* loci. ChIP assays revealed that binding of RNA pol II to *POR* loci was significantly elevated in Col-0 seedlings, but such elevation was not observed in *fca* seedlings at 28 ºC (Fig. 85). Together with the temperature-sensitive binding of FCA to *POR* promoter regions, these observations suggest that FCA would mediate epigenetic modifications in *POR* loci to recruit RNA pol II at high ambient temperatures.

A critical question was whether FCA-mediated thermal adaptation of chlorophyll biosynthesis also occurs under natural conditions. I buried *fca* seeds 1 cm below the soil surfaces and grew them at 28 ºC. As seen on Murashige and Skoog agar plates, growth of *fca* seedlings was significantly disturbed and chlorophyll content of *fca-11* seedlings was largely decreased at high ambient temperatures (Fig. 86). I designed a controlled culture system that mimics natural soil environments, whereby the temperatures of air and soil were separately controlled (Fig. 87A). Developing *fca-11* seedlings exhibited albino phenotypes when grown in warm soil, while Col-

PORA	m-CG (%)	m-CHG (%)	m-CHH (%)	Total (%)
Col-0 23°C	11.90	4.17	4.84	5.38
Col-0 28°C	9.18	1.43	2.88	3.25
fca-9 23°C	15.24	2.00	4.30	4.98
fca-9 28°C	12.99	3.64	2.79	3.80
fca-11 23°C	13.19	3.85	3.23	4.19
fca-11 28°C	14.29	1.43	4.15	4.70

PORB	m-CG (%)	m-CHG (%)	m-CHH (%)	Total (%)
Col-0 23°C	7.14	5.36	3.43	4.08
Col-0 28°C	15.87	0.00	4.57	5.90
fca-9 23°C	10.26	7.69	4.00	5.13
fca-9 28°C	7.14	1.79	3.14	3.63
fca-11 23°C	13.49	0.00	4.71	5.67
fca-11 28°C	9.40	3.85	3.85	4.64

Fig. 84. DNA methylation status at *PORA* and *PORB* loci.

Three-day-old seedlings grown at either 23ºC or 28ºC were used for genomic DNA extraction. DNA methylation assays were performed as described previously (Cheminant et al., 2011). Genomic DNA was subjected to bisulfite conversion. Promoter regions of *PORA* and *PORB* loci were amplified from the bisulfite-treated DNA and subcloned into the pTOP TA V2 plasmid (Enzynomics, Dae-Jeon, Korea). Methylation patterns were determined by direct DNA sequencing.

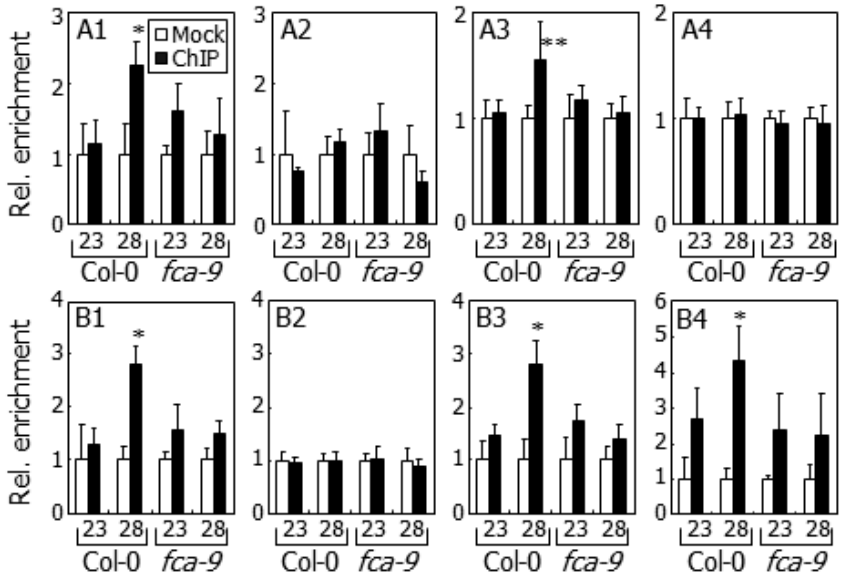

Fig. 85. ChIP assays on RNA pol II binding to *POR* loci.

ChIP assays were performed as described in Fig. 81. An anti-RNA pol II antibody was used for immunoprecipitation. Three measurements were statistically treated (*t*-test, **P* < 0.01, **P* < 0.05, difference from 23°C). Bars indicate SEM.

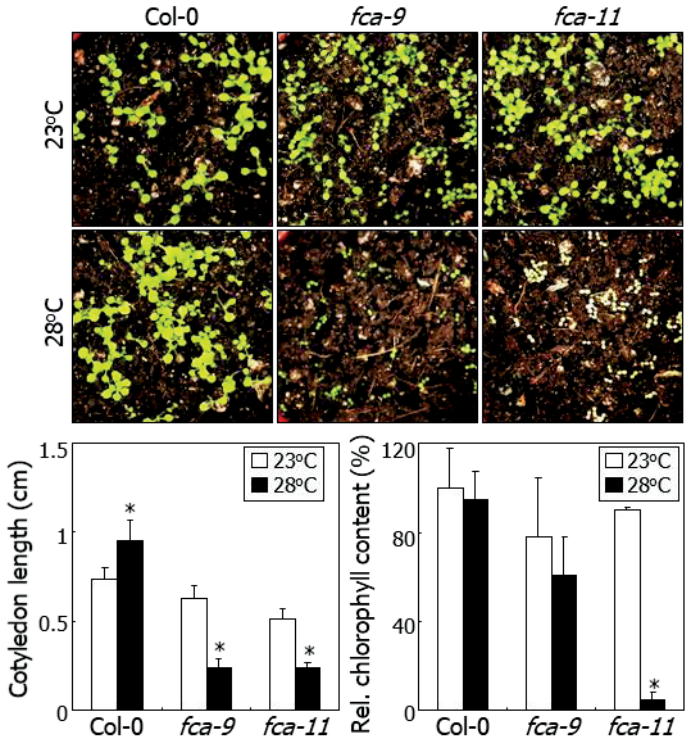

Fig. 86. phenotype of *fca* seedlings grown in soil at 28°C.

Seedlings were germinated and grown in soil for 7 d at either 23°C or 28°C (upper panel). Lengths of cotyledons were measured using ~15 seedlings and statistically treated (*t*-test, **P* < 0.01) (lower left panel). Three measurements of chlorophyll contents were averaged and statistically treated (*t*-test, **P* < 0.01) (lower right panel). Bars indicate SEM.

0 seedlings exhibited normal growth and greening (Fig. 87B). Accordingly, levels of POR proteins were drastically reduced in *fca-11* seedlings under the warm soil conditions (Fig. 87C), strongly supporting that the FCA-mediated thermal adaptation of developing seedlings is critical for autotrophic transition under natural conditions.

My data provide a thermal adaptation strategy for chlorophyll biosynthesis during early seedling development (Fig. 88A). Under natural conditions, the warming rate of soil temperature exceeds that of air temperature because soil absorbs solar heat (Lamberti and Basile, 1991). Developing seedlings would encounter high temperature when they move through the surface soil layer (Fig. 88B, left panel). I thus concluded that during the period of autotrophic transition, FCA is required for the induction of *POR* genes and suppression of POR protein degradation to trigger the conversion of pchlide to chlide and, thus, chlorophyll biosynthesis (Fig88B, right panel).

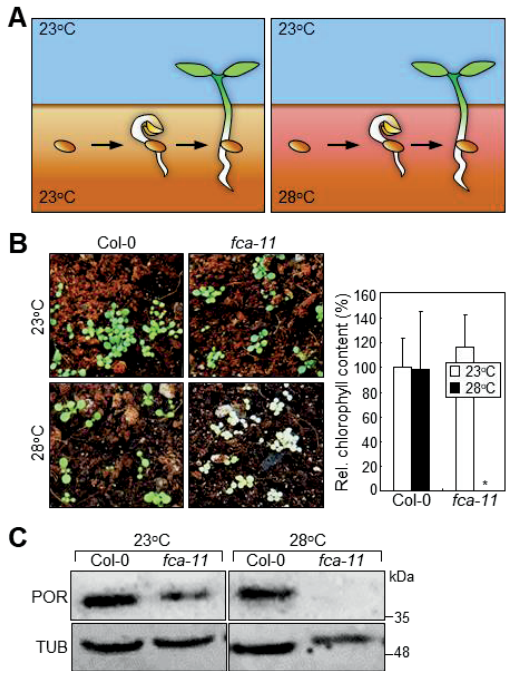

Fig. 87. *fca* seedlings exhibit albinism in warm soil.

(**A**) Schematic drawing of warm soil culture. While air temperature was 23°C, soil temperature was either 23°C or 28°C. Seedlings were germinated and grown for 7 d.

(**B**) Seedling phenotypes in warm soil. Seven-day-old seedlings were photographed (left panel). Three measurements of chlorophyll contents were statistically treated (*t*-test, $*P < 0.01$, difference from 28°C-treated Col-0) (right panel). Bars indicate SEM.

(**C**) Levels of POR proteins. Whole seedlings were used for the preparation of total protein extracts. POR proteins were immunologically detected using an anti-POR antibody.

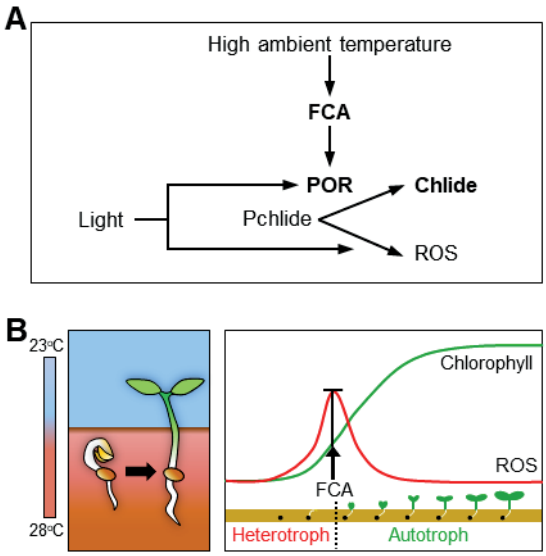

Fig. 88. FCA is essential for thermal adaptation of autotrophic development.

(**A**) FCA-mediated maintenance of PORs at warm temperatures.

(**B**) Functional relevance of FCA in autotrophic development. Under natural conditions, developing seedlings would encounter high ambient temperatures in the soil surface layer (Lamberti and Basile, 1991). FCA promotes the elevation of chlide production with a reduction of ROS production, providing a thermal adaptation strategy.

DISCUSSION

Thermomorphogenesis is a recently emerging field of interests in plant biology in conjunction with global warming. It is widely documented that under high ambient temperature conditions, plants exhibit distinct morphological and developmental traits, such as accelerated hypocotyl growth, leaf hyponasty, reduction of stomatal density, and early flowering (Crawford et al., 2012; Koini et al., 2009; Lee et al., 2013). However, it is largely unknown how warm temperatures affect the heterotrophic-to-autotrophic transition, which is a critical developmental process for plant survival and propagation.

In this work, I found that the maintenance of POR proteins is a prerequisite for autotrophic transition at warm temperatures and FCA is required for both the thermal induction of *POR* genes and the suppression of thermal degradation of POR proteins. Developing seedlings undergo autotrophic transition while they move across the heat-absorbing soil surface layer. Considering the wide conservation of PORs and its upstream regulator FCA in various plant species (Armstrong et al., 1995; Buhr et al., 2008; Forreiter and Apel, 1993; Iwamoto et al., 2001; Jang et al., 2009; Kumar et al., 2011; Lee et al., 2014; Masuda et al., 2002; Oosawa et al., 2000; Sakurabe et al., 2013), it is likely that the FCA-mediated thermal

adaptation of autotrophic development would be a general adaptation scheme in plants.

Upon light exposure, POR-bound pchlide is converted to chlide, leading to chlorophyll biosynthesis for autotrophic growth. Meanwhile, free pchlide triggers ROS production. Because of the toxic effects of ROS on cellular components, over-accumulation of pchlide and thus ROS production would cause photooxidative damages in developing seedlings (Huq et al., 2004; Zhong et al., 2009). However, it is currently unclear why plants have evolved such photosensitizer to induce autotrophic transition. Previous studies have shown that ROS contribute to cell elongation (Foreman et al., 2003). Therefore, it is possible that ROS produced during autotrophic development would contribute to hypocotyl elongation at high ambient temperatures. Developing seedlings would modulate the balance between ROS and chlorophyll levels by adjusting the production of POR enzymes. Further works on the physiological relationship between ROS and early seedling development would provide clues as to the relevance of my working model for FCA function in triggering autotrophic transition at high ambient temperature.

My data suggest that FCA induces *PORA* and *PORB* expressions by facilitating the DNA accessibility of RNA pol II. I found that PORB plays a major role in the thermal control of chlorophyll biosynthesis in light-grown seedlings and FCA directly regulates *PORB* expression. Expression of

PORC gene might be regulated indirectly through downstream regulators of FCA in response to high ambient temperatures. Meanwhile, while FCA binds to *POR* loci at high ambient temperatures, it should be clarified how the RNA-binding protein FCA mediates the thermal induction of *POR* genes. It has been reported that FCA binds to DNA through physical interactions with transcription factors (Lee et al., 2014; Lee et al., 2015). Various transcription factors, such as EIN3, EIL1, and PIF1, are known to regulate *POR* gene expression (Moon et al., 2008; Zhong et al., 2009). However, none of these transcription factors interacted with FCA. It will be worth of searching for FCA-interacting partners that are involved in autotrophic transition during thermomorphogenesis.

I found that POR proteins are destabilized at 28ºC in the absence of FCA. However, treatment of fca mutant seedlings with protease and proteasome inhibitors did not rescue the thermally induced degradation of POR proteins, obscuring the biochemical nature of POR degradation. I used total protein extracts to analyze the levels of POR proteins. Thus it is unlikely that the reduction of POR protein levels in the fca mutants is due to protein denaturation/aggregation. While proteins are targeted for degradation by proteases or 26S proteasome in most cases, it has been reported that treatments with known protease and proteasome inhibitors do not block the degradation of several proteins, suggesting that they are degraded through as yet unknown proteolytic pathways. Karrikin is a growth regulator recently identified in the smoke of burning plants, and its

putative receptor KARRIKIN INSENSITIVE 2 is destabilized in the presence of karrikin (Waters et al., 2015). It has been reported that known protease and proteasome inhibitors are unable to block the ligand-dependent degradation of the receptor protein. Searching for gene mutations that revert the thermally induced albino phenotypes of *fca* mutants will be helpful to uncover the underlying proteolytic mechanism of POR degradation.

ACKNOWLEGEMENTS

I thank for H. J. Lee for scientific discussion. I also thank for J. H. Jung for providing *pFCA*:*FCA-FLAG* transgenic plants.

RFERENCES

Abdalla, K. O., Thomson, J. A. and Rafudeen, M. S. (2009). Protocols for nuclei isolation and nuclear protein extraction from the resurrection plant *Xerophyta viscosa* for proteomic studies. *Anal*. *Biochem*. 384, 365-367.

Albertos, P., Romero-Puertas, M. C., Tatematsu, K., Mateos, I., Sánchez-Vicente, I., Nambara, E. and Lorenzo, O. (2015) S-nitrosylation triggers ABI5 degradation to promote seed germination and seedling growth. *Nat. Commun.* 6, 8669.

Ang, L. H., Chattopadhyay, S., Wei, N., Oyama, T., Okada, K., Batschauer, A. and Deng X. W. (1998) Molecular interaction between COP1 and HY5 defines a regulatory switch for light control of *Arabidopsis* development. *Mol. Cell* 2, 213-222.

Armstrong, G. A., Runge, S., Frick, G., Sperling, U. and Apel, K. (1995). Identification of NADPH:protochlorophyllide oxidoreductases A and B: a branched pathway for light-dependent chlorophyll biosynthesis in *Arabidopsis thaliana*. *Plant Physiol*. 108, 1505-1517.

Barrero, J. M., Piqueras, P., González-Guzmán, M., Serrano, R., Rodríguez, P. L., Ponce, M. R. and Micol, J. L. (2005) A mutational analysis of the *ABA1* gene of *Arabidopsis thaliana* highlights the involvement of ABA in vegetative development. *J. Exp. Bot.* 56, 2071-2083.

Bäurle, I., Smith, L., Baulcombe, D.C. and Dean, C. (2007). Widespread role for the flowering-time regulators FCA and FPA in RNA-mediated chromatin silencing. *Science* 318, 109-102.

Böhmer, M. and Schroeder, J. (2011) Quantitative transcriptomic analysis of abscisic acid-induced and reactive oxygen species-dependent expression changes and proteomic profiling in *Arabidopsis* suspension cells. *Plant J.* 67, 105-118.

Box, M.S. et al. (2015). ELF3 controls thermoresponsive growth in *Arabidopsis*. *Curr*. *Biol*. 25, 194-199.

Briggs, W. R. and Christie, J. M. (2002) Phototropins 1 and 2: versatile plant blue-light receptors. *Trends Plant Sci.* 7, 204-210.

Buhr, F., El Bakkouri, M., Valdez, O., Pollmann, S., Lebedev, N., Reinbothe, S. and Reinbothe, C. (2008). Photoprotective role of NADPH:protochlorophyllide oxidoreductase A. *Proc*. *Natl*. *Acad. Sci. USA* 105, 12629-12634.

Canamero, R. C., Bakrim, N., Bouly, J. P., Garay, A., Dudkin, E. E., Habricot, Y. and Ahmad M. (2006) Cryptochrome photoreceptors cry1 and cry2 antagonistically regulate primary root elongation in *Arabidopsis thaliana*. *Planta* 224, 995-1003.

Casal, J. J., Sánchez, R. A. and Botto, J. F. (1998) Modes of action of phytochromes. *J. Exp. Bot.* 49, 127-138.

Castells, E., Molinier, J., Drevensek, S., Genschik, P., Barneche, F. and Bowler, C. (2010) *det1-1*-induced UV-C hyposensitivity through *UVR3* and *PHR1* photolyase gene over-expression. *Plant J.* 63, 392-404.

Chai, T., Zhou, J., Liu, J. and Xing, D. (2015) LSD1 and HY5 antagonistically regulate red light induced-programmed cell death in *Arabidopsis. Front. Plant Sci*. 6, 292.

Cheminant, S., Wild, M., Bouvier, F., Pelletier, S., Renou, J. P., Erhardt, M., Hayes, S., Terry, M.J., Genschik, P. and Achard, P. (2011). DELLAs regulate chlorophyll and carotenoid biosynthesis to prevent photooxidative damage during seedling deetiolation in *Arabidopsis*. *Plant Cell* 23, 1849-1860.

Chen, X., Yao, Q., Gao, X., Jiang, C., Harberd, N. P. and Fu, X. (2016) Shoot-to-root mobile transcription factor HY5 coordinates plant carbon and nitrogen acquisition. *Curr. Biol.* 26, 640-646.

Cho, M. H., Lim, H., Shin, D. H., Jeon, J. S., Bhoo, S. H., Park, Y. and Hahn, T. R. (2011). Role of the plastidic glucose translocator in the export of starch degradation products from the chloroplasts in *Arabidopsis thaliana*. *New Phytol*. 190, 101-112.

Choi, K. et al. (2011). The FRIGIDA complex activates transcription of FLC, a strong flowering repressor in *Arabidopsis*, by recruiting chromatin modification factors. *Plant Cell* 23, 289-303.

Clough, S. J. and Bent, A. F. (1998) Floral dip: a simplified method for *Agrobacterium*-mediated transformation of *Arabidopsis thaliana*. *Plant J.* 16, 735-743.

Cluis, C. P., Mouchel, C. F. and Hardtke, C. S. (2004) The *Arabidopsis* transcription factor HY5 integrates light and hormone signaling pathways. *Plant J.* 38, 332-347.

Correll, M. J. and Kiss, J. Z. (2005) The roles of phytochromes in elongation and gravitropism of roots. *Plant Cell Physiol.* 46, 317-323.

Costigan, S. E., Warnasooriya, S. N., Humphries, B. A. and Montgomery, B. L. (2011) Root-localized phytochrome chromophore synthesis is required for photoregulation of root elongation and impacts root sensitivity to jasmonic acid in *Arabidopsis*. *Plant Physiol.* 157, 1138-1150.

Crawford, A. J., McLachlan, D. H., Hetherington, A. M. and Franklin, K. A. (2012). High temperature exposure increases plant cooling capacity. *Curr*. *Biol*. 22, R396-R397.

Dyachok J., Zhu L., Liao F., He J., Huq E. and Blancaflor E. B. (2011) SCAR mediates light-induced root elongation in *Arabidopsis* through photoreceptors and proteasomes. *Plant Cell* 23, 3610-3626.

Flors, C., Fryer, M. J., Waring, J., Reeder, B., Bechtold, U., Mullineaux, P. M., Nonell, S., Wilson, M. T. and Baker, N. R. (2006). Imaging the production of singlet oxygen in vivo using a new fluorescent sensor, Singlet Oxygen Sensor Green. *J. Exp. Bot*. 57, 1725-1734.

Foreman, J. et al. (2003). Reactive oxygen species produced by NADPH oxidase regulate plant cell growth. *Nature* 422, 442-446.

Forreiter, C. and Apel, K. (1993). Light-independent and light-dependent protochlorophyllide-reducing activities and two distinct NADPH-protochlorophyllide oxidoreductase polypeptides in mountain pine (*Pinus mugo*). *Planta* 190, 536-545.

Franklin, K. A. et al. (2011). Phytochrome-interacting factor 4 (PIF4) regulates auxin biosynthesis at high temperature. *Proc. Natl. Acad. Sci. USA* 108, 20231-20235.

Frick, G., Su, Q., Apel, K. and Armstrong, G. A. (2003). An *Arabidopsis* porB porC double mutant lacking light-dependent NADPH:protochlorophyllide oxidoreductases B and C is highly chlorophyll-deficient and developmentally arrested. *Plant J.* 35, 141-153.

Ghassemian, M., Nambara, E., Cutler, S., Kawaide, H., Kamiya, Y. and McCourt, P. (2000) Regulation of abscisic acid signaling by the ethylene response pathway in *Arabidopsis*. *Plant Cell*, 12, 1117-1126.

Gray, W. M., Ostin, A., Sandberg, G., Romano, C. P. and Estelle, M. (1998). High temperature promotes auxin-mediated hypocotyl elongation in *Arabidopsis*. *Proc. Natl. Acad. Sci. USA* 95, 7197-7202.

Hardtke, C. S., Gohda, K., Osterlund, M. T., Oyama, T., Okada, K. and Deng, X. W. (2000) HY5 stability and activity in *Arabidopsis* is

regulated by phosphorylation in its COP1 binding domain. *EMBO J*. 19, 4997-5006.

Heyes, D. J. and Hunter, C. N. (2005). Making light work of enzyme catalysis: protochlorophyllide oxidoreductase. *Trends Biochem*. *Sci*. 30, 642-649.

Hu, J., Huang, X., Chen, L., Sun, X., Lu, C., Zhang, L., Wang, Y. and Zuo, J. (2015). Site-specific nitrosoproteomic identification of endogenously S-nitrosylated proteins in *Arabidopsis*. *Plant Physiol*. 167, 1731-1746.

Huq, E., Al-Sady, B., Hudson, M., Kim, C., Apel, K. and Quail, P. H. (2004). Phytochrome-interacting factor 1 is a critical bHLH regulator of chlorophyll biosynthesis. *Science* 305, 1937-1941.

Ikegami, K., Okamoto, M., Seo, M. and Koshiba, T. (2009) Activation of abscisic acid biosynthesis in the leaves of *Arabidopsis thaliana* in response to water deficit. *J*. *Plant Res*. 122, 235-243.

Iwamoto, K., Fukuda, H. and Sugiyama, M. (2001). Elimination of *POR* expression correlates with red leaf formation in *Amaranthus tricolor*. *Plant J*. 27, 275-284.

Jang, Y. H., Park, H. Y., Kim, S. K., Lee, J. H., Suh, M. C., Chung, Y. S., Paek, K. H. and Kim, J. K. (2009). Survey of rice proteins interacting with OsFCA and OsFY proteins which are homologous to the *Arabidopsis* flowering time proteins, FCA and FY. *Plant Cell Physiol.* 50, 1479-1492.

Jeong, A. R., Lee, S. S., Han, Y. J., Shin, A. Y., Baek, A., Ahn, T., Kim, M. G., Kim, Y. S., Lee, K. W., Nagatani, A. and Kim, J. I. (2016) New constitutively active phytochromes exhibit light-independent signaling activity. *Plant Physiol*. pp.00342.

Jiao, Y., Lau, O. S. and Deng, X. W. (2007) Light-regulated transcriptional networks in higher plants. *Nat. Rev. Genet.* 8, 217-230.

Jung, J. H., Lee, S., Yun, J., Lee, M. and Park, C. M. (2014) The *miR172* target TOE3 represses *AGAMOUS* expression during *Arabidopsis* floral patterning. *Plant Sci.* 215, 29-38.

Kim, Y., Lim, J., Yeom, M., Kim, H., Kim, J., Wang, L., Kim, W. Y., Somers, D. E. and Nam, H. G. (2013) ELF4 regulates GIGANTEA chromatin access through subnuclear sequestration. *Cell Rep.* 3, 671-677.

Kim, D. H., Yamaguchi, S., Lim, S., Oh, E., Park, J., Hanada, A., Kamiya, Y. and Choi, G. (2008) SOMNUS, a CCCH-Type zinc finger protein in *Arabidopsis*, negatively regulates light-dependent seed germination downstream of PIL5. *Plant Cell*, 20, 1260-1277.

Kircher, S. and Schopfer, P. (2012) Photosynthetic sucrose acts as cotyledon-derived long-distance signal to control root growth during early seedling development in *Arabidopsis*. *Proc. Natl. Acad. Sci. U. S. A.* 109, 11217-11221.

Koini, M. A., Alvey, L., Allen, T., Tilley, C. A., Harberd, N. P., Whitelam, G. C. and Franklin, K. A. (2009). High temperature-mediated

adaptations in plant architecture require the bHLH transcription factor PIF4. *Curr. Biol*. 19, 408-413.

Kumar, S., Jiang, S., Jami, S. K. and Hill, R. D. (2011). Cloning and characterization of barley caryopsis FCA. *Physiol. Plant* 143, 93-106.

Kwak, J. M., Mori, I. C., Pei, Z. M., Leonhardt, N., Torres, M. A., Dangl, J. L., Bloom, R. E., Bodde, S., Jones, J. D. and Schroeder, J. I. (2003) NADPH oxidase *AtrbohD* and *AtrbohF* genes function in ROS-dependent ABA signaling in *Arabidopsis*. *EMBO J.* 22, 2623-2633.

Lamberti, F. and Basile, M. (1991). Soil solarization. Proceedings of the First international conference on Soil Solarization. (Rome: FAO press).

Leasure, C. D., Tong, H., Yuen, G., Hou, X., Sun, X. and He, Z. H. (2009) ROOT UV-B SENSITIVE2 acts with ROOT UV-B SENSITIVE1 in a root ultraviolet B-sensing pathway. *Plant Physiol.* 150, 1902-1915.

Lee, J., He, K., Stolc, V., Lee, H., Figueroa, P., Gao, Y., Tongprasit, W., Zhao, H., Lee, I. and Deng X. W. (2007) Analysis of transcription factor HY5 genomic binding sites revealed its hierarchical role in light regulation of development. *Plant Cell* 19, 731-749.

Lee, D. Y., Hayes, J. J., Pruss, D. and Wolffe, A. P. (1993). A positive role for histone acetylation in transcription factor access to nucleosomal DNA. *Cell* 72, 73-84.

Lee, H. J. et al. (2016b) Stem-piped light activates phytochrome B to trigger light responses in *Arabidopsis thaliana* roots. *Sci*. *Signal*. 9, ra106.

Lee, H. J., Ha, J. H. and Park. C. M. (2016a) Underground roots monitor aboveground environment by sensing stem-piped light. *Commun. Integr. Bio.* 9, e1261769.

Lee, H. J., Jung, J. H., Cortés Llorca, L., Kim, S. G., Lee, S., Baldwin, I. T. and Park, C. M. (2014). FCA mediates thermal adaptation of stem growth by attenuating auxin action in *Arabidopsis*. *Nat*. *Commun*. 5, 5473.

Lee, J. H., Ryu, H. S., Chung, K. S., Posé, D., Kim, S., Schmid, M. and Ahn, J. H. (2013). Regulation of temperature-responsive flowering by MADS-box transcription factor repressors. *Science* 342, 628-632.

Lee, S., Lee, H. J., Jung, J. H. and Park, C. M. (2015) The *Arabidopsis thaliana* RNA-binding protein FCA regulates thermotolerance by modulating the detoxification of reactive oxygen species. *New Phytol.* 205, 555-569.

Lee, S., Seo, P. J., Lee, H. J. and Park, C. M. (2012). A NAC transcription factor NTL4 promotes reactive oxygen species production during drought-induced leaf senescence in *Arabidopsis*. *Plant J*. 70, 831-844.

Li, X., Chen, L., Forde, B. G. and Davies, W. J. (2017) The biphasic root growth response to abscisic acid in *Arabidopsis* involves interaction with ethylene and auxin signalling pathways. *Front*. *Plant Sci*. 8, 1493.

Li, Y. and Tollefsbol, T. O. (2011). DNA methylation detection: bisulfite genomic sequencing analysis. *Methods Mol*. *Biol*. 791, 11-21.

Lin, Y. P., Lee, T. Y., Tanaka, A. and Charng, Y. Y. (2014). Analysis of an *Arabidopsis* heat-sensitive mutant reveals that chlorophyll synthase is involved in reutilization of chlorophyllide during chlorophyll turnover. *Plant J*. 80, 14-26.

Liu, F., Marquardt, S., Lister, C., Swiezewski, S. and Dean, C. (2010). Targeted 3' processing of antisense transcripts triggers *Arabidopsis* FLC chromatin silencing. *Science* 327, 94-97.

Liu, F., Quesada, V., Crevillén, P., Bäurle, I., Swiezewski, S. and Dean, C. (2007). The *Arabidopsis* RNA-binding protein FCA requires a lysine-specific demethylase 1 homolog to downregulate FLC. *Mol. Cell* 28, 398-407.

Lopez-Molina, L., Mongrand, S. and Chua, N. H. (2001) A postgermination developmental arrest checkpoint is mediated by abscisic acid and requires the ABI5 transcription factor in *Arabidopsis*. *Proc. Natl. Acad. Sci. USA,* 98, 4782-4787.

Lorrain, S., Allen, T., Duek, P. D., Whitelam, G. C. and Fankhauser, C. (2008). Phytochrome-mediated inhibition of shade avoidance involves degradation of growth-promoting bHLH transcription factors. *Plant J*. 53, 312-323.

Lu, X. D., Zhou, C. M., Xu, P. B., Luo, Q., Lian, H. L. and Yang, H. Q. (2015) Red-light-dependent interaction of phyB with SPA1 promotes COP1-SPA1 dissociation and photomorphogenic development in *Arabidopsis*. *Mol. Plant* 8, 467-478.

Ma, L., Gao, Y., Qu, L., Chen, Z., Li, J., Zhao, H. and Deng, X. W. (2002) Genomic evidence for COP1 as a repressor of light-regulated gene expression and development in *Arabidopsis*. *Plant Cell* 14, 2383-2398.

Macknight, R. et al. (1997). *FCA*, a gene controlling flowering time in *Arabidopsis*, encodes a protein containing RNA-binding domains. *Cell 89*, 737-745.

Mandoli, D. F., Ford, G. A., Waldron, L. J., Nemson, J. A. and Briggs, W. R. (1990) Some spectral properties of several soil types: implications for photomorphogenesis. *Plant Cell Environ.* 13, 287-294.

Mansfield, S. G. and Briarty, L. G. (1996). The dynamics of seedling and cotyledon cell development in *Arabidopsis thaliana* during reverse mobilization. *Int. J. Plant Sci*. 157, 280–295.

Marsch-Martínez, N., Franken, J., Gonzalez-Aguilera, K. L., de Folter, S., Angenent, G. and Alvarez-Buylla, E. R. (2013) An efficient flat-surface collar-free grafting method for *Arabidopsis thaliana* seedlings. *Plant Methods*, 9, 14.

Masuda, T., Fusada, N., Shiraishi, T., Kuroda, H., Awai, K., Shimada, H., Ohta, H. and Takamiya, K. (2002). Identification of two differentially regulated isoforms of protochlorophyllide oxidoreductase (*POR*) from tobacco revealed a wide variety of light- and development-dependent regulations of *POR* gene expression among angiosperms. *Photosynth. Res*. 74, 165-172.

McAdam, S. A., Brodribb, T. J. and Ross, J. J. (2016) Shoot-derived abscisic acid promotes root growth. *Plant Cell Environ.* 39, 652-659.

Meskauskiene, R., Nater, M., Goslings, D., Kessler, F., op den Camp, R. and Apel, K. (2001). FLU: a negative regulator of chlorophyll biosynthesis in *Arabidopsis thaliana*. *Proc. Natl. Acad. Sci. USA* 98, 12826-12831.

Mo, M., Yokawa, K., Wan, Y. and Baluška, F. (2015) How and why do root apices sense light under the soil surface? *Front. Plant. Sci*. 6, 775.

Moon, J., Zhu, L., Shen, H. and Huq, E. (2008). PIF1 directly and indirectly regulates chlorophyll biosynthesis to optimize the greening process in *Arabidopsis*. *Proc. Natl. Acad. Sci. USA* 105, 9433-9438.

Mubarakshina, M. M., Ivanov, B. N., Naydov, I. A., Hillier, W., Badger, M. R. and Krieger-Liszkay, A. (2010) Production and diffusion of chloroplastic H_2O_2 and its implication to signalling. *J. Exp. Bot.* 61, 3577-3587.

Oosawa, N., Masuda, T., Awai, K., Fusada, N., Shimada, H., Ohta, H. and Takamiya, K. (2000). Identification and light-induced expression of a novel gene of NADPH-protochlorophyllide oxidoreductase isoform in *Arabidopsis thaliana*. *FEBS Lett*. 474, 133-136.

Osterlund, M. T., Hardtke, C. S., Wei, N. and Deng, X. W. (2000) Targeted destabilization of HY5 during light-regulated development of *Arabidopsis*. *Nature* 405, 462-466.

Oyama, T., Shimura, Y. and Okada, K. (1997) The *Arabidopsis HY5* gene encodes a bZIP protein that regulates stimulus-induced development of root and hypocotyl. *Genes Dev.* 11, 2983-2995.

Paddock, T. N., Lima, D., Mason, M. E., Apel, K. and Armstrong, G. A. (2012). *Arabidopsis* light-dependent protochlorophyllide oxidoreductase A (PORA) is essential for normal plant growth and development. *Plant Mol*. *Biol*. 78, 447-460.

Paddock, T. N., Mason, M. E., Lima, D. F. and Armstrong, G. A. (2010). *Arabidopsis* protochlorophyllide oxidoreductase A (PORA) restores bulk chlorophyll synthesis and normal development to a *porB porC* double mutant. *Plant Mol*. *Biol*. 72, 445-457.

Piskurewicz, U., Jikumaru, Y., Kinoshita, N., Nambara, E., Kamiya, Y. and Lopez-Molina, L. (2008). The gibberellic acid signaling repressor RGL2 inhibits *Arabidopsis* seed germination by stimulating abscisic acid synthesis and ABI5 activity. *Plant Cell* 20, 2729-2745.

Reinbothe, C., Apel, K. and Reinbothe, S. (1995). A light-Induced protease from barley plastids degrades NADPH:protochlorophyllide oxidoreductase complexed with chlorophyllide. *Mol*. *Cell*. *Biol*. 15, 6206-6212.

Reinbothe, C., Lebedev, N. and Reinbothe, S. A. (1999). Protochlorophyllide light-harvesting complex involved in de-etiolation of higher plants. *Nature* 397, 80-84.

Reinbothe, S., Reinbothe, C., Holtorf, H. and Apel, K. (1995). Two NADPH:protochlorophyllide oxidoreductases in barley: evidence for the selective disappearance of PORA during the light-induced greening of etiolated seedlings. *Plant Cell* 7, 1933-1940.

Reinbothe, S., Reinbothe, C., Lebedev, N. and Apel, K. (1996). PORA and PORB, two light-dependent protochlorophyllide-reducing enzymes of angiosperm chlorophyll biosynthesis. *Plant Cell* 8, 763-769.

Rensing, S. A. and Sheerin, D. J. (2016) A. Hiltbrunner, Phytochromes: more than meets the eye. *Trends Plant Sci.* 21, 543-546.

Sakuraba, Y., Rahman, M. L., Cho, S. H., Kim, Y. S., Koh, H. J., Yoo, S. C. and Paek, N. C. (2013). The rice faded green leaf locus encodes protochlorophyllide oxidoreductase B and is essential for chlorophyll synthesis under high light conditions. *Plant J.* 74, 122-133.

Schafer, E. and Bowle, C. (2002) Phytochrome-mediated photoperception and signal transduction in higher plants. *EMBO Rep.* 3, 1042-1048.

Schäfer, M., Brütting, C., Baldwin, I. T. and Kallenbach, M. (2016) High-throughput quantification of more than 100 primary- and secondary-metabolites and phytohormones by a single solid-phase extraction based sample preparation with analysis by UHPLC-HESI-MS/MS. *Plant Methods*, 12, 30.

Schoefs, B. and Franck, F. (2003). Protochlorophyllide reduction: mechanisms and evolutions. *Photochem. Photobiol.* 78, 543-557.

Seo, E., Lee, H., Jeon, J., Park, H., Kim, J., Noh, Y. S. and Lee, I. (2009) Crosstalk between cold response and flowering in *Arabidopsis* is mediated through the flowering-time gene *SOC1* and its upstream negative regulator *FLC*. *Plant Cell* 21, 3185-3197.

Seo, K. I., Lee, J. H., Nezames, C. D., Zhong, S., Song, E., Byun, M. O. and Deng, X. W. (2014) ABD1 is an *Arabidopsis* DCAF substrate receptor for CUL4-DDB1-based E3 ligases that acts as a negative regulator of abscisic acid signaling. *Plant Cell*, 26, 695-711.

Seo, P. J., Kim, M. J., Park, J. Y., Kim, S. Y., Jeon, J., Lee, Y. H., Kim, J. and Park, C. M. (2010). Cold activation of a plasma membrane-tethered NAC transcription factor induces a pathegen resistance response in *Arabidopsis*. *Plant J.* 61, 661-671.

Sharrock, R. A. and Clack, T. (2002) Patterns of expression and normalized levels of the five *Arabidopsis* phytochromes. *Plant Physiol.* 130, 442-456.

Shibuya, K., Fukushima, S. and Takatsuji, H. (2009). RNA-directed DNA methylation induces transcriptional activation in plants. *Proc. Natl. Acad. Sci. USA* 106, 1660-1665.

Smith, H. (1982) Light quality, photoperception and plant strategy. *Ann. Rev. Plant Physiol.* 33, 481-518.

Smith, S. and De Smet, L. (2012) Root system architecture: insights from *Arabidopsis* and cereal crops. *Philos. Trans. R. Soc. Lond. B. Biol. Sci.* 367, 1441-1452.

Su, Q., Frick, G., Armstrong, G. and Apel, K. (2001). POR C of *Arabidopsis thaliana*: a third light- and NADPH-dependent protochlorophyllide oxidoreductase that is differentially regulated by light. *Plant Mol. Biol*. 47, 805-813.

Sun, Q., Yoda, K. and Suzuki, H. (2005) Internal axial light conduction in the stems and roots of herbaceous plants. *J. Exp. Bot.* 56, 191-203.

Sun, Q., Yoda, K., Suzuki, M. and Suzuki, H. (2003) Vascular tissue in the stem and roots of woody plants can conduct light. *J. Exp. Bot.* 54, 1627-1635.

Sun, F., Zhang, W., Hu, H., Li, B., Wang, Y., Zhao, Y., Li, K., Liu, M. and Li, X. (2008) Salt modulates gravity signaling pathway to regulate growth direction of primary roots in *Arabidopsis thaliana*. *Plant Physiol.* 146, 178-188.

Sun, J., Qi, L., Li, Y., Chu, J. and Li, C. (2012). PIF4-mediated activation of YUCCA8 expression integrates temperature into the auxin pathway in regulating *Arabidopsis* hypocotyl growth. *PLoS Genet*. 8, e1002594.

Suzuki, A. et al. (2011) *Lotus japonicus* nodulation is photomorphogenetically controlled by sensing the red/far red (R/FR) ratio through jasmonic acid (JA) signaling. *Proc. Natl. Acad. Sci. U. S. A.* 108, 16837-16842.

Taiz, L. and Zeiger, E. (Sinauer Associates, Sunderland, MA, ed. 5, 2010) “Phytochrome and light control of plant development” in *Plant Physiology* pp. 497-498.

Tester, M. and Morris, C. (1987) The penetration of light through soil. *Plant Cell Environ.* 10, 281-286.

Tomas, H. (1997). Chlorophyll: a symptom and a regulator of plastid development. *New Phytol*. 136, 163-181.

Tong, H., Leasure, C. D., Hou, X., Yuen, G., Briggs, W. and He, Z. H. (2008) Role of root UV-B sensing in *Arabidopsis* early seedling development. *Proc. Natl. Acad. Sci. U. S. A.* 105, 21039-21044.

Tsukagoshi, H. (2016) Control of root growth and development by reactive oxygen species. *Curr. Opin. Plant. Biol.* 29, 57-63.

Tsukagoshi, H., Busch, W. and Benfey, P. N. (2010) Transcriptional regulation of ROS controls transition from proliferation to differentiation in the root. *Cell*, 143, 606-616.

Udvardi, M. K., Czechowski, T. and Scheible, W. R. (2008) Eleven golden rules of quantitative RT-PCR. *Plant Cell*, 20, 1736–1737.

Vidal, E. A., Moyano, T. C., Canales, J. and Gutiérrez, R. A. (2014). Nitrogen control of developmental phase transitions in *Arabidopsis thaliana*. *J. Exp. Bot*. 65, 5611-5618.

Warnasooriya, S. N. and Montgomery, B. L. (2011) Spatial-specific regulation of root development by phytochromes in *Arabidopsis thaliana. Plant Signal. Behav.* 6, 2047-2050.

Wei, Q., Zhou, W., Hu, G., Wei, J., Yang, H. and Huang, J. Y. (2008) Heterotrimeric G-protein is involved in phytochrome A-mediated cell death of *Arabidopsis* hypocotyls. *Cell Res.* 18, 949-960.

Xu, X., Paik, I., Zhu, L. and Huq, E. (2015) Illuminating progress in phytochrome-mediated light signaling pathways. *Trends Plant Sci.* 20, 641-650.

Yokawa, K., Fasano, R., Kagenishi, T. and Baluška, F. (2014) Light as stress factor to plant roots - case of root halotropism. *Front. Plant Sci*. 5, 718.

Yokawa, K., Kagenishi, T. and Baluška, F. (2016) UV-B induced generation of reactive oxygen species promotes formation of BFA-induced compartments in cells of *Arabidopsis* root apices. *Front. Plant Sci*. 13, 1162.

Zheng, X. et al. (2013) *Arabidopsis* phytochrome B promotes SPA1 nuclear accumulation to repress photomorphogenesis under far-red light. *Plant Cell* 25, 115-133.

Zhong, S., Zhao, M., Shi, T., Shi, H., An, F., Zhao, Q., and Guo, H. (2009). EIN3/EIL1 cooperate with PIF1 to prevent photo-oxidation and to promote greening of *Arabidopsis* seedlings. *Proc. Natl. Acad. Sci. USA* 106, 21431-21436.

Zhou, X. et al. (2015) SOS2-LIKE PROTEIN KINASE5, an SNF1-RELATED PROTEIN KINASE3-type protein kinase, is important for abscisic acid responses in *Arabidopsis* through phosphorylation of ABSCISIC ACID-INSENSITIVE5. *Plant Physiol.* 168, 659-676.

PUBLICATION LIST

*equal contribution.

1. Gil, K. E., **Ha, J. H.** and Park, C. M. Abscisic acid-mediated phytochrome B signaling promotes primary root growth in *Arabidopsis*. (2018) *Plant Signal Behav*. **25**, 1-3.
2. **Ha, J. H.**, Kim, J. H., Kim, S. G., Sim, H. J., Lee, G., Halitschke, R., Baldwin, I. T., Kim, J. I. and Park, C. M. Shoot phytochrome B modulates root ROS homeostasis via abscisic acid signaling in *Arabidopsis*. (2018) *Plant J*. **94**, 790-798.
3. **Ha, J. H.**, Han, S. H., Lee, H. J. and Park, C. M. Environmental adaptation of the heterotrophic-to-autotrophic transition: the developmental plasticity of seedling establishment. (2017) *Crit. Rev. Plant Sci.* **36**, 128-137.
4. Lee, H. J., Park, Y. J., **Ha, J. H.**, Baldwin, I. T. and Park, C. M. Multiple routes of light signaling during root photomorphogenesis. (2017) *Trends Plant Sci.* **10**, 1360-1385.
5. Park, Y. J., Lee, H. J., **Ha, J. H.**, Kim, J. Y. and Park, C. M. COP1 conveys warm temperature information to hypocotyl thermomorphogenesis. (2017) *New Phytol.* **215**, 269-280.

6. Lee, H. J., **Ha, J. H.** and Park, C. M. A FCA-mediated epigenetic route towards thermal adaptation of autotrophic development in plants. (2017) *BMB Rep.* **29**, 3832.
7. **Ha, J. H.***, Lee, H. J.*, Jung, J. H. and Park, C. M. Thermo-induced maintenance of photo-oxidoreductases underlies plant autotrophic development. (2017) *Dev. Cell.* **41**, 1–10.
8. Lee, H. J., **Ha, J. H.** and Park, C. M. Underground roots monitor aboveground environment by sensing stem-piped light. (2016) *Commun. Integr. Biol.* **9**, e1261769.
9. Lee, H. J.*, **Ha, J. H.***, Kim, S. G.*, Choi, H. K., Kim, Z. H., Han, Y. J., Kim, J. I., Oh, Y., Fragoso, V., Shin, K., Hyeon, T., Choi, H. G., Oh, K.H., Baldwin, I. T. and Park, C. M. Stem-piped light activates phytochrome B to trigger light responses in Arabidopsis thaliana roots. (2016) *Sci. Signal*. **9**, ra106.
10. Lee, S.*, Lee, H. J.*, Huh, S. U., Paek, K. H., **Ha, J. H.** and Park, C. M. The *Arabidopsis* NAC transcription factor NTL4 participates in a positive feedback loop that induces programmed cell death under heat stress conditions. (2014) *Plant Sci*. **227**, 76-83.

ABSTRACT IN KOREAN (국문 초록)

식물은 지표면에 뿌리를 내려 주변 환경의 영양소를 흡수하여 에너지를 만들어 생활한다. 이동성이 없는 특성으로 인해 식물은 발달 및 성장에 있어 빛, 온도, 수분과 그 속에 녹아있는 영양소 및 무기 염류 등 매우 다양한 환경요소들의 영향을 받는다. 환경 변화에 대응하는 식물의 반응 메커니즘에 대한 분자생물학적 연구는 과거부터 현재까지 매우 활발하게 진행되어오고 있다. 식물의 빛 반응에 관한 기존 연구는 식물의 상층부에서 일어나는 광형태형성에 관한 연구가 주로 이루어져 왔다. 또한, 온도 변화에 대응하는 식물의 메커니즘 연구는 줄기 생장 등의 묘목 단계에서 일어나는 열형태형성 과정에 집중되어 연구가 진행되어 왔다. 환경 변화에 대응하는 반응 메커니즘은 어떤 조직에서 일어나는지, 어느 시기에 일어나는 지에 따라 다르게 나타난다. 그러나, 특정 조직에서나 특정 시기에서 일어나는 환경 변화 대응 메커니즘 연구는 많이 이루어지지 않았다. 본 연구에서는 빛 반응과 뿌리 조직 간의 상호작용 및 독립영양체계로의 전환 단계에서의 온도 반응에 관한 연구를 진행하였다.

제 1장에서는 식물의 뿌리가 빛에 직접적으로 노출되어 있지

않음에도 광 반응성을 보이며 뿌리에도 광 수용체가 존재한다는 기존 보고들을 토대로, 어떻게 뿌리가 빛을 인식하는 지 알아보고, 어떤 광 반응을 일으키는 지 연구하였다. 물리화학적 실험을 통해 적외선 파장의 빛이 식물 줄기를 통해 뿌리로 전달된다는 사실을 밝혀 내었으며, 식물 뿌리에 존재하는 광 수용체인 phytochrome B (phyB) 가 줄기를 통해 내려온 빛에 의해 활성화되어 ELONGATED HYPOCOTYL (HY5) 단백질을 안정화 시킨다. 안정화된 HY5 단백질은 뿌리의 중력굴성 조절에 필수적이다. 본 연구를 통해 식물의 뿌리가 지상부의 환경을 모니터링 하고 환경 변화에 반응하는 능동적 역할을 수행한다는 사실을 밝혀내었다.

제 2장에서는 식물의 뿌리가 빛에 직접적으로 노출된 환경에서 어떠한 반응을 보이는 지 연구하였다. 식물 뿌리가 빛에 노출된 환경에서 광 수용체인 phyB 단백질은 스트레스 호르몬인 앱시스산 (ABA)의 합성을 촉진시켜 ABA 신호체계를 활성화 시킨다. 활성화 된 ABA 신호는 뿌리로 전달되어 뿌리에서 ABA INSENSITIVE5 (ABI5) 유전자의 발현을 촉진함과 동시에 단백질을 안정화 시킨다. 안정화된 ABI5 단백질에 의해 만들어진 PEROXIDASE 1 (PER1) 효소가 활성산소의 과 축적을 억제하여 뿌리의 광산화 피해를 막아주어 빛에 노출된 조건에서도 뿌리가 원활하게 생장할 수 있도록 한다. 본 연구를 통해 광 수용체가

ABA 신호체계를 통해 식물 상층부와 뿌리의 균형적 발달 및 성장에 기여한다는 사실을 밝혀내었다.

제 3장에서는 약 고온 환경에서의 식물의 발달 과정에 대한 연구를 수행하였다. 식물은 독립영양생장을 위하여 엽록소를 합성한다. 빛에 노출되기 전 식물체는 엽록소 전구체인 protochlorophyllide (pchlide) 를 축적하고 pchilde는 빛과 반응하여 PROTOCHLOROPHYLLIDE OXYDOREDUCTASE (POR) 효소에 의해 chlorophyllide (chlide)로 전환된다. POR 효소와 결합되지 않은 pchilde는 빛과 반응하여 활성산소를 만들어 식물 세포에 피해를 입힌다. 때문에 POR 단백질의 활성을 유지시켜 pchlide의 양을 적절하게 조절하는 것이 필수적이다. 이 과정에서 RNA 결합 단백질로 알려진 FCA 단백질이 POR 유전자의 전사 촉진 및 단백질 안정화를 통해 pchlide 가 고온 환경에서도 원활하게 chlide로 전환될 수 있게 한다. 본 연구를 통해 FCA 단백질을 통한 독립영양체계 구축 메커니즘이 자연 환경에서 식물이 열에 의해 뜨거워진 지표면을 지나면서 발아하는 과정을 가능하게 한다는 사실을 밝혀내었다.

주요어: 빛 신호체계, 광수용체, 뿌리 성장, 빛 이동, 앱시스산, 약 고온, 독립영양체계, 엽록소 합성, 활성 산소

학 번: 2014-21242